VALIDATION OF TWO NOVEL MOUSE MODELS OF CONDITIONAL MEIS1 DELETION TO STUDY ROLES IN ADULT MOUSE HEMATOPOIESIS

by

MICHELLE ERIN MILLER
B.Sc., The University of British Columbia, 2005

A THESIS SUBMITTED IN PARTIAL FUFILLMENT OF THE REQUIREMENTS FOR THE DEGREE OF
DOCTOR OF PHILOSOPY

in

THE FACULTY OF GRADUATE AND POSTDOCTORAL STUDIES

(Medical Genetics)

THE UNIVERSITY OF BRITISH COLUMBIA

(Vancouver)

April 2014

Abstract

Meis1 is recognized as an important transcriptional regulator in hematopoietic development and is strongly implicated in the pathogenesis of leukemia, both as a Hox transcription factor co-factor and independently. Despite the emerging recognition of *Meis1*'s importance in the context of both normal and leukemic hematopoiesis, there is not yet a full understanding of *Meis1*'s functions and the relevant pathways and genes mediating its functions. In this thesis, I provide the groundwork for a novel model system to explore *Meis1* function. Mice with a loxP flanked *Meis1* allele were crossed with two different conditional Cre-recombinase expressing strains, MxCre mouse and the ERTCre mouse. I validated conditional deletion of the *Meis1* allele and the resultant decrease in mRNA and protein expression. I additionally studied expression of *Meis1* related (MEINOX family) transcription factors in highly purified hematopoietic populations to generate an atlas of gene expression and focus our future studies. The inducible *Meis1*-deletion mice were then used to study if *Meis1* is a requirement to maintain hematopoietic homeostasis in adult mice. I provide evidence for a critical role for *Meis1* in hematopoietic stem cell maintenance and megakaryocytic and erythroid progenitor expansion in vivo. I furthermore identified two novel candidate effectors of *Meis1* in the adult hematopoietic system, *Hlf* and *Msi2* using Affymetrix expression analysis. As recent studies have suggested a role for *Meis1* in the regulation of hypoxia-induced reactive oxygen species (ROS), I examined the impact of the ROS-scavenger N-acetyl-L-cysteine on the $Meis1^{-/-}$ phenotype in vivo. The results highlighted in this thesis provide direction and an experimental platform for further dissection of the mechanisms of *Meis1* function in both normal and leukemic hematopoiesis.

Preface

The work in this thesis was completed for the purposes of a Doctorate of Philosophy in the department of Medical Genetics at The University of British Columbia under the supervision of Dr. R. Keith Humphries (Terry Fox Laboratory, Vancouver, BC).

All experimental designs are my own, however, several people made invaluable contributions. The conditional-knock out mouse line on which the experiments are based, C57BL/6 J *Meis1*$^{tmloxP/+}$ (*Meis1*$^{fl/+}$), was a generous gift from Drs N. Jenkins and N. Copeland (McLaughlin Research Institute, Great Falls, MT, USA). B6;129-*Gt(ROSA)26Sor*$^{tm1(cre/ERT)Nat}$/J mice were a gift from Dr. A. Weng (Terry Fox Laboratory, BC Cancer Agency, Vancouver, BC, CAN). Dr. Weng also provided his expertise in the examination of histology slides. All animal breeding protocols and experimental procedures were approved by the UBC Research Ethics Board Animal Care Committee (Ethics certificate A13-0063, Genetic control and manipulation of normal and malignant hematopoiesis).

Wenbo Xu and David Lai of the Flow Core Lab in the Terry Fox Laboratory, BC Cancer Agency were an important resource for flow cytometric analysis and sorting. Staff at the BC Cancer Agency Centre for Translational Genomics (Vancouver, BC) prepared histology slides and ran provided samples on the Affymetrix expression array. The Affymetrix data processing and statistical analysis was performed by Dr. Madeleine Lemieux (Bioinfo, Ottawa, ON) and independently by Dr. Lars Palmqvist (University of Gothenburg, Germany), although only Dr. M. Lemieux's are reported here. Mature megakaryocyte RNA was provided by Dr. Susie K. Nilsson (CSIRO, Australia).

Patty Rosten (Terry Fox Laboratory) provided expertise and manpower in the design and execution of the various molecular methods including Southern blot, PCR, Q-PCR and Q-RT-PCR. Fellow lab members Courteney Lai, Donald Lai and Harry Chang provided occasional assistance with mouse work (bleeds, irradiation). Donald Lai additionally performed the CFC-replating experiments under my supervision as a Research Student. All Humphries lab members must be acknowledged for their contribution of ongoing discussion and generosity.

Table of contents

List of tables

List of figures

List of abbreviations

Abbreviation	Name
4-OHT	4-hydroxy-tamoxifen
AML	Acute myeloid leukemia
APC	Allophycocyanin
BFU-E	Burst forming unit - erythroid
BM	Bone marrow
BrdU	Bromodeoxyuridine
CFC	Colony forming cell
CFU-GEMM	Colony forming unit - granulocyte/erythrocyte/monocyte/megakaryocyte
CFU-GM	Colony forming unit - granulocyte/monocyte
CFU-Mk	Colony forming unit - megakaryocyte
CLP	Common lymphoid progenitor
CML	Chronic myeloid leukemia
CMP	Common myeloid progenitor
CRU	Competitive repopulating unit
CTD	C-terminal domain
Cy	Cyanine
DAPI	4',6-diamidino-2-phenylindole
DMEM	Dulbecco's Modified Eagle's Medium
DNA	deoxy-nucleic acid
dpc	Days post coitus
EDTA	Ethylenediaminetetraacetic acid
EtOH	Ethanol
FACS	Fluorescence activated cell sorting
FBS	Fetal bovine serum
FITC	Fluroescein isothiocyanate
FSC	Forward scatter
GFP	Green fluorescent protein
GMP	Granulocytic-monocytic progenitor
HEPES	4-(2-hydroxyethyl)-1-piperazineethanesulfonic acid
HM	Homothorax-Meis
HRP	Horseradish peroxidase
HSC	Hematopoietic stem cell
IL	Interleukin
IP	intraperitoneal
IV	intravenous
LSC	Leukemic stem cell
LTC-IC	Long-term culture initiating cell

LTRC	Long-term repopulating cell
MEP	Megakaryocytic-erythrocytic progenitor
MES	2-(N-morpholino)ethanesulfonic acid
mRNA	messenger ribonucleic acid
NAC	N-acetyl-L-cysteine
PA	Phoenix Ampho
PB	Peripheral blood
PBS	Phosphate buffered saline
PCR	Polymerase chain reaction
PE	Phycoerythrin
PerCP	Peridinin chlorophyll
PHZ	phenylhydrazine
PI	Propidium iodide
PolyI:C	polyinosinic:polycytidylic acid
PURO	Puromycin
Q-PCR	Quantitative PCR
Q-RT-PCR	Quantitative-RT-PCR
RNA	ribonucleic acid
ROS	Reactive oxygen species
RT-PCR	Reverse transcriptase PCR
SA	Streptavidin
SCF	Stem cell factor
SQ	Subcutaneous
SSC	Side scatter
TBS	Tris-buffered saline
TBS-T	TBS-Tween
Tris	Tris(hydroxymethyl)aminomethane
YFP	Yellow fluorescent protein

Acknowledgements

Thank-you so much to my committee members Dr. Gerald Krystal, Dr. Peter Lansdorp and Dr. Fabio Rossi for their contributions to this work in the form of critical appraisal and discussion. Their patience and understanding is also greatly appreciated. Humphries Lab and Terry Fox Laboratory members past and present are to be acknowledged for their unhesitating willingness to provide expertise, resources and discussion. A heartfelt thank-you to Dr. Keith Humphries for his ongoing guidance, support and outstanding example of a researcher dedicated to the pursuit of scientific advancement, irrespective of personal gain.

Dedication

To my Mother for teaching me what was possible. To Patty for making the journey fun. And to Nick for his unwavering support.

Chapter 1 : Introduction

Thesis Overview: *Meis1* as a key regulator in both normal and leukemic hematopoiesis

Self-renewal, that is the ability to generate a cell with equivalent potential upon division, is a characteristic shared by a specific subset of cells across a number of tissue types and species (reviewed in Orford & Scadden, 2008). This potential defines the tissue stem cell and makes it possible to maintain a tissue for the lifetime of the organism, especially in tissues with high cell turnover, such as the gut and blood. Of these tissue stem cell systems, the hematopoietic system is perhaps the best studied. Indeed, studies focused on the hematopoietic system over the last 50 years (reviewed in Spangrude *et al.*, 1991; Akala & Clarke, 2006; Orkin & Zon, 2008) have led to significant insights and experimental approaches relevant not only to hematopoiesis but to a wide range of stem cell based systems.

Through the study of the hematopoietic system, certain stem cell characteristics have been established. For one, progeny of the stem cell must have the ability to give rise to the differentiated, functional cell types comprising the tissue. Another essential property of HSCs is their ability to undergo self-renewal divisions in which one or both progeny cells retain essentially all of the self-renewal and differentiation functions of the parent cell. We thus now appreciate that the hematopoietic stem cell (HSC) sits at the apex of a hierarchy from which progenitors with increasingly restricted differentiation and self-renewal potential arise (Figure 1.1; modified from Orkin & Zon, 2008). Given the central role of HSC in initiating and sustaining lifelong hematopoiesis, a major and ongoing research challenge is to identify and understand the key regulators underlying the origin and function of normal HSC.

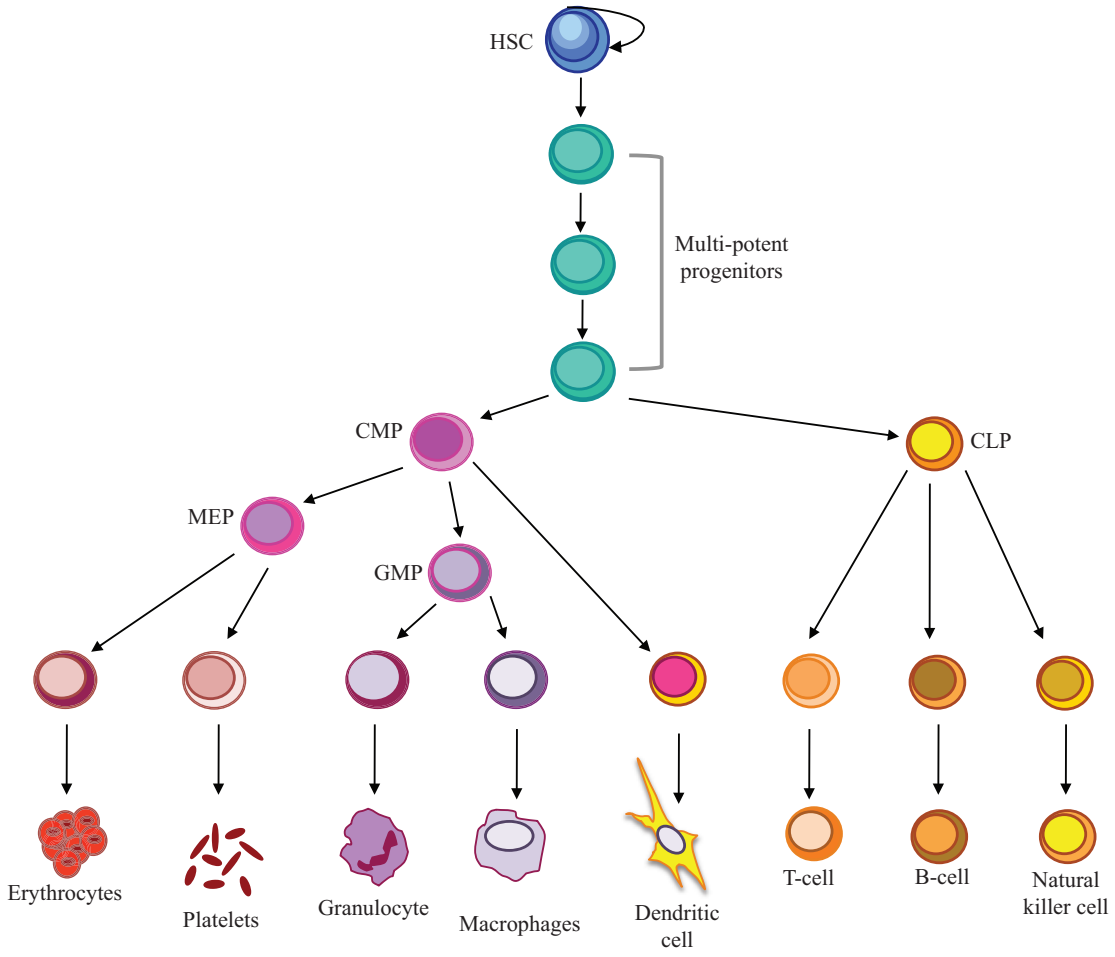

Figure 1.1: Simplified schematic representation of the hematopoietic hierarchy. The hematopoietic stem cell (HSC) sits at the apex at the hierarchy. Through the process of self-renewal, the HSC pool is maintained. To maintain homeostasis, however, the HSC undergoes commitment to multi-potent progenitors with variable long-term reconstitution capacity and narrowing lineage commitment. Lineage committed progenitors undergo successive transient amplification and differentiation to fully differentiated and function cell types.

In a similar fashion, there is a growing understanding of the processes by which key regulatory mechanisms can be eroded and ultimately lead to the emergence of transformed hematopoietic cells and resultant hematologic malignancies. For several such malignancies, including acute and chronic myeloid leukemia, a striking feature now recognized is that the leukemic population is also hierarchical in nature with self-renewing

leukemic stem cells (LSCs) at the apex (Bonnet & Dick, 1997; reviewed in Jordan, 2004; Buzzeo, Scott & Cogle, 2007; Dick, 2008). This "stem cell model" of leukemia again draws critical attention to questions about the origin and properties of LSCs and the key underlying regulators (reviewed Gilliland *et al.*, 2004; Jordan & Guzman, 2004; Misaghian *et al.*, 2008).

This parallel between normal and malignant hematopoiesis has been reinforced by the elucidation of many shared regulators. Notable among the common regulators now identified are a number of transcription factors that on the one hand can be essential for the early development or maintenance of normal HSCs (e.g. Runx1 and Tel/Etv6 respectively) but on the other hand, can acquire leukemogenic potential by a variety of mechanisms including deregulated expression or being part of translocations with creation of fusion genes (eg. AML-ETO and ETV6-FLT3) (Mulloy *et al.*, 2002; Vu, *et al.*, 2006).

In the thesis work described here, I have focused on a transcription factor *Meis1*, as one such candidate regulator implicated in both normal and leukemic hematopoiesis. These studies have in large part been based on a novel conditional knockout mouse model for *Meis1* that I have validated for use *in vitro* and *in vivo.* The results of this work highlight a critical requirement of *Meis1* in the maintenance of adult HSC potential, cell fate determination and expansion of differentiated erythroid and megakaryocytic progenitors. Use of this model combined with RNA expression analyses has also provided an opportunity for further identification of potential effectors of MEIS1 function. This model now provides a framework for future examination and comparative analyses of *Meis1*'s role in both normal and leukemia hematopoiesis.

The following sections provide further background on the stem cell models as they relate to normal and leukemic hematopoiesis, an overview of some of the key known

regulators of primitive normal and leukemic cells, and finally a more extensive review of emerging evidence of the central role of members of the Hox family of transcription factors and their co-factors, most notably, *Meis1* in these processes.

Normal and leukemic hematopoiesis as stem cell driven hierarchies

The HSC exists in a bone marrow niche, a relatively protected environment whereby cues from the surrounding environment maintain a state of relative proliferative quiescence and reduced metabolic activity (reviewed Zon, 2008; Haylock & Nilsson, 2006). Cues from the environment promote HSC division at which point it can give rise to progeny that will undergo further rounds of replication and division to generate terminally differentiated, but functional, cell types with limited replicative potential including T-cells, B-cells, granulocytes, natural killer, megakaryocytes and erythroid cells. Incompletely differentiated progenitors exist at various branch points in the hierarchy that can amplify in numbers but only give rise to a limited number of cell types. For example, once committed to the megakaryocyte-erythroid lineage, the progenitor appears to preclude alternative fates (Akashi *et al.*, 2000). This progressive restriction of potential but gain of physiological and immunological function coincides with loss of self-renewal potential.

These characteristics have been elegantly shown in mouse experimental models whereby populations at various stages of the hierarchy are isolated by virtue of cell surface markers and transplanted into irradiated recipients (Figure 1.2). The blood system is widely accessible and advances in multi-colour fluorescence activated cell sorting (FACS) technology, along with the identification and validation of markers has made it possible to isolate enriched populations of cells with defined potential (reviewed in Fulwyler, 1980) and

to track their output in the peripheral blood and bone marrow of immune-compromised recipient mice (Szilvassy *et al.*, 1990). *In vitro* assays have also been developed to measure the potential of multi-potent progenitors; however, the *in vivo* transplantation models remain the gold standard for qualitative and quantitative measurement of HSC function (reviewed in Purton & Scadden, 2007). The ability to purify these cell populations and measure their function has paved the way for genetic studies that have allowed study into what cellular processes underpin hematopoietic cell function and potential.

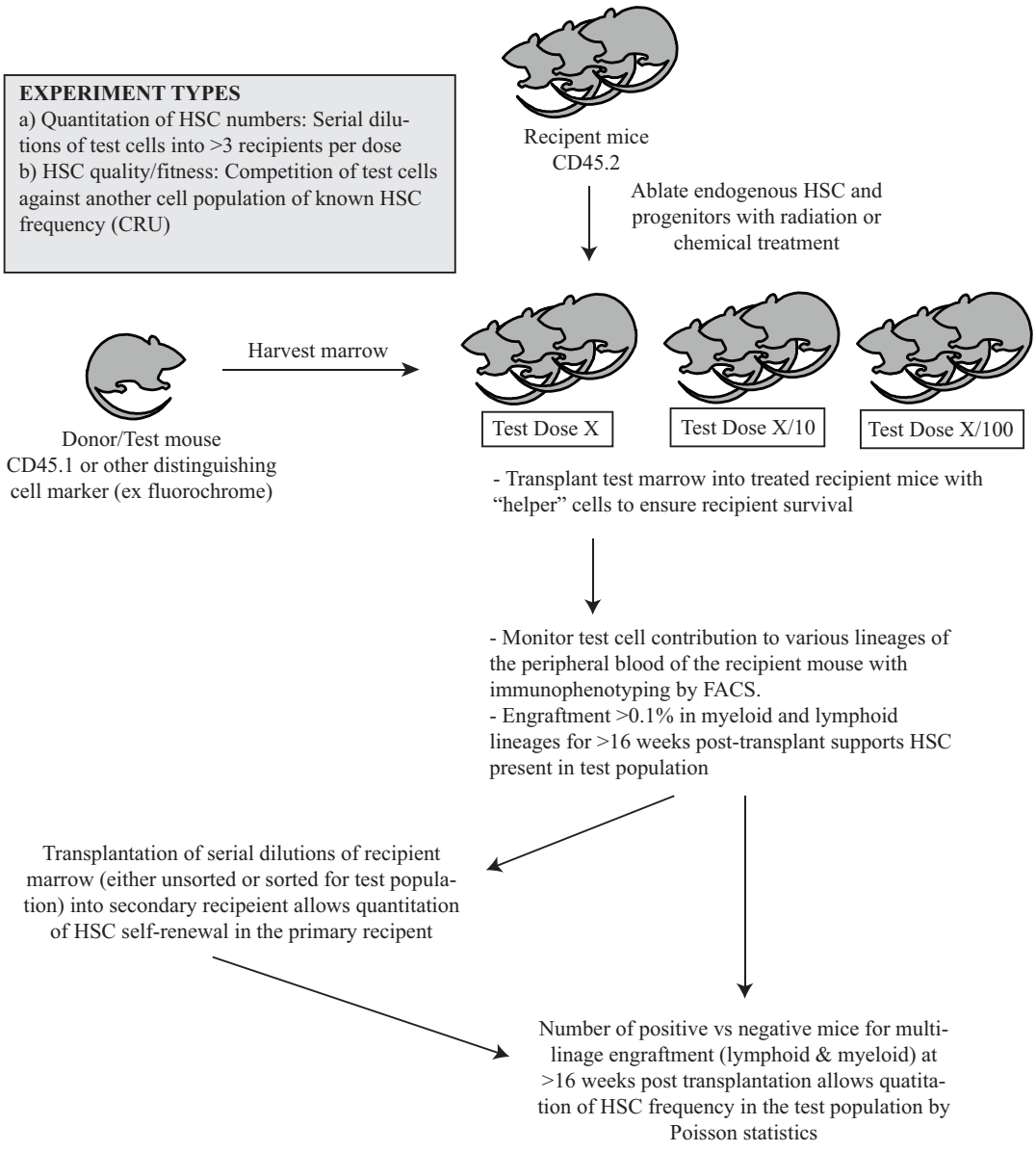

Figure 1.2: Schematic representation of quantitative and qualitative long-term repopulation assays

Deregulation of self-renewal and differentiation leads to the generation of leukemia

These same techniques have also paved the way to enhancing our understanding of mechanisms underlying leukemogenesis, that is the process by which key regulatory

mechanisms are eroded and a cell population acquires malignant potential. The paths to malignancy are many, such that there is considerable heterogeneity between patients in terms of the molecular underpinnings be it fusion genes, deregulated gene expression, acquired mutations and various combinations of these. In brief, these aberrations result in enhanced proliferation, a loss of differentiation and deregulated apoptosis such that non-functional leukemic cells overwhelm the hematopoietic system.

A growing body of evidence has revealed that leukemias can mimic the normal hematopoietic system in several aspects. Notably, the leukemic population is also heterogeneous within a given individual in terms of phenotype and potential. Some of the first demonstrations of this were colony forming assays undertaken in the 70's and 80's where it was shown that only a small set both human and mouse tumor cells had the ability to read out as colonies in *in vivo* and *in vitro* assays (reviewed in Huntly & Gilliland, 2005). Using FACS analysis, researchers have been able to enrich for cells that, while not forming the bulk of the leukemic population, have the capacity to form transplantable leukemias *in vivo.* These cells have been coined leukemic initiating cells (LIC) based on their ability to recapitulate the leukemia when transplanted into mice (reviewed in Hope, Jin & Dick, 2003; Passegué *et al.*, 2003, Warner *et al.*, 2004; Becker & Jordan, 2011). Serial transplantation studies provide further evidence that LICs can undergo self-renewal and thus satisfy key criteria to be termed Leukemic Stem Cells (LSC). Indeed in many situations, the terms LIC and LSC have become to be used interchangeably. In this thesis the term LSC is primarily used as a way to discuss the concept of a cell at the top of a hierarchically structured leukemia and LIC is used in an operational sense when LSC are being detected by functional readouts. Importantly, a stem cell model of leukemia does not imply the origin of the LSC

but leaves open the possibility that it arises from a preexisting HSC or from later progenitors that reacquire crucial stem cell functions such as self-renewal.

Genetic programs underpin self-renewal and differentiation in normal and leukemic hematopoiesis.

Genetic studies have shown that a large number of interconnected networks underlying different mechanisms are in play for proper function, maintenance and differentiation within the hematopoietic hierarchy. Aberrations in these networks are not well tolerated and invariably result in cell death or favor the selection of further alterations that can lead to the evolution of grossly distorted cell function that can culminate in malignancy. These mechanisms include regulation of self-renewal potential (reviewed in Reya, 2003; Zon, 2008), cell-cycle (reviewed in Matsumoto & Nakayama, 2012), epigenetic modification (reviewed in Sashida & Iwama, 2012), cell signaling (reviewed in Rizo *et al.*, 2006), cell survival and differentiation. Transcription factors are centrally poised to influence these mechanisms by virtue of regulation of gene expression. One such family, HOX genes and their co-factors, have been established as key components of HSC function during ontogeny and in the pathogenesis of leukemia.

Hox genes are critical for embryonic patterning

Hox genes were first characterized in the fruit fly *Drosophila melanogaster* in mutagenesis screens. Two mutations were identified, *antennapedia* and *bithorax,* that caused significant alterations to the normal body segmentation of the fly. The genes underlying this phenomemon were termed homeobox genes and were found in two clusters: the *bithorax* complex (*BX-C: Ubx, Abd-A, Abd-B*) and the *antennapedia* complex (*Ant-C: Lab*, *Pb*, *Dfd,*

Scr, Antp). Homologs have been found in most species, including fish, fungi and plants, indicating an ancient origin with evolutionary significance. Gene and cluster duplication over the years have left vertebrate mammals with 4 clusters of Hox genes (A through D) that are scattered through the genome. Each cluster consists of 9 to 11 members of 13 paralog groups that are assigned on the basis of sequence similarity and location to the *Drosophila Ant-C* cluster and *Abdominal-B (Abd-B)* gene of the *bithorax* cluster. Thus paralog groups 1 through 8 are *Ant*-C-like, and paralogs 9 through 13 are *Abd-B*-like. During development, Hox genes are expressed in temporal and positional colinearity, that is, 3' genes are expressed more anteriorly and earlier than those at 5' positions. Their expression patterns define domains along the anterior-posterior axis of the embryo and specify the development of structures within these domains (Reviewed in Grier *et al.*, 2005).

Hox genes have low DNA binding affinity and specificity in isolation and thus require co-factors for function

Interestingly, despite the number of Hox genes and their critical role in development, each Hox gene has remarkably low DNA binding specificity and affinity and indeed, functional specificity cannot be achieved on the basis of DNA binding alone (reviewed in Rauskolb & Wieschaus, 1994). One candidate co-factor, *extradenticle* (*exd)* was identified in *Drosophila* that, when mutated, caused similar homeotic transformation of body segments to loss of the *bithorax* or *antenepedia* clusters. A mutation in *exd*, however, did not result in changes in expression of the homeotic genes themselves, nor was expression of *exd* regulated by these genes, suggesting action in parallel (Peifer & Wieschaus, 1990).

Exd was found to be homologous to *PBX1*, a human proto-oncoprotein found in one-quarter of pediatric pre-B-cell acute lymphoblastc leukemias as a fusion with *E2A* in t(1;19) translocation (Rasukolb, Peifer & Wieschaus, 1993). *In vitro* experiments revealed that Pbx1

could enhance the DNA binding specificity and affinity of numerous 3' *Ant-C*-like Hox genes (HoxB4, B6 and B7) but not *Abd-B*-like HoxA10 (Chang *et al.*, 1995). Discovery of a novel homeodomain-containing protein, *Meis1*, in a mouse model of leukemia would provide further insight into the complexity of interactions required for execution of HOX programs.

The discovery of **Meis1** *is entrenched in the leukemic process*

Myeloid ecotropic virus insertion site 1 (Meis1) was first described in 1995 as a common viral integration site in the BXH-2 model of myeloid leukemogenesis (Moskow *et al*., 1995). BXH-2 mice develop granulocytic leukemia by 1 year of age due to activation of cellular proto-oncogenes and/or inactivation of tumor suppressor genes by retroviral insertion of two endogenous ecotropic proviruses, *Emv1* and *Emv2*. As the insertion is relatively random, a number of genes will be disrupted during the process, many of which do not contribute to the pathogenesis of the malignancy. Disruption of a gene in multiple independently arising tumors, however, is strongly suggestive of a causative role in the generation of leukemia in these mice. In this model, disruption of *Meis1* was found in 15% of tumors, in contrast to the known oncogene *c-myb* locus that was only disrupted in 3% of tumors. Viral integrations at the *Meis1* locus did not disrupt exon coding sequences and were localized into two clusters at the 5' and 3' regions of the locus. Northern blotting analysis of these tumors and subsequent studies (described below) demonstrated increased expression of *Meis1* in these leukemias, supporting a role for *Meis1* as an oncogene in this context.

In this seminal work on Meis1, Moskow *et al*. additionally localized the mouse *Meis1* locus to chromosome 11 (11.11 cM, NC_000077.6: 18880428..19018969, complement) and identified the cDNA transcript from adult mouse lung and spleen libraries. The *Meis1* transcript contains 12 exons and encodes a protein of 390 amino acids. Two isoforms of the

transcript were postulated to exist based on alternative splicing within exon 10. In comparison to the prototypic *Meis1a* transcript, *Meis1b* has a novel 93-amino acid C-terminal region. Two isoforms of *Meis1* are currently validated in the mouse and humans (Figure 1.3a). *Meis1a* is considered the canonical sequence in mouse and has 99.7% amino acid identity to the canonical MEIS1 protein in humans, differing by only 1 amino acid. The protein is characterized by a 63 amino acid DNA binding TALE-type homeodomain (Figure 1.3b domains). MEIS1 protein is highly conserved between species, with identity at 356 of the 390 amino acids between *Mus musculus*, *Homo sapiens*, *Xenopus laevis*, *Rattus norvegicus, Bos taurus, Danio rerio* and *Pan troglodytes* (Uniprot alignment, August 2013).

a)

```
241  GDNSSEQGDGLDNSVASPSTGDDDDPDKDKKRHKKRGIFPKVATNIMRAWLFQHLTHPYP  300  MEIS1A
241  GDNSSEQGDGLDNSVASPSTGDDDDPDKDKKRHKKRGIFPKVATNIMRAWLFQHLTHPYP  300  MEIS1B
     ************************************************************
301  SEEQKKQLAQDTGLTILQVNNWFINARRRIVQPMIDQSNRAVSQGTPYNPDGQPMGGFVM  360  MEIS1A
301  SEEQKKQLAQDTGLTILQVNNWFINARRRIVQPMIDQSNRAVSQGTPYNPDGQPMGGFVM  360  MEIS1B
     ************  *  *  :.  *           *
361  DGQQHMGIRAPGPMSGMGMNMGMEGQW-------HYM-----------------------  390  MEIS1A
361  DGQQHMGIRAPGLQSMPGEYVARGGPMGVSMGQPSYTQAQMPPHPAQLRHGPPMHTYIPG  420  MEIS1B

391  ---------------------------------------------  390  MEIS1A
421  HPHHPAVMMHGGQPHPGMPMSASSPSVLNTGDPTMSAQVMDIHAQ  465  MEIS1B!
```

b)

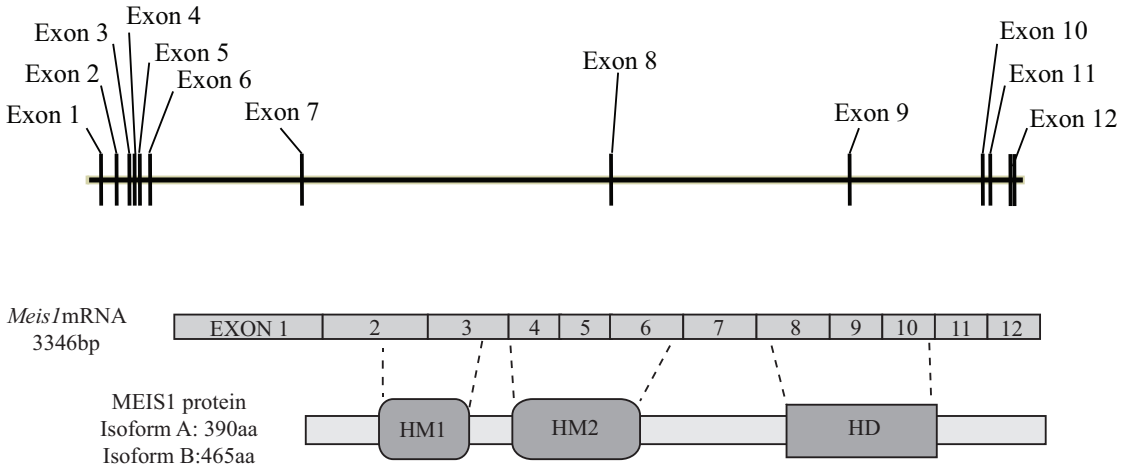

Figure 1.3: *Meis1* Exon structure, mRNA and MEIS1 protein.
a) Comparison of the C-terminal of MEIS1A and MEIS1B. The proteins are identical until the splice site in exon 10. The homeodomain (HD) is underlined. The designation of isoform A or B is consistent with the historical literature and UniProt database as of August 2013. b) Relative exon positions within the genomic sequence. Schematic representation of *Meis1* mRNA and relative exon contributions to MEIS1 protein domains. The Homothorax-Meis (HM) domain is highly conserved within the MESI/PREP family of proteins and is considered to be composed of two subdomains (HM1 and HM2), the sequence intervening the region and 8 amino acids C-terminal to the HM2 subdomain. The subdomains are also referred to in literature as HM^A(HM1) and HM^B(HM2). The HM domain is required for interaction with PBX-family members (Ryoo *et al.*, 1999).

Meis1 ***confers Hox binding specificity and affinity in conjunction with other Hox co-factors***

At the time of the Moskow *et al.* study, the only region of similarity of MEIS1 to known proteins was that for the homeodomain of human proteins *PBX1, PBX2, PBX3* and *Drosophila* extradenticle (*exd)* and Knotted (*Kn1).* This homology would prove to be a key guide to understanding the role of MEIS1 in the context of leukemia and normal hematopoietic function. *Hth* was identified as the *Drosophila* homolog of murine *Meis1* based on sequence similarity (88% identity in the C-terminal region including 93% identity in the homeodomain, Pai *et al.*, 1998) and was shown to be essential for Hox patterning of *Drosophila* (Rieckhof *et al.*, 1997).

MEIS, PBX and their homologs are classified based on homology as TALE-type homeoproteins. TALE-type homeodomains are distinguished by the presence of three extra amino acids between the first and second alpha helices of the homeodomain as compared to the homeobox (Hox) family of proteins that defined the domain. The TALE family of genes in the mouse now includes the MEINOX family, which includes *Meis1, Meis2*, *Meis3*, *Pknox1* and *Pknox2*, and the PBC family consisting of *Pbx1*, *Pbx2*, *Pbx3* and *Pbx4* (reviewed in Moens & Selleri, 2006). Both PBC and MEINOX families were found to serve as *HOX* co-factors and to enhance DNA-binding specificity and affinity via MEIS1 or PBX-HOX duplexes or MEIS-PBX-HOX trimeric complexes (Shen *et al.*, 1997; Shen *et al*, 1999; Shanmugam *et al*., 1999).

In contrast to PBX proteins that were found to bind *Ant-C* like HOX proteins (HOX 1 through 8), MEIS1 is complementary to PBX such that MEIS1 directly binds the *Abd-B*-like proteins of paralogs 9-13 (Shen *et al.*, 1997). Through *in vitro* binding assays, a model was developed whereby HOX proteins from paralogs 1-8 preferentially form heterodimers with

PBX proteins, whereas HOX paralogs 9-13 form heterodimers with MEIS1. This preferential binding is highly influenced by the presence of DNA in the assay as yeast-two hybrid interaction assays have demonstrated interaction between MEIS1 and *Ant*-C-like paralogs 2, 4, 5 and 8 (Williams *et al.,* 2005). Additional binding of the alternate co-factor to both PBX-HOX and MEIS-HOX complexes confers additional binding affinity but does not alter target specificity (Shanmugam *et al.,* 1999).

These studies and additional mutagenesis studies established that HOX-PBX dimer bind to a 5'-ATGATTNATNN-3' consensus motif (Lu *et al.*, 1995, Chang *et al.*, 1996) that requires a core YPWMK N-terminal to the HOX homeodomain (Phelan *et al.*, 1995) to interact with the 3 amino acid loop extension of the PBX homeodomain (Piper *et al.*, 1999). The N-terminal PBC-A domain of PBX1 is required for interaction with MEIS1 through the HM1 and HM2 domains at the N-terminal of MEIS1 proteins (Ryoo *et al.*, 1999, Wang *et al.*, 2005, Mamo *et al.,* 2006). The C-terminal of MEIS1 (18 amino acids MEIS1a, 93 amino acids MEIS1b) is required for interaction with various domains in the N-terminus of HOX proteins, however, this was not tested in the context of DNA binding (Williams *et al.*, 2005) and the exact domains mediating MEIS-HOX interaction remain unclear. While the HOX core binding sequence remains unchanged, the MEIS binding consensus sequence is 5'-TGACAG-3'.

In addition to influencing Hox binding, Hox co-factors influence the cellular localization of other co-factors

Interaction between PBX and MEIS proteins may be important for more than just DNA binding. In several models, the presence or absence of one co-factor influences the localization of the other. For example, in a *Drosophila* study exploring the factors influencing HOX function, the expression of *hth* in cells was found to strongly correlate with

nuclear localization of EXD (Rieckhof *et al.*, 1997). Enforced expression of either *Meis1* or *hth* was found to trigger nuclear localization of EXD, even when the DNA-binding homeodomain was altered. Additional studies in *Drosophila* and mouse suggest that in the absence of HTH/MEIS1, EXD/PBX is exported from the nucleus by a nuclear export signal and masking of N-terminal nuclear localization sequences (Berthelsen *et al.,* 1999; Abu-Shaar *et al.,* 1999; Jaw *et al.* 2000; Saleh *et al.* 2000). Interestingly, in *Xenopus*, Xpbx1b localizes to the nucleus in the absence in the absence of ectopic Xmeis1b, and indeed Xmeis1b is cytoplasmic in the absence of Xpbx1b (Maeda *et al.*, 2002).

In addition to organism specificity, the requirement for localization may be context specific, as in mouse fibroblasts overexpression of PBX1 results in nuclear localization in the absence of MEIS1 or other family members. In the developing *Drosophila*, although EXD is nuclear in all cells where *hth* is expressesd, *hth* is not expressed in all cells where EXD is nuclear (Rieckhof *et al.*, 1997). Other molecules have been identified in the fly (Wingless and Decapentaplegic) that induce EXD nuclear translocation in endoderm of the midgut (Mann and Abu-Shaar, 1996).

The combinatorial interactions between HOX, PBX and MEIS suggest numerous possibilities for regulation of gene expression

HOX-PBX-MEIS signaling is likely to be very complex and not governed by a few simple principles as the diversity of partnerships between the 47 players is immense (38 *Hox*, 3 *Meis*, 2 *Pknox* and 4 *Pbx* genes), even without accounting for the contribution of the various splice isoforms of these genes. Much of this regulation is likely accomplished by tissue specific expression of various combinations of HOX, PBX and MEIS family genes. In the hematopoietic system, *Pbx1, Pbx2, Meis1* and an assortment of *Hox* are preferentially expressed in fetal liver and adult bone marrow populations enriched for hematopoietic stem

cells with long-term repopulation capacity (Sauveageau *et al.* 1994; Pineault *et al.*, 2002). Expression of *Meis1* is highest in the HSC-enriched bone marrow compartment and progressively down-regulated in progenitors, with the exception of increased expression in megakaryocytic progenitors (Pineault *et al.*, 2002; Hu *et al.,* 2009; Okada *et al.*, 2003), suggesting a role in regulation in these progenitor cells.

Regardless of tissue limited expression, however, the functional reach of *Meis1* is likely substantial as either directly or indirectly it can interact with Hox and additional non-Hox co-factors. Given the roles in normal and aberrant hematopoiesis described below, it may thus constitute a critical regulatory node in these processes.

Knock-out & overexpression studies of Meis, Pbx and Hox reveal critical roles in normal and leukemic hematopoiesis.

Manipulation of gene expression in the embryo and adult organism are powerful tools with which to study gene function. Gene deletion in the zygote allows for investigation of whether genes are essential for embryogenesis, and if so, at what stage. If a gene is embryonic lethal, conditional deletion during development or in the adult allows powerful studies into pathways regulated by the gene. Use of these models has yielded insights into key processes regulated by *Hox, Meis* and *Pbx* in both normal and leukemic hematopoiesis.

Pbx, Meis and Hox knock-outs in normal hematopoiesis

Despite the apparent interconnectedness and requirement for HOX-PBX-MEIS complexes at a variety of targets, knockout phenotypes are quite unique to each of the Hox co-factors. *Pbx1* or *Meis1* are expressed in sites of hematopoietic development in the embryo, that is, the 11.5dpc aorta-goanad-mesonephros (AGM) and 14.5dpc fetal liver (FL) (DiMartino *et al.*, 2001; Hisa *et al.*, 2004; Azcoitia *et al.* 2005). Constitutive knock-out of

Pbx1, *Meis1* or conditional mis-localization of MEIS1 in the developing embryo result in a decline in hematopoietic colony forming cells (CFC) and poor reconstitution in competitive transplant experiments. Although both knockouts are embryonic lethal, the physiological mechanisms underpinning this process appear to be different in important ways. *Pbx1*$^{-/-}$ embryos are anemic, edematous and show skewing of progenitor differentiation at the expense of erythroid progenitors. *Meis1*$^{-/-}$ embryos, in contrast, show massive hemorrhaging from a lack of megakaryopoiesis and vascular patterning anomalies.

Most *Hox* genes of the A, B, C and D clusters are expressed in hematopoietic cells, with, in general, preferential expression in HSC-enriched populations and down regulation during differentiation (Sauvageau *et al.*, 1994; Lawrence *et al.*, 1997; Kawagoe *et al.*, 1999; Pineault *et al.*, 2002). Due to high homology between Hox genes, and thus likely redundancy, knock-out of individual genes have relatively mild hematopoietic phenotypes (reviewed in Gier *et* al. 2005; Argipopoulos & Humphries, 2007). For example, over-expression of *HoxB4 in vivo* or as an exogenous protein enhances HSC self-renewal and expansion (Sauavgeau *et al.*, 1995; Antonchuck *et al*. 2002; Krosl *et al.*, 2003); however, in contrast to loss of *Meis1* or *Pbx1*, *Hoxb4-/-* mice are viable and born at expected Mendelian frequencies (Brun *et al.*, 2004). Cells have a subtle reduction in repopulating ability and frequency, although this has little impact on steady-state hematopoiesis. Greater impairment in hematopoietic potential is seen in compound *Hoxb3* and *Hoxb4* mutant mice, although differences again are not dramatic in the steady-state (Björnsson *et al.*, 2003). Similarly, *Hoxa9-/-* bone marrow has an 8-fold reduction in repopulating activity and 30-40% reduced numbers of total leukocytes and lymphocytes, although normal red blood cell, hematocrit and platelet counts (Lawrence *et al.*, 1997; Lawrence *et al.*, 2005).

Hox and Meis overexpression are potent contributors to leukemogenesis

The role of *Pbx* for *Hox* gene specification during embryogenesis had been previously well established as had an independent role for *PBX* in the generation of acute lymphoid leukemia as partner in the translocation arising in the fusion gene *E2A-PBX1* (Kamps *et al.,* 1990; Chang *et al.*, 1995). From the outset of its cloning from BHX-2 mice, *Meis1* had been described as *Pbx*-like, however, a similar role in leukemogenesis to *Pbx* had yet to be described. In a study published shortly after their initial publication identifying *Meis1* (Moskow *et al.* 1995), the group headed by Drs Jenkins and Copeland highlighted the strong link between *Meis1* and *Hox* in the generation of myeloid leukemias that would prove to be the foundation of a growing body of work investigating this phenomenon. Cloning of retroviral insertion sites in CpG islands of BHX-2 mice was undertaken in an effort to identify insertions likely to influence gene expression (Nakamura *et al.*, 1996). 4 insertion sites were identified using this method, 2 of which clustered to *Hoxa7* and *Hoxa9* and were found to enhance gene expression. Although one common insertion site remained unidentified, the other was found to correspond to *Meis1.* Strikingly, although 9.6% of the tumors screened had retroviral insertions in *Meis1* that enhanced gene expression, 95% of these also had insertions in either *Hoxa9* or *Hoxa7.* The preference for Hox/Meis co-expression in the development of these leukemias was further enforced by the finding that of 21 leukemias with *Hox* dysregulation, only 3 lacked *Meis1* insertion.

Meis1 ***is commonly overexpressed in patient AML samples***

Many mouse and human studies have followed that point to a role for deregulated/overexpression of *Meis1* and *Hox* in the generation of leukemias. In examining expression of *MEIS1* in leukemia, interesting patterns have emerged. *MEIS1* was found to be expressed in a selection of patient bone marrow samples from all recognized FAB AML

subtypes with the exception of the promyelocytic (M3) subtype (Kawagoe *et al.*, 1999; Lawrence *et al.,* 1999; Afonja *et al*., 2000; Drabkin *et al.,* 2002; Roche *et al.,* 2004; Camós *et al.,* 2006; Grubach *et al.*, 2008; Zangenberg *et al.,* 2009). In AML samples where *MEIS1* expression is present, there also exist high levels of *HOX*-family member expression (*HOXA4, HOXA7, HOXA9, HOXA10*). It is worthwhile to note that although *HOX* genes are not expressed in the FAB-M3 AML subtype (Lawrence *et al.,* 1999), there are also leukemias in which high *HOX*-family member expression is not accompanied by a concurrent increase in *MEIS1* expression (Drabkin *et al.*, 2002, Afonja, *et al.,* 2000).

Levels of *MEIS1* expression may have a prognostic significance. In normal karyotype AML, low *HOXA4* expression levels is associated with shorter overall survival (Grubach *et al.* 2008). When these samples are subdivided on the basis of *MEIS1* expression, patients with high levels of *MEIS1* expression had significantly worse outcomes than those with low *MEIS1* expression (Zangenberg *et al.*, 2009). This study, however, did not take into account expression levels of other *HOX*-family members in the samples. Other studies looking at broader sets of *HOX* and *MEIS* expression have found associations between high levels of *HOX* expression in AML with intermediate risk cytogenetics (normal karyotype and translocations not falling into the high or low risk categories). Within these samples, high levels of *HOX* expression were associated with high levels of *FLT3* (receptor for growth factor FLT3L) expression, with the highest correlation between *HOXA7* and *MEIS1* expression (Roche *et al.,* 2004). In cell lines derived from un-selected AML patient samples, most co-express *MEIS1*, *HOXA7* and *HOXA9* (Afonja *et al.,* 2000, Lawrence *et al.*, 1999).

Meis1 ***overexpression in patient samples is often found in conjunction with dysregulated Hox gene expression***

This level of association between *HOX* and *MEIS1* expression is unlikely to be random and indeed enforced co-expression of *HOX* and *MEIS1* by retroviral overexpression in mouse models of leukemia supports a causative role in leukemogenesis. Nucleophosmin (NPM) mutated AML with high levels of cytoplasmic NPM accumulation ($NPMc^+$) are also associated with high levels of *Hox* and *Meis1* expression (Alcalay *et al.*, 2005). Knock-down of *Meis1* by shRNA impairs expansion of primary $NPMc^+$ AML cells *in vitro* and triggers increased levels of apoptosis compared to NPMwt AML (Woolthuis *et al.*, 2012).

Examination of *MLL*-rearranged leukemias in both human samples and mouse models provides some of the most compelling evidence for the involvement of *MEIS1* in leukemogenesis. *MLL* is a transcriptional activator that plays an essential role in regulating *HOX* and other gene expression during embryogenesis through histone H3 lysine-4 methyltransferase activity. Rearrangements of *MLL* at 11q23 are frequent anomalies in both adult and pediatric acute leukemias whereby N-terminal of *MLL* is fused to a variety of C-terminal partners in 20% of ALL and 5-6% of AML samples (Somervaille & Cleary, 2010; Tamai & Inokuchi, 2010). All samples with t(4:11) translocations express high levels of *MEIS1* (Rozovskaia *et al.*, 2001; Kohlmann *et al.*, 2005; Trentin *et al.*, 2009). Common t(4:11) fusion partners *MLL-ENL*, *MLL-AF4* have shown a characteristic expression profile of *HOX* and *MEIS1* over-expression (Rozovskaia *et al.*, 2001; Zeisig *et al.*, 2004). Furthermore, cells susceptible to transformation by the *MLL-AF9* fusion gene express high levels of *MEIS1* and *Meis1* is a component of the expression profile in mouse models of *MLL-AF9* induced transformation (our data, Chen *et al.*, 2008; Kumar *et al.,* 2010). In a study using mouse models by Wong and colleagues, the decreasing time to the onset of

leukemia of various *MLL*-fusions was shown to be linked in a dose dependent manner to the extent in which they triggered up-regulation of *Meis1* (Wong *et al.*, 2007). These leukemias exhibited a more immature phenotype and had higher colony-forming capacity, suggestive of a primitive cell type with extensive replicative potential. In addition, *Meis*$^{-/-}$ fetal liver derived cells could not be transformed with the fusions, supporting that expression of *Meis1* is an essential and rate-limiting set in leukemogenesis in the context of *MLL*-fusions. Other fusion genes characterized by high levels of *MEIS1* expression in the context of AML include *MYST3-CREBBP* (Camós *et al.*, 2006), *NUP98-HOXA9* (Takeda *et al*., 2006) and *NUP98-NSD1* (Wang *et al.*, 2007).

Although initial studies of *MEIS1* expression in acute leukemia suggested *MEIS1* is not expressed in lymphoblastic leukemia (Lawrence *et al.*, 1999), expression in phenotypically lymphoid *MLL*-fusion samples as well as infant and adult ALL samples suggests *MEIS1* also may play a role in these leukemias. Compared to normal cells, ALL cell lines and patient samples express increased levels of *MEIS1* and *MEIS2,* and knock-down of *MEIS1* expression decreases their proliferation (Rozovskaia *et al.*, 2001; Imamura *et al.*, 2002; Ferrando *et al.*, 2003). Strikingly, *MEIS1* and *HOXA9* are co-expressed at high frequency (74%) in infant (under age 5) *MLL*-rearranged and non-*MLL* rearranged leukemias (Imamura *et al.*, 2002). Decrease in proliferation following down-regulation of *MEIS1* may be the mechanism by which some ALL-cell lines manifest resistance to chemotherapeutics (Rosales-Aviña *et al.*, 2011). ShRNA knock-down of *MEIS1* in a B-cell leukemic line expressing *MLL-AF4* resulted in impaired engraftment in mouse transplantation studies, likely due impaired proliferation and chemotaxis to the appropriate niche (Orlovsky *et al.*, 2011).

Mouse models demonstrate overexpression of* Meis1 *and a Hox gene are sufficient for leukemogenesis

Molecular manipulation of genetic sequence and expression in mouse models has proved to be invaluable in furthering our understanding of critical domains underpinning the leukemic process. Building on the initial studies demonstrating frequent retroviral co-activation of *Hoxa9* and *Meis1* in BHX-2 leukemias (Moskow *et al.,* 1995), subsequent studies in mice have greatly expanded the range of *Hox* genes and *Hox*-fusions with which *Meis* cooperates as well as defined domains and contributory genetic pathways in this process. In studies designed to address whether all *HOX* genes have intrinsic leukemogenic properties, either as intact genes or as *NUP98* fusions, *Meis1* was found to reduce the latency to leukemia with all constructs tested (Pineault *et al.*, 2005). Overexpression of *Meis1, 2* or *3,* in isolation, however, does not have an oncogenic effect and fails to immortalize progenitors *in vitro* or cause leukemias when overexpressing cells are transplanted *in vivo* (Kroon *et al.,* 1998; Calvo *et al.*, 2000).

Collaboration between *Hox, Nup98*-Hox and *Meis1* appears to be a universal property as, to date, no reports exist of *Meis1* failing to cause transformation in the presence of *Hox* or *Nup98-Hox* overexpression (summarized in Table 1). *Hox* and *Nup98-Hox* partners tested to date include those found in human and mouse leukemias as well as other family members not overexpressed in leukemias or engineered fusions. *Meis1* clearly contributes to the oncogenic process in these leukemias, as opposed to reinforcing programs established by the *Hox* or *Nup98-Hox* partner. This is most clearly illustrated by studies with the engineered fusion *Nup98-Hoxa10-homeodomain* (NA10HD), where the *Hoxa10* is pared down to the DNA binding homeodomain in the fusion. Overexpression of NA10HD in HSCs results in nearly exclusive self-renewal divisions *in vitro*, resulting in a hugely expanded stem cell pool.

When transplanted *in vivo*, however, the cells respond appropriately to their environment and although engraftment is robust, leukemias do not form (Ohta & Sekulovic *et al*., 2007). Co-expression of *Meis1* with *NA10HD*, however, results in transformation and leukemias *in vivo* (Pineault *et al*., 2004), supporting the idea that *Meis1* triggers a unique program for transformation, independent of the *Hox* partner. Of further interest, NA10HD lacks any known motifs for direct interaction with MEIS1, thus raising questions about the basis for the powerful functional interaction seen with co-overexpression of MEIS1 and NA10HD.

Co-operation between *Meis1* and *Hox* is extremely powerful and is synergistic, providing further support for independent programs regulated by *Hox* and *Meis1*. For example, *Meis1* overexpression fails to generate transplantable leukemia cells and *Hoxa9* overexpression does so at a relatively low frequency (1 in 9, Wang *et al.*, 2005) after a long latency (280 days). The *Hoxa9*-leukemias that do result invariably have accumulated additional mutations that activate *Meis1* expression. When co-expressed, however, the frequency of leukemia-initiating cell is minimally increased 9-fold and the latency to disease is reduced 4-fold to roughly 72 days. The decreased latency and increased frequency in *Hox* plus *Meis1* co-expressing leukemias supports a synergistic effect between the two genes whereby the genetic programs triggered are more powerful than simply an additive effect enhanced expression of a shared program. This synergism is also true in *Hox*-expressing *MLL*-fusion leukemias where enforced *Meis1* expression reduces the latency to disease and increases leukemia-initiating cell frequency (Wong *et al.*, 2007).

Table 1.1: Models of *Meis1*-overexpression studied to date

Mutations/Overexpression Found in Patient Samples	Gene	Reference
	HoxA9	Kroon *et al.*, 1998; Wang *et al*, 2005
	HoxA7	Wang *et al*, 2004
	HoxA10	Pineault *et al.*, 2004
	HoxB3	Sauvageau *et al.,* 1997
	Nup98-HoxD13	Pineault *et al.*, 2003
	Nup98-HoxA9	Kroon *et al.*, 2001; Iwasaki *et al.*, 2005
	Nup98-HoxA10	Pineault *et al.*, 2004
	Nup98-PMX1	Hirose *et al.*, 2008
	MLL-GAS7	Wong *et al.*, 2007
	MLL-AF10	Wong *et al.*, 2007
	MLL-LAF4	Wong *et al.*, 2007
	MLL-ENL	Ferrando *et al.*, 2003
	MLL-AF5q31	Imamura *et al.*, 2002
	NPMc+	Woolthuis *et al.,* 2012
	MN1	Heuser *et al.*, 2011
Artificial/Engineered Mutations/Overexpression	HoxB4	Pineault *et al.*, 2004
	HoxB6	Fischbach *et al.*, 2005
	Nup98-HoxA10-homeodomain	Pineault *et al.*, 2004
	Nup98-HoxD13-homeodomain	Pineault *et al.*, 2004
	Nup98-HoxB3	Pineault *et al.*, 2004
	Nup98-HoxB4	Pineault *et al.*, 2004

Meis1 ***and Hox gene expression may constitute a core expression program that accommodates transformation***

For many leukemias, if not all, there is evidence to suggest that *Meis1* and some *Hox* expression are required for a cell to be susceptible to transformation. Previous studies have demonstrated that committed progenitors, such as common myeloid and granulocyte-macrophage progenitors (CMPs and GMPs, respectively) can be transformed, provided that the oncogenic event confers or enhances self-renewal properties to allow for expansion of the leukemic clone. The self-renewal capacity of and HSC is not universally sufficient, however.

This is exemplified in chronic myelogenous leukemia (CML) where the *BCR-ABL* fusion gene is present in HSC population, but it is the outgrowth of a more committed cell that causes disease (Maguer-Satta *et al.*, 1996). In addition, no terminally differentiated cells have been successfully transformed by leukemia-associated oncogenes to date, suggesting there is a limited population of cells susceptible to transformation with given properties.

Cells susceptible to transformation appear limited for each oncogene and are likely defined somewhat by the extent to which the oncogene can exploit naïve cellular programs. In a seminal work, B.J.P Huntly *et al.* tested the hypothesis that all leukemia oncogenes have the capacity to confer self-renewal to committed progenitors to generate leukemic stem cells/leukemia initiating cells. They found that while the fusion *MOZ-TIF* could transform committed myeloid progenitors at the CMP and GMP level, *BCR-ABL* could not and that transformation by this gene was limited to cells with inherent self-renewal potential, that is, the hematopoietic stem cell (Huntly *et al.*, 2004). Recent work implicates the *Meis1* program in conferring target cell susceptibility for transformation. Using the *MN1* model of leukemogenesis, Heuser *et al.* were able to show that expression of *Meis1* is a requirement for target cell transformation and that dominant negative *M33-Meis1* abolishes leukemogenicity (Heuser *et al.,* 2011). When they examined the expression profiles of cells susceptible to transformation by *MN1* and MN1-leukemias, they found a high degree of correlation between *Meis1* and *Meis1*-associated factor expression (*Flt3, Mef2c*). Enforced expression of *Meis1* expands the range of cells that can be immortalized by *MN1*, however, *AbdB*-like *Hox* expression is required for full transformation. These studies and others have suggested a "code" of expression required for full transformation and that both the oncogene and target cell play a complementary role in contributing to full expression of the code. This

provides further support for the concept that *Meis1*, in conjunction with *Hox* gene expression, may be a cornerstone in this code relevant to normal and leukemic hematopoiesis,.

Identifying the targets and downstream effectors of *Meis1*

Despite its role as a transcription factor, identification of specific targets genes and pathways for *Meis1* remains limited despite a number of studies looking at gene expression changes in both over-expression and knock-out models. Cell surface receptor *Flt3* has been shown to be up-regulated with *Hox* and *Meis1* in several leukemic expression studies, although it is not a requirement for transformation (Morgado *et al.*, 2007). Several cell cycle molecules have been identified in similar over-expression and knock-down studies, including *Cdk2* and *Ccnd3* (Kumar *et al.*, 2009; Argiropoulous *et al.,* 2010). A whole genome chromatin immunoprecipitation and sequencing (ChIP-seq) approach in mouse ES-derived hematopoietic progenitors identified >8000 regions bound by MEIS1 (Wilson *et al.,* 2010). A similar approach in and *Hoxa9* and *Meis1*-overexpressing mouse cell lines identified 624 regions bound by MEIS1 (Huang *et al.*, 2012). Reassuringly, previously identified targets were confirmed in these studies, however, the cell populations in which the studies were performed may differ from naïve cell populations in important respects. This highlights the need for a conditional model of gene expression at physiological levels in purified cell populations of interest. Below is a summary of our current understanding of genes regulated by *Meis1* in normal and leukemic hematopoiesis.

To date, few targets of* Meis1 *have been identified in normal hematopoiesis

Expression of *Meis1* is enriched in the most primitive HSC populations and progressively down-regulated with differentiation, with the exception of the megakaryocyte,

suggesting a key role in regulation of these cell types. Genome-wide ChIP-seq in the ES derived hematopoietic progenitor cell line HPC-7, suggests that *Meis1* binding is enriched in promoter regions at >8000 MEIS1 sites in the genome (Wilson *et al.*, 2010). An inducible model of *Meis1* expression in the mouse ES system suggests that *Meis1* expression inhibits commitment to erythroid fate via inhibition of erythroid specific genes (*Hba-a1/2* and *Gypa*) and expression of *Ptger3* (Cai *et al.*, 2012). *Ptger3* encodes for prostaglandin E2, a factor known to promote short-term reconstituting hematopoietic progenitor proliferation (Frisch *et al.*, 2009).

Bona fide targets for *Meis1* in adult HSC populations at physiological levels have not been reported to date, with the exception of recent studies implicating regulators of anaerobic metabolism, the hypoxia-inducible factors (*Hif*s). Studies published during the conduct and writing of this thesis work support a model whereby HSC employ anaerobic metabolism to restrict the generation of reactive oxygen species (ROS) in the low-oxygen bone marrow niche. Regulation of metabolism by restricting the generation of ROS is significant as increased levels of ROS are associated with loss of HSC potential (Ito *et al.*, 2006; Miyamoto *et al.*, 2007; Takubo *et al.*, 2010). *Meis1* was found to directly bind the promoter of master regulators of anaerobic metabolism *Hif1* α (Simsek *et al.*, 2010) and *Hif2* α (Kocabas *et al.*, 2012) and positively influence gene transcription. Conditional knock-out of *Meis1* in the adult mouse results in decreased HSC function that can be rescued by ROS-scavenging compounds, supporting a causative role for *Meis1* in regulating aneorobic metabolism and hence HSC function (Kocabas *et al.*, 2012; Unnisa *et al.*, 2012). This is a powerful demonstration of how conditional knock-out models can be exploited to identify physiologically relevant target gene expression.

Consistent with *Meis1* up-regulation of expression in megakaryocytic progenitors (Okada *et al.*, 2003) and requirement of *Meis1* for embryonic megakaryopoiesis (Hisa *et al.*, 2004; Azcoitia *et al.*, 2005), *Platelet factor 4* (*Pf4* or *Cxcl4*), is a direct target of MEIS1 with PBX1B and PBX2 (Okada *et al.*, 2003). MEIS1 was recently shown to regulate a transcription of dynamin isoform *DMN3* via a promoter uniquely used in megakaryopoiesis (Nürnberg *et al.*, 2012). Inhibition of dynamin activity in megakaryocytes inhibited platelet generation *in vitro*, supporting a role of *Meis1* regulation in megakaryopoiesis. *Meis1* may also suppress erythropoiesis in the developing embryo once cells are committed to the megakaryocytic lineage. Overexpression of *Meis1* in embryonic cell (ES) cultures resulted in increased levels of megakaryocyte progenitors based on CD41 expression and colony formation (Cai *et al.*, 2012). This result is somewhat in contrast with studies in zebrafish whereby knockdown of *meis1* also results in impaired definitive erythropoiesis (Cvejic *et al.*, 2011). Regardless of species differences, collectively these results implicate *Meis1* as a regulator of erythro- and megakaryopoeisis. Further studies using a conditional adult model of *Meis1* deletion would help to delineate roles in maintaining normal, adult homeostasis in these linages.

Although there are several candidate targets for* Meis1 *in leukemogenesis, few have been validated as essential for transformation

In leukemia, *Meis1* expression is invariably linked to *Hox* gene over-expression, and as such, the majority of studies looking a targets of *Meis1* are preformed in the context of overexpression of both factors. In contrast to ChIP-seq in the ES derived progenitor population, only 5% of *Meis1* and *Hoxa9* DNA binding appears to localize to promoter regions (Huang *et al.*, 2012). The majority of DNA binding that influences gene expression in this model occurred in enhancer regions, distal from transcription start sites, and was

associated with H3 and H4 acetylation of CBP binding, marks of active enhancer regions. Further interrogation of these regions validated enhancer and repressive activity of gene expression in ~50% of the regions tested (12/22). This study confirmed gene regulation by *Meis1* and *Hoxa9* of *Erg1, CD34* and *Flt3,* targets identified by gene expression analysis in a previous overexpression study (Wang *et al.*, 2005).

Growth factor receptor *Fms*-related tyrosine kinase 3 (*FLT3)* appears to be an important, although not essential, target for MEIS1 in the transformation process, and indeed is one of the best-characterized targets to date. FLT3 is a tyrosine protein kinase receptor expressed in virtually all patients with AML and in a large portion of ALL samples. Co-expression of *Meis1* in *Hoxa9* immortalized mouse progenitors up-regulated *Flt3* expression and chromatin immune-precipitation experiments demonstrate direct binding of *Hoxa9* and *Meis1* to the *Flt3* promoter (Wang *et al.* 2005; Wang *et al.*, 2006). Moreover, engineered overexpression could replace Meis1 for leukemic transformation by NUP98-Hox fusion genes (Palmqvist *et al.,* 2006). However, *Flt3* is not essential for transformation , as Meis1 mutants that do not trigger upregulation of Flt3 can still cooperate with NUP98-Hox fusions (Argiropoulos *et al*.,2008) and *Flt3* $^{-/-}$ cells are readily transformed by *Hoxa9+Meis1* overexpression and cause leukemias with similar phenotype and latency to wild-type marrow (Morgado *et al.*, 2007). This is likely due to an ability of MEIS1 to trigger expression of downstream *Flt3* targets in response to FL signaling, that is, activation of ERK1/2, Akt and nuclear factor- κ B (Argiropoulos *et al.*, 2008).

One mechanism by which oncogenes transform cells is through enforced cell cycle progression. Evidence for a role for *Meis1* in influencing cell cycle is inconsistent and may vary with cell context. In leukemia models of *Hoxa9* overexpression, addition of *Meis1* does

not increase levels of cell cycle mRNA nor does *Vp16-Meis1* confer enhanced growth properties to fibroblasts, suggesting *Meis1* oncogenicity is not related to enhanced proliferation. In *MLL* leukemia models, however, increased *Meis1* expression is associated with increased cell cycle entry (Wong *et al.*, 2007). Additionally short-hairpin RNA against *Meis1* in *MLL-Af9* overexpressing cell-lines reduced expression of several genes regulating DNA replication and cell-cycle entry, including *Cdk2, Cdk6, Cdkn3, Ccna2, Cdc7, Cdc42, Rbl1* and *Wee1* and resulted in cell cycle arrest at G_o/G_1 (Kumar *et al.*, 2009). Further support for *Meis1* as a modulator of cell-cycle comes from experiments with an engineered dominant repressive form of *Meis1*, *M33-Meis1.* Enforced expression of *M33-Meis1* results in a partial G_1 block in AML leukemia lines, mediated by a decrease in Cyclin D3 levels and reduced Rb phosphorylation (Argiropoulos *et al.*, 2010). Outside of leukemogenesis, *Meis1* enforces *cyclin D1* and *c-myc* expression in the developing zebrafish retina (Bessa *et al.*, 2008). Collectively this data implicates *Meis1* as a regulator of cell cycle progression although perhaps only minimally in the leukemic context.

Of interest given recent studies suggesting a role for *Meis1* in the regulation of ROS in the HSC, regulation of ROS in the LSC by MEIS1 may also be significant. Low levels of ROS were recently found to be associated with LSC frequency in a *Hoxa9+Meis1* mouse model of leukemia (Herault *et al.*, 2012). The expression levels of *Meis1* are equivalent between the lines used in the study, however, and the authors linked low level of ROS in high frequency LSCs to expression levels of the ROS scavenger *Gpx3.* This does not preclude the importance of *Meis1* in enforcing expression of *Gpx3* or other regulators of ROS in these leukemias, and in fact, a *Meis1* binding site exists in the 3'UTR of *Gpx3*, suggesting regulation may be possible. The sum of these studies support *Meis1* as master

regulator of a complex genetic program that has strong oncogenic potential when dysregulated. Further investigations are required to precisely pinpoint which of the many genes with DNA binding and altered expression in the presence of *Meis1* are fundamental to the transformation process.

To date, no putative *Meis1* effector genes, including *Flt3*, can substitute for *Meis1*-overexpression in transformation models. For example, In a NUP98-HOXD13 overexpression model, *Trib2, Dlk1, Ccl3, Ccl4* and *Rgs1* were identified as up-regulated and bound by *Meis1* in the transformation process. Only *Trib2*, however, could replace *Meis1* to cause leukemia with *NUP98-HOXD13* overexpression although the latency to leukemia was much longer (140 days vs 50 days with *Meis1*), suggesting further collaborating mutations are required for transformation (Argiropoulos *et al.*, 2008). These studies highlight the complexity of understanding effectors of *Meis1* activity, as there are likely several key effectors that have complementary and additive effects, as well as redundancy in the system.

Delineating functional domains of MEIS1

Deletion mutant studies have delineated several important domains of *Meis1* required for its function in normal and leukemic hematopoiesis. While many of these studies have been conducted in the context of leukemia models, likely the findings are largely also relevant to *Meis1* roles in normal hematopoiesis. For transformation, the DNA binding by MEIS1 and the C-terminal domain are critical in the context of *Hoxa9* and *MLL*-fusion leukemia. DNA binding mutant MEIS(N51S) does not collaborate with Hoxa9 overexpression (Wang *et al.*, 2005) in the animal models or rescue transformation capacity by *MLL-AF9* on a *Meis*$^{-/-}$ background (Wong *et al.*, 2007). Interaction with PBX also

appears to be essential as mutations or deletions in the HM domains required for PBX interaction abrogate *Hoxa9*-overexpression transformation and fail to rescue transformation by *MLL-AF9* (Mamo *et al.*, 2006; Wang *et al.*, 2006; Wong *et al.*, 2007).

The C-terminal domain of *MEIS1* is also essential for transformation, likely due to transactivation of expression as opposed to direct HOX-interaction. Deletion of the C-terminal domain (CTD) after the homeodomain (amino acid 334) or at the distal C-terminus (amino acid 371) results in a mutant MEIS1A protein that cannot cooperatively bind PBX-HOX to trigger gene expression in cell lines expressing reporter constructs nor collaborate with *Hoxa9* overexpression *in vivo* (Mamo *et al.*, 2006; Wang *et al.*, 2006). These truncations also fail to rescue *MLL-AF9* serial replating *in vitro* on a *Meis*$^{-/-}$ background. While it may be temping to assume this is due to a loss of HOX and DNA-binding activity, this does not appear to be the case. A more restricted truncation mutant that results in the loss of the terminal 18-amino acids responsible for HOX protein interaction, Meis370T, retains the ability to immortalize progenitors and cause AML *in vivo* with *Hoxa9* over-expression (Wang *et al*. 2005). In addition, loss of the CTD does not appear to influence DNA binding in the context of HOX and PBX1, despite abrogation of reporter gene activity with the loss of the terminal 18 amino acids of MEIS1A (Huang *et al,* 2005).

Current theories suggest that loss of function as a result of CTD truncation may be due to a transactivation function localized in the domain that is activated following chromatin remodeling on PBX-HOX-MEIS hetero-trimer or PBX-MEIS heterodimer responsive genes (Huang *et al.*, 2005). C-terminal mutants of *Meis1a* and *Meis1b* were examined for transactivation and DNA binding with PBX1, HOXA1 and HOXB1 on endogenous promoter elements. Researchers found that MEIS1 appeared to be recruited to

the promoter where PBX1 and HOX were already bound following activation by either PKA signaling or HDAC inhibition. They propose a model by which PBX exerts a repressive function on transcription from PBX-MEIS or MEIS-PBX-HOX complexes until cellular signaling triggers chromatin remodeling to a permissive state that permits recruitment of these complexes to genes or recruitment of MEIS to PBX-HOX bound promoters. Furthermore, evidence in zebrafish suggests MEIS may act in these complexes to maintain HistoneH4 acetylation and transcription via recruitment of transcriptional activator and histone acetyltransferase CBP (Choe *et al.*, 2009). Although these studies are on developmentally regulated promoter regions, and not necessarily those involved in leukemia, the role of the C-terminal domain of *MEIS1* is likely linked to transactivation of transcription as mutations abrogate function in both contexts.

The transactivation function of the *MEIS1* CTD is supported by studies with *Pknox1*, a MEIS-family member. *Pknox1* and *Meis1* share high sequence similarity the conserved HM motifs and homeodomain but diverge significantly in the CTD region. PKNOX1, however, appears to have a tumor suppressive role as overexpression in mouse models prolongs the latency of *Hoxa9* overexpressing cells and additionally *PKnox1*$^{-/-}$ mice are tumor prone in the context of *Eμ-Myc* (Thorsteinsdottir *et al*., 2002; Longobardi *et al.*, 2010). The CTD of PKNOX1 appears devoid of transactivation capacity (Huang *et al.*, 2005), however, replacement of the CTD of *Pknox1* with *Meis1a* converts PKNOX1 into a collaborating oncogene with HOXA9, with similar latency and phenotype to HOXA9+MEIS. Supporting a role in transactivation is similar activity of PKNOX-VP16 where the CTD of PKNOX is replaced with VP16 (Bisaillon *et al*. 2011). That the CTD of MEIS1 can convert PKNOX into an oncoprotein, and that lack of transactivating and

transformation capacity in C-terminal *Meis1* mutants, argues that a key role for MEIS1 is regulation of gene expression in the context of *Hox*-mediated leukemogenesis.

Roles for *Meis1* outside of hematopoiesis

While a large bulk of study into *MEIS1* function has been in the context of mammalian development and hematopoiesis, studies have implicated *MEIS1* in a diverse array of other processes. In concert with PBX partners, *Meis1* or homologs have been implicated in regulation of neural development of the hindbrain and eye in *Drosophila*, *Xenopus*, *Zebrafish* and mammalian systems (Pai *et al.*, 1998; Waskiewicz *et al.*, 2001; Zhang *et al.*, 2002; Hisa *et al.*, 2004; Azcoitia *et al.*, 2005; Heine *et al.*, 2008; Bessa *et al.,* 2008). In the developing eye, regulation of *cyclin D1* and *c-myc* by *Meis1* is required to maintain proliferation of the multipotent cells of the early eye (Bessa *et al.*, 2008). SOX3, one of the earliest neural markers in vertebrates is directly bound and regulated by Pbx1/Meis1 binding (Mojsin & Stevanovic*,* 2009). Pbx/Meis heterodimer-regulated expression also appears to be important in the developing heart as haploinsufficiency for *Pbx1* (via reduction of *Pbx2 or Pbx3)* or loss of *Meis1* leads to phenotypically similar abnormalities of heart development, resembling tetralogy of Fallot (Stankunas *et al.*, 2008).

Outside the embryo, there is evidence that *Meis1* expression in the maternal endometrium is required for embryo implantation via integrin expression (Xu *et al.*, 2008). Expression of *Meis1* is high in adult human endometrium, myometrium and cervical tissues as well as in ovarian cancer samples (Crijns *et al.*, 2007). Other tumor tissues may require *Meis1* to varying extents. Down-regulation of TGF-β type II receptor occurs in a number of lung cancers, resulting in loss of function of the tumor suppressor TGF-β. *Meis1* was found

to bind the TGF-β type II receptor promoter to repress gene transcription (Halder *et al.*, 2011). In neuroblastoma, both expression and the chromosomal loci of *Meis1* are amplified (Jones *et al.,* 2000; Spieker *et al.*, 2001). In conjunction with the developmental regulator OCT-1, MEIS1 and other TALE homeodomain transcription factors may regulate neuronal specific expression of gonadotropin-releasing hormone in the adult hypothalamus (Rave-Harel *et al.*, 2004). Together, these studies suggest a far larger role for *Meis1* beyond the hematopoietic system in regulating gene programs that may be subverted in oncogenesis.

Knowledge of regulation of *Meis1* expression is relatively limited

Although *Meis1* is a key regulator of gene expression in many processes, as of yet, little is known about regulation of its expression. Studies in zebrafish suggest there is at a minimum 13 highly conserved *cis*-regulator regions with enhancer activity and differing degrees of tissue specificity (Royo *et al.*, 2012, Zhou *et al*.,2013). Evidence of multiple cis-regulator regions in the human *MEIS1* gene are also emerging (Xiang *et al*., 2010; Zhou *et al.*, 2013). In the immortalized myeloid leukemia line K562, deletion of E-twenty six (ETS) binding sites in a reporter construct for the *MEIS1* promoter abrogates reporter gene expression, whereas mutation of C/EBPα, SRF or RUNX1 binding sites have minimal impact (Xiang *et al.*, 2010). Binding of ETS family member ELF1 was observed in myeloid leukemia lines, primary samples and cord blood at the native *MEIS1* promoter in these studies, supporting a role for ELF1 in transcriptional regulation of *MEIS1* expression. Interestingly, ETS-1 is required for MEIS1 regulated expression of *Pf4*, suggesting both regulation and co-operative expression with ETS family members. The *MEIS1* promoter additionally contains a partial cyclic AMP response element (CRE) that may respond to

increased levels of transcriptional activator CREB (cAMP responsive element binding protein 1). Elevation of CREB levels in AML samples leads to a 40-fold increase in *MEIS1* expression, although direct binding to the *MEIS1* promoter was not demonstrated (Esparza *et al.*, 2008). Elevation in CREB, and hence *MEIS1* expression, may be one of the oncogenic mechanisms in AML as expression is lower in patients in remission and marrow of healthy donors (Crans-Vargas *et al.,* 2002).

A complex circuit of HOX, PBX and MEIS family member co-regulation may additionally be crucial for appropriate *MEIS1* expression (Zhou *et al.*, 2013). In AML patient samples there is a linear correlation between *HOXA9* and *MEIS1* mRNA expression, which is mirrored in normal hematopoietic progenitor populations (Hu *et al.*, 2009). *Hoxa9*$^{-/-}$ mutant bone marrow shows a profound reduction in *Meis1* expression that can be partially rescued by *Creb1* expression, a direct target of HOXA9 and direct regulator of *Meis1* expression (Hu *et al.,* 2009; Esparza *et al.,* 2008). Interestingly, *Hoxa9* expression does not appear to be involved in the up-regulation of *Meis1* in megakaryocytic progenitors, further enforcing Hox-independent roles for MEIS1 (Hu *et al.*, 2009).

MEIS family member *Pknox1* also rescues *Meis1* expression in *Hoxa9* deficient bone marrow and appears to be crucial for *Meis1* expression during embryogenesis (Hu *et al.*, 2009; Ferretti *et al.*, 2006). *Pknox1*$^{-/-}$ embryos exhibit a similar phenotype to *Meis1*$^{-/-}$ mutants, that is, embryonic lethality due to anemia, impaired angiogenesis and retinal anomalies. *Pknox1*-deficient embryos additionally show reduction in MEIS1, PBX1 and PBX2 protein levels and concomitant DNA binding activity. The authors suggest this supports *Pknox1* as a master regulator of *Meis1* expression, however, this is not consistent with later embryonic lethality in *Pknox1*$^{-/-}$ embryos (17.5 dpc) compared to *Meis1*$^{-/-}$ embryos

(11.5 – 14.5dpc) (Hisa *et al.*, 2004; Azcoitia *et al.,* 2005). Epigenetic changes are also crucial for regulation of *Meis1* expression. In the context of *MLL* leukemias, histone H3 methyltransferase DOT1 is required for *MLL* transformation, in part by increasing H3K79 methylation around *Hoxa9* and *Meis1* promoters and hence expression (Chang *et al.*, 2010).

Meis1 **is a powerful player in the context of normal and malignant hematopoiesis, however fundamental characteristics remain unknown**

While *Meis1* has been extensively studied in a number of contexts, many questions remain. The extent to which other members of the MEINOX family (*Meis2, Meis3, Pknox1* and *Pknox2*) are expressed in appreciable amounts in the hematopoietic hierarchy is not well studied. The expression level of these members is of interest in light of the possibility of functional redundancy between the related genes.

In addition, while *Meis1* is clearly required for embryonic hematopoiesis and viability, requirements in adult mammalian hematopoiesis remain unclear. While the maintenance of HSC in *Meis1*$^{-/-}$ mice is compromised, the extent to which the defining property of the HSC, that is self-renewal, has not been examined. In addition, little evidence exists as to how *Meis1* influences megakaryocytic or erythroid differentiation in the adult mammalian system. While *Meis1* is implicated as a critical regulator of leukemia and hematopoiesis, very few effectors of this role have been validated to date. As previous studies of other transcription factors, such as *MLL* and *AML1/RUNX1,* have demonstrated, knowledge in either the normal or leukemic context may be highly informative in the other.

The work presented in this thesis sought to build upon research into *Meis1* function in several ways. Firstly, we validated two conditional models of *Meis1* deletion that we then exploited to investigate some of the most pressing questions regarding *Meis1* function. We

additionally examined MEINOX family expression in sorted hematopoietic fractions to compile a complete picture of MEINOX expression through the hierarchy. Once robust deletion *in vitro* and *in vivo* was established, we used the model to examine the requirement for *Meis1* in adult hematopoiesis. Our results support a role for *Meis1* in HSC self-renewal and additionally in maintenance of megakaryocyte and erythroid potential. HSC lacking *Meis1* fail to expand *in vivo* while lineage differentiation remains largely intact. Erythropoiesis is impaired in adult mice lacking *Meis1* as erythroid progenitors fail to expand in response to stress. Our studies also provide clarification in the adult mammalian system that *Meis1* is required for both megakaryopoieis and erythropoiesis as opposed to favoring differentiation along either lineage as seen in the embryonic and zebrafish models of *Meis1* deletion and overexpression. We additionally identified several genes that may be relevant to *Meis1* function in adult hematopoiesis by expression analysis of HSC-enriched populations following *Meis1* deletion. Building on recent studies highlighting an interplay between ROS and *Meis1* function in the HSC, we used an *in vivo* model of ROS scavenging to examine if this mechanism extends to other hematopoietic populations requiring *Meis1* expression, including megarkaryocyte and erythroid progenitors. We additionally examined if expression of our candidate effectors of *Meis1* function in the HSC are altered by ROS-scavenging in both HSC and megakaryocyte progenitor-enriched populations. In summary, the work validates a powerful tool for the study of *Meis1* function and provides novel insights into roles in the adult HSC and differentiated progenitor populations.

Chapter 2 : Materials & Methods

In vivo methods

Mice

All mice were bred and maintained at the British Columbia Cancer Research Centre Animal Resource Centre with all protocols approved by the University of British Columbia Animal Care Committee (Certificate: A13-0063). Male *Meis1*$^{tmloxP/+}$ (*Meis1*$^{fl/+}$) mice on the CD45.2 C57BL/6 J (B6) background were a generous gift from Drs N. Jenkins and N. Copeland. Little information was available at the time with respect to the exact method of engineering the mice or targeted sequence. The CD45.2 background was confirmed by FACS analysis of peripheral blood (see below), following which *Meis1*$^{fl/+}$ mice were bred with female B6 mice and the resulting offspring interbred. *Meis1*$^{fl/fl}$ or *Meis1*$^{fl/+}$ mice were then bred with B6;129-*Gt(ROSA)26Sor*$^{tm1(Cre/ERT)Nat}$/J (*ERTCre;* Gift from Dr. A. Weng) or B6.Cg-Tg(Mx1-Cre)1Cgn/J (*MxCre;* Jackson Laboratory) for inducible expression of *Cre* recombinase and subsequent deletion of *Meis1* exon 8 (*MxCre/Meis1* or *ERTCre/Meis1*). The *ERTCre* strain was engineered to express Cre recombinase with a modified estrogen receptor ligand binding domain from the ubiquitous *Gt(ROSA)26Sor* promoter. In the absence of the synthetic ligand tamoxifen (4-OHT), the Cre protein remains cytoplasmic, however administration of 4-OHT allows localization to the nucleus and recombinase activity (Badea *et al.*, 2003). The *MxCre* system is based on controlled expression of the Cre recombinase as opposed to localization. Normally, the *Mx1* promoter is expressed in response to interferon signaling triggered by double-stranded RNA virus infection. Expression of the Cre gene in *MxCre* mice is driven by the *Mx1* promoter when the synthetic double-stranded RNA analog

polyinosinic:polycytidylic acid (PolyI:C) is administered, or alternatively interferon alpha or beta (Kühn *et al.*, 1995).

Progeny of the *MxCre/Meis1* or *ERTCre/Meis1* crosses were further interbred to yield the described genotypes. Wild-type *Meis1* alleles are denoted as $Meis1^{+}$, while the floxed allele prior to Cre recombinase expression is termed $Meis1^{fl}$. Following expression of Cre recombinase, the allele with excised sequence intervening the LoxP sites is designated as $Meis1^{-}$. For example, a mouse heterozygous for the targeted *Meis1* allele on the *ERTCre* background following Cre expression would be denoted as $ERTCre/Meis1^{-/+}$. Investigation of the targeted sequence and validation of Cre-mediated deletion is described in Chapter 3.

For transplantation assays, wild-type B6.SJL-PtprcaPeb3b/BoyJ (Peb3b, Animal Resource Centre (ARC), BC Cancer Research Centre, Vancouver, BC) were used as transplant recipients such that donor cell contribution in the peripheral blood of mice could be monitored by differential expression of CD45 antigen isoforms. Mice on the B6 background express CD45.2 on hematopoietic cells, whereas Pep3b mice express the CD45.1 isoform. Bone marrow from Peb3b mice were used to assay MEINOX family expression in sorted cell fractions as well as for cell line studies.

***Induction of Cre recombinase expression/localization* in vivo**

In vivo deletion of *Meis1* exon 8 was achieved via two methods employing the Cre/LoxP system. Induction of *Cre* expression was achieved in *MxCre/Meis1* mice by intraperitoneal (IP) injection of 300µg polyinosinic:polycytidylic acid (poly I:C; VWR/EMD Biosciences, Radnor, PA, USA), dissolved in phosphate buffered saline (PBS; STEMCELL Technologies Inc., Vancouver, BC, CAN) per mouse every 48 hours for 18 days. To induce deletion in the *ERTCre/Meis1* mice, 4-hydroxytamoxifen (4-OHT; Sigma, St. Louis, MO,

USA) was first dissolved at 25mg/mL into filtered >99% ethanol (EtOH) and homogenized with a hand-held homogenizer. This was further diluted into autoclaved corn oil (Sigma) to achieve a 5mg/mL 4-OHT suspension. 1mg 4-OHT was injected IP into *ERTCre/Meis1* mice every 48 hours for 12 days to trigger *Cre* expression.

Phenylhydrazine induced model of hemolytic anemia

Phenylhydrazine treatment is an experimental model for hemolytic anemia (Capron *et al*, 2011) and was used to examine the capacity of *Meis1*$^{-/-}$ erythroid-progenitors to expand in response to stress. At 48-hours following the last of nine PolyI:C injections, *MxCre/Meis1*$^{-/+}$ or *MxCre/Meis1*$^{-/-}$ mice were given IV injections of phenylhydrazine hydrochloride (PHZ; Sigma) at 40mg/Kg. Four days later, mice were euthanized and analyzed for phenotype and CFC (described below) capacity.

Reactive oxygen species scavenging by* in vivo *N-acetyl-L-cysteine treatment

Very recent work implicates *Meis1* in the regulation of *hypoxia-inducible factor* (*Hif*s) regulation and that this may be one mechanism through which reactive oxygen species (ROS) are regulated in the HSC. In order to assess the impact of ROS on the phenotypic anomalies and putative target genes we identified in *MxCre/Meis1*$^{-/-}$ mice, we used *in vivo* N-acetyl-L-cysteine (NAC) treatment. NAC has several functions in cells, but the ROS scavenger function in cells by the provision of substrate for H_2O_2 decomposition pathways (Yang *et al*., 2007) has been postulated to be of importance in the study of *Meis1* function (Kocabas *et al.*, 2012; Unnisa *et al*, 2012). Cre expression in *MxCre/Meis1* mice was induced with PolyI:C according to the protocol outlined above. Following 2 PolyI:C injections (4 days), mice were then also given daily subcutaneous (SQ) injections of 100mg/Kg NAC

(Sigma) for 14 days. Mice were analyzed 5 to 7 days following the final PolyI:C/NAC injections.

Isolation of bone marrow and peripheral blood for analysis

Peripheral blood parameters following induction were monitored using the tail prick method and collection into heparinized capillaries. For peripheral blood complete blood count and differential, blood was transferred to ETDA-coated blood collection tubes (microtainer 365973, BD, Franklin Lakes, NJ, USA) and counts performed by a scil Vet abc automatic blood cell counter (Vet Novations, Viernheim, Germany). If mice were euthanized prior to blood collection, blood was collected from the heart of euthanized mice. Bone marrow was isolated from euthanized mice by flushing the marrow cavities of femurs, tibias and iliac crests with 2% FBS in PBS using an 18G to 24G needle.

Long-term repopulating cell (LTRC) and competitive repopulating unit (CRU) assays

Bone marrow was flushed from the tibias, femurs and iliac Crests of mice in 2% PBS with fetal bovine serum (FBS; STEMCELL Technologies Inc.) and nucleated cell counts performed using 3% v/v acetic acid with methylene blue. If no further manipulation (such as cell sorting) was required prior to transplantation, appropriately diluted Ly5.2+ cell suspensions were made and transplanted into recipient $Ly5.1^{+}$ Pep3b mice irradiated at 780 cGy using an X-ray source. Whole Pep3b bone marrow was used as helper or competitor cells as indicated in the results.

Engraftment of test cells into recipients was monitored by peripheral blood collection from the tail-vein of recipient mice at various intervals. Approximately 50μL of peripheral blood was collected, lysed (Pharmlyse, BD) and incubated at $4^{o}C$ with a combination of fluorochrome conjugated anti-mouse antibodies against CD45.2-FITC (anti-Ly5.2), CD4-PE,

CD8-PE, B220-PE, B220-APC-Cy7, Gr1-APC-Cy7 and Mac1-APC-Cy7 (see Table 2 for clones and suppliers). Samples were washed and re-suspended in 2% PBS and 1ug/mL propidium iodide (PI) prior to acquisition on a modified FACSCalibur (BD with Cytek laser and digital detector upgrades, Fremont, CA, USA). Analysis of FACS data was performed using FlowJo analysis software (TreeStar, Ashland, OR, USA). Mice were scored as positive for multi-lineage engraftment if >1% of total peripheral blood nucleated cells were donor-derived $Ly5.2^+$ cells and within this population, the contribution of T cells ($CD4CD8^+$), B-cells ($B220^+$) and myeloid cells ($Gr1^+Mac1^+$) to was >1%. Long-term repopulating cell frequency and test for significant differences between groups was performed using the Extreme Limiting Dilution Analysis (ELDA) online tool (http://bioinf.wehi.edu.au/software/elda).

Cell sorting and FACS analysis

Isolation of retrovirally transduced producer cells and 5-FU pre-treated marrow

Green and yellow fluorescent proteins (GFP, YFP) are useful tools to monitor gene transfer efficiency following retroviral transduction (construct and infection details below). GFP and YFP expression is linked to that of the gene of interest through an internal ribosome entry site (IRES), thusly allowing monitoring of expression and sorting by expression for the gene of interest. We used FACS to sort both viral producer cells and retrovirally transduced 5-flurouracil (5-FU). Cells were harvested from culture, then washed with 2% PBS and prepared for sorting by staining with propidium idodide (PI, Sigma) for viability. An Influx I (Cytopia/BD Biosciences) or FACSDIVA (BD Biosciences) machine with a 488nm argon

laser source, was used to sort cells on the basis of viability (PI negative) and YFP (527nm emission) and/or GFP positivity (509nm emission).

Isolation and phenotypic analysis of primary marrow progenitor and mature cell populations

For phenotypic analysis and isolation of purified hematopoietic populations, the following isolation and staining protocols were used. *MxCre/Meis1* mice were analyzed 5-7 days following the final PolyI:C injection as trials at earlier time-points yielded FACS profiles with indistinct separation between positive and negative populations. Sorting and analysis of *ERTCre/Meis1* mice was done 2-4 days following the final 4-OHT injection. Bone marrow was flushed from the tibias, femurs and iliac crests of mice in 2% PBS with FBS. Red blood cells were lysed with PharmLyse (BD Biosciences) reagent according to the manufacturers instructions. A viable cell count was then performed using 0.4% trypan blue in PBS. Unless the cells were destined for a myeloid progenitor sort (common myeloid progenitor (CMP), granulocyte-monocyte progenitor (GMP) or megakaryocyte-erythroid progenitor (MEP)), cells were blocked for 20 minute on ice in 5% rat sera and 1μg/1x10^6 cells Fc receptor (FcR, also known as CD16/32), then washed with 2% FBS in PBS. Cells were then incubated with the antibody stains outlined in Table 2.1 for 20 min on ice (BD Pharmingen; eBioScience, San Diego, CA USA; BioLegend, San Diego, CA USA, STEMCELL Technologies). Cells were then washed and re-suspended at roughly 1x10^7 cells/mL with 3μM 4',6-diamidino-2-phenylindole (DAPI, Life Technologies, Carlsbad, CA, USA)) for viability and 10μg/mL DNaseI solution (STEMCELL Technologies) to prevent clumping. Cells were then filtered through a 45μm filter prior sorting.

An Influx II or Aria cytometer with 488nm argon, 350/405nm UV and 634nm red diode laser sources were used for cell sorting and phenotyping from primary marrow. Cells

were sorted/analyzed according to the gating strategies outlined in Table 2.2. Annexin V staining for apoptosis and BrDU for cell cycle staining were done according to the kit manufacturer's instructions (BD Biosciences). Following sorting, purity of the sorted sample was assessed by running a small fraction of the sorted sample through the cytometer. Purity of >98% was deemed to be acceptable. Analysis of FACS data was performed using FlowJo analysis software (TreeStar). Unpaired two-tailed, Student's T-tests were perfomed to determined statistical significance between *Meis1*$^{-/-}$ and control samples.

Table 2.1: Dilution, clone and source of antibodies for FACS phenotyping and cell sorting

PURPOSE	ANTIBODY	CLONE	DILUTION (FINAL)	SUPPLIER
Donor cell and lineage distribution of mouse peripheral blood	CD45.2-APC	104	1:1000	BD Pharmingen
	CD4-PE	L3T4	1:1600	eBioscience
	CD8-PE	Ly-2	1:1600	eBioScience
	B220-PE	RA3-6B2	1:2000	BD Pharmingen
	B220-APC-Cy7	RA3-6B2	1:2000	BD Pharmingen
	Gr1-APC-Cy7	RB6-8C5	1:6000	BD Pharmingen
	Mac1-APC-Cy7	M1/70	1:5000	BD Pharmingen
ESLAM HSC for expression profiling (Kent *et al.*, 2009)	CD45-FITC	30-F11	1:100	BioLegend
	EPCR-PE	RMEPCR1560	1:100	STEMCELL Technologies
	CD48-APC	HM48-1	1:100	BioLegend
	CD150-biotin	TC15-12F12.2	1:100	BioLegend
	SA-PE-TxRed	Streptavidin	1:400	BD Pharmingen
CD150 HSC for phenotyping (Kiel *et al.*, 2005)	Lineage-PerCP-Cy5.5	See below	See below	See below
	cKit-APC	2B8	1:100	BD Pharmingen
	Sca-PE	E13-161.7	1:100	BD Pharmingen
	CD48-FITC	HM48-1	1:100	BioLegend
	CD150-PE-Cy7	SLAM	1:100	BioLegend
LSK for Affymetrix expression analysis	Lineage-PerCP-Cy5.5	See below	See below	See below
	cKit-APC	2B8	1:100	BD Pharmingen
	Sca-PE	E13-161.7	1:100	BD Pharmingen
Myeloid	Lineage-PerCP-	See below	See below	See below

PURPOSE	ANTIBODY	CLONE	DILUTION (FINAL)	SUPPLIER
progenitors for expression and phenotyping (Akashi *et al.*, 2000)	Cy5.5			
	Sca1-PE-Cy7	E13-161.7	1:150	BD Pharmingen
	cKit-APC	2B8	1:100	BD Pharmingen
	CD34-FITC	RAM34	1:400	eBioscience
	CD16/32-PE	2.4G2	1:300	BD Pharmingen
Common lymphoid progenitors (CLP) for expression and phenotyping (Kondo *et al.*, 1997)	Lineage-FITC	See below	See below	See below
	cKit-APC	2B8	1:100	BD Pharmingen
	Sca1-PE	E13-161.7	1:100	BD Pharmingen
	CD127-biotin	B12-1	1:100	BD Pharmingen
	SA-PerCP-Cy5.5	Streptavidin	1:100	BD Pharmingen
Megakaryocyte progenitors for expression and phenotyping (Pronk *et al.*, 2007)	Lineage-PerCP-Cy5.5	See below	See below	See below
	Sca1-PE	E13-161.7	1:200	BD Pharmingen
	cKit-APC	2B8	1:100	BD Pharmingen
	CD150-PE-Cy7	SLAM	1:100	Biolegend
	CD41-FITC	MWReg30	1:100	BD Pharmingen
Mature megakaryocytes (Heazlewood *et al.*, 2013)	CD41 (as per Nilsson lab)			
Erythroblast maturation series for expression profiling *unlysed (Socolovsky *et al.*, 2001)	Ter119-PerCP-Cy5.5	TER-119	1:150	BD Pharmingen
	CD71-PE	C2	1:100	BD Pharmingen
Lineage-FITC for expression profiling and phenotyping of CLP	Gr1-FITC	RB6-8C5	1:2400	BD Pharmingen
	Ter119-FITC	TER-119	1:150	BD Pharmingen
	B220-FITC	RA3-6B2	1:600	BD Pharmingen
	CD3-FITC	L3T4	1:300	BD Pharmingen
	CD4-FITC	Ly-2	1:600	BD Pharmingen
	CD8a-FITC	53-6.7	1:600	BD Pharmingen
Lineage-PerCP-Cy5.5 for expression profiling and phenotyping of HSC and myeloid	Gr1-PerCP-Cy5.5	1A8	1:2400	BD Pharmingen
	Ter119- PerCP-Cy5.5	TER-119	1:150	BD Pharmingen
	B220- PerCP-Cy5.5	RA3-6B2	1:600	BD Pharmingen
	CD3- PerCP-	L3T4	1:300	BD Pharmingen

PURPOSE	ANTIBODY	CLONE	DILUTION (FINAL)	SUPPLIER
lineages	Cy5.5			
	CD4- PerCP-Cy5.5	Ly-2	1:600	BD Pharmingen
	CD8a- PerCP-Cy5.5	53-6.7	1:600	BD Pharmingen
Mature lymphoid for expression profiling	B220-APC-Cy7	RA3-6B2	1:500	BD Pharmingen
	CD4-PE	L3T4	1:400	eBiosciences
	CD8-PE	Ly-2	1:400	eBiosciences
Mature myeloid for expression profiling (Song *et al.*, 2005)	Gr1-APC-Cy7	RB6-8C5	1:500	BD Pharmingen
	Mac1-FITC	M1/70	1:800	BD Pharmingen
Apoptosis	AnnexinV-PE		kit instructions	BD Pharmingen
Cell Cycle	BrDU-APC		kit instructions	BD Pharmingen

Table 2.2: Cell sorting and phenotyping gating strategies.
Note all samples first gated on SSC-A/FSC-A for size and complexity, DAPI for viability and FSC-A/FSC-H for singlets

Populations of Interest	Subpopulations assessed	Enrichment Gate	First Purity Gate	Second Purity Gate
LSK HSC for sorting and Affymetrix expression analysis	n/a	Lin^-	$cKit^+Sca1^+$	
ESLAM HSC for expression profiling	n/a	Generous first and second purity gates	$CD45^+EPCR^+$	$CD48^-CD150^+$
CD150 HSC for phenotyping	n/a	Lin^-	$cKit^+Sca1^+$	$CD48^-CD150^+$
Myeloid Progenitors for expression and phenotyping	CMP	Lin^-	$cKit^+Sca1^-$	$CD16/32^{low}CD34^+$
	GMP	Lin^-	$cKit^+Sca1^-$	$CD16/32^{hi}CD34^+$
	MEP	Lin^-	$cKit^+Sca1^-$	$CD16/32^{low}CD34^{low}$
Common lymphoid progenitors	n/a	Lin^-IL7R^+ (generous)	$IL7R^+$	$cKit^{mid}Sca1^{mid}$

Populations of Interest	Subpopulations assessed	Enrichment Gate	First Purity Gate	Second Purity Gate
for expression and phenotyping				
Megakaryocyte progenitors for expression and phenotyping	n/a	Lin^-	$cKit+Sca1^-$	$CD150^+CD41^+$
Erythroblast maturation series for expression profiling	Proerythroblasts & basophilic erythroblasts	n/a	$Ter119^+CD71^{hi}$	
	Late basophilic and chromatophilic erythroblasts	n/a	$Ter119^+CD71^{mid}$	
	Orthochromatophilic erythroblasts	n/a	$Ter119^+CD71^{lo}$	
Lineage defined T-cells		n/a	$CD4^+CD8^+$	
Mature B-cells		n/a	$B220^+$	
Mature Myeloid	Granulocyte precursor		$Gr1^+Mac1^+$	
	Granulocyte		$Gr1^-Mac1^+$	
Mature megakaryocytes		Lin^-	$CD41^+SSC^{hi}$	

Table 2.3: References for Sorting Gates
Lineage refers to the lineage cocktail referred to as Lin- (IL7R is excluded in the CLP stain)

Stain	Markers	Reference
Lineage	Gr1, Mac1, Ter119, B220, CD3, CD8 (IL7R)	-
ESLAM HSC	$CD45^{mod}EPCR^{+}CD48^{-}CD150^{+}$	Kent *et al.*, 2009
CD150 HSC	$Lin^{-}cKit^{+}Sca1^{+}CD48^{-}CD150^{+}$	Kiel *et al*., 2005
CMP	$Lin^{-}cKit^{+}Sca1^{-}CD16/32^{low}CD34^{+}$	Akashi *et al.*, 2000
GMP	$Lin^{-}cKit^{+}Sca1^{-}CD16/32^{hi}CD34^{+}$	Akashi *et al.*, 2000
MEP	$Lin^{-}cKit^{+}Sca1^{-}CD16/32^{low}CD34^{low}$	Akashi *et al.*, 2000
MkP	$Lin^{-}cKit^{+}Sca1^{-}CD150^{+}CD41^{+}$	Pronk *et al.*, 2007
CLP	$Lin^{-}IL7R^{+}cKit^{mid}Sca1^{mid}$	Kondo *et al.*, 1997
Immature Erythroblast	$Ter119^{+}CD71^{hi}$	Socolovsky *et al.*, 2001
Maturing Erythroblast	$Ter119^{+}CD71^{mid}$	Socolovsky *et al.*, 2001
Mature Erythroblast	$Ter119^{+}CD71^{low}$	Socolovsky *et al.*, 2001
Granulocyte Precursor	$Gr1^{+}Mac1^{+}$	Song *et al*., 2005
Granulocyte	$Gr1^{-}Mac1^{+}$	Song *et al*., 2005
Mature Megakaryocyte	$CD41^{+}SSC^{hi}$	Heazlewood *et al.*, 2013

In vitro studies

Retroviral vectors and transduction

Stable ecotropic retroviral producer lines for transduction of mouse bone marrow cells, were derived from GP+E-86 packaging cells following infection with virus transiently produced from Phoenix Ampho (PA) packaging cells as previously described (protocol in Kalberer, Antonchuk & Humphries, 2002).

In brief, PA cells were transfected with DNA constructs using a calcium phosphate-based system (CellPhect, GE Healthcare, Little Chalfont, Buckinghamshire, UK) for the retroviral constructs of interest (MSCV-CRE-PURO, pSF91-MN1-GFP, MSCV-ND13-GFP, MSCV-MEIS1a-YFP, MSCV-MEIS1b-YFP or MSCV-MEIS251-YFP). MSCV-Meis1b-YFP and MSCV-Meis251-YFP were generated by cloning from cDNA using primers specific to the region with additional restriction enzyme sequence for compatibility

into the existing MSCV-Meis1a-YFP vector. In the case of MEIS251, a stop codon was introduced into the sequence at amino acid 251 in the MEIS1 sequence. Other viral vectors are described in Heuser *et al.*, 2007 (pSF91-MN1-GFP), Pineault *et al.,* 2003 (MSCV-ND13-GFP, MSCV-Meis1a-YFP). Amphotropic virus containing supernatant was then harvested 12 hours later, filtered with a 0.45μm filter to remove cellular debris and transferred to dishes containing GP+E86 cells ecotropic packaging cells and 5μg/mL protamine sulfate. The cycle of removing the media from GP+E86 cells and replacing with PA supernatant containing viral particles was repeated every 12 hours for 2 days. Following this process, virally transduced GP+E86 cells were selected by fluorescence activated cell sorting (FACS) (for GFP or YFP expressing viruses) or by antibiotic selection (1.6 – 3.2μg/mL puromycin for MSCV-CRE-PURO, Life Technologies, Carlsbad, CA, USA).

To transduce primary mouse marrow, Peb3b or C57BL/6J mice were pre-treated with 5-FU (150mg/Kg by intravenous (IV) injection; Hospira, Montral, QC, CAN) and 4 days later, bone marrow harvested (Van Zant, 1984). Red blood cells were lysed (Pharm Lyse, BD Biosciences, Franklin Lakes, NJ, USA) and stimulated for 2-days in culture in medium containing 15% fetal bovine serum (FBS), 6ng/mL mouse Interleukin 3 (mIL-3, STEMCELL Technologies, Vancouver, BC, CAN), 10ng/mL human IL-6 (STEMCELL Technologies) and 100ng/mL mouse stem cell factor (mSCF, STEMCELL Technologies) (cytokine cocktail 3/6/SCF) in Dulbecco's Modified Eagle's Medium (DMEM, STEMCELL Technologies). After pre-stimulation, bone marrow cells were harvested and plated onto irradiated GP+E86 viral producer cells (40Gy from an X-ray source) for 48 hours culture in growth factor containing media as above supplemented with 5μg/mL protamine sulfate (Life Technologies). Non-adherent and loosely adherent bone marrow cells were then recovered

transduced cells selected by FACS or antibiotic selection (MSCV-CRE-PURO). Transduced cells were then maintained in 15% FBS with the mIL-3/hIL-6/mSCF cocktail in DMEM.

Hematopoietic colony-forming cell (CFC) assays

In vitro assays of colony forming cell (CFC) content are used as a surrogate to measure the capacity and frequency lineage committed hematopoietic progenitors in a test cell population, from culture or a primary cell source (reviewed in Purton & Scadden, 2007). We used CFC assays to examine the frequency of muti-potent (CFU-GEMM), myeloid (CFU-GM), erythroid (BFU-E) and megakaryocyte (CFU-Mk) progenitors from freshly euthanized experimental animals. The assay was also used to examine if over-expression of the *Meis1* truncation (MEIS251) transcript had a gross impact on cell proliferation.

BM cells were flushed from the tibias, femurs and iliac crests of mice in 2% FBS/PBS while spleen cells were isolated by maceration through a 0.2μM screen. Nucleated cell counts were performed and cells further diluted in 2% FBS in Iscoves Modified Dulbecco Medium (2%FBS/IMDM, STEMCELL Technologies). Bone marrow or spleen cells were mixed with methylcellulose media containing cytokines to support CFU-GEMM, CFU-GM, and BFU-E colony growth (CAT: M3434, STEMCELL Technologies) according to manufacturer's protocol at a concentration of $2x10^4$ cells per dish for bone marrow or $2x10^5$ cells per dish for spleen. As this cocktail supports myeloid colony growth that can overwhelm the less frequent erythroid progenitor, an alternate methylcellulose media optimized for BFU-E growth (CAT: M3436, STEMCELL Technologies) was also used. For the erythroid colony cultures, $4x10^4$ bone marrow or $4x10^5$ spleen cells per dish was used. Cells were cultured for 10-12 days in a humidified incubator at 37^oC and 5% CO_2 for

myeloid-biased cultures and 14 days for erythroid-biased cultures. CFC morphology and numbers were assessed using an inverted microscope.

CFU-Mk are difficult to detect using in situ morphological assessment and are therefore more accurately enumerated by detection in collagen gels that have been dehydrated, fixed and treated with a cytochemical stain for acetylcholinesterase enzyme activity (Shivdasani & Schulze, 2005, manufacturer's instructions at www.STEMCELL.com). Bone marrow was plated at a concentration $1x10^5$ cells per culure slide into collagen-based media suuplemented with cytokines and lipids (CAT 4964, STEMCELL, Technologies) according to manufacturer's instructions.

Cultures were incubated at 37^o 5% CO_2 and >95% humidity for 7 days, then fixed using acetone following dehydration with Whatman paper. Slides were then stained (acetylthiocholiniodide, sodium citrate, copper sulfate, and potassium ferricyanide - all reagents SIGMA) according to manufacturer's protocol to identify megakaryocytes on the basis of acetylcholinesterase activity (STEMCELL Technologies). Mouse megakaryocytes and early megakaryocyte progenitors, which express acetylcholinesterase, have brown granular deposits of copper ferrocyanide in the cytoplasm resulting from the enzymatic reaction. Granules may appear light red-brown in cells with low acetylcholinesterase content and ranges from orange-brown to dark brown/ black in cells with high acetylcholinesterase content. Harris hematoxylin solution (Sigma) was used as a counterstain for cell nuclei. CFU-Mk colonies range in size from three to approximately 50 megakaryocytes per colony, mixed CFU-Mk contain megakaryocytes and cells of granulocyte/macrophage lineages. Non-Mk colonies containing cells with stained nuclei only are also present.

For retroviral overexpression studies to determine if MEIS1 truncation transcript (MEIS251) had a dominant negative effect, CFCs with potential self-renewal capacity were detected using re-plating assays. 2000 retrovirally transduced (see below) bone marrow cells were plated immediately after the infection procedure dish in myeloid-biased methylcellulose media for 7 days at 37^{o}C and 5% CO_2. Following enumeration of colony number, the entire culture was then harvested by rinsing the plate gently with 4x 1 mL volumes of 2% FBS/IMDM. Pooled cells were washed twice by centrifugation at 300 g and replated (1500 cells per dish) onto secondary methylcellulose plates. Two rounds of replating were performed for each experiment. For all colony forming assays, unpaired two-tailed, Student's T-tests were perfomed to determined statistical significance between *Meis1*$^{-/-}$ and control samples.

Long-term culture initiating cell (LTC-IC) assay

The *in vitro* long-term culture initiating cell (LTC-IC) assay, detects and quantifies a subset of primitive hematopoietic cells (termed LTC-IC) based on their capacity to continuously produce myeloid cells for ≥ 4 weeks when cultured on a suitable feeder layer (Collins & Dorshkind, 1987). This assay consists of two steps: The first step is to co-culture test cells on a supportive feeder layer in a limiting dilution assay for 4 to 6 weeks to allow the differentiation of less primitive hematopoietic cells (present in the input cell suspension), while maintaining or expanding LTC-IC numbers. The second step is to detect LTC-IC-derived myeloid hematopoietic progenitors using the CFC assay. The frequency of LTC-IC is determined using Poisson statistics and method of maximum likelihood.

In the LTC-IC studies, S17 stromal line cells (Collins & Dorshkind, 1987) were irradiated at 2000cGy and seeded at 1.5x10^{4} cell per well into a flat-bottom tissue culture

treated 96-well plate. Cultures were then seeded with un-separated BM cells at various concentrations ($3x10^4$, $1.5x10^4$, $7.5x10^3$, $3.75x10^3$) from induced *ERTCre/Meis*$^{+/-}$, *ERTCre/Meis*$^{-/-}$, *MxCre/Meis*$^{+/-}$ or *MxCre/Meis*$^{-/-}$mice. Cells were prepared in mouse MyeloCult™ M5300 (12.5% horse serum, 12.5% FBS, 0.2 mM i-inositol, 20 mM folic acid, 10^{-4} M 2-mercaptoethanol, 2 mM L-glutamine, STEMCELL Technologies) supplemented with freshly prepared 10^{-6} M hydrocortisone (21-hemisuccinate sodium salt)(mLTCM). Weekly one-half media changes were performed according to manufacturers protocol. Following 4 weeks in culture, adherent and non-adherent cells were harvested from individual wells and plated into methycellulose media supplemented with cytokines (CAT:3434, STEMCELL Technologies), then cultured as described for CFC assays. The number of CFCs was counted and the wells were recorded as negative if no CFC were present and positive if ≥ 1 CFC is present. LTC-IC frequency and test for significant differences between groups was performed using the Extreme Limiting Dilution Analysis (ELDA) online tool (http://bioinf.wehi.edu.au/software/elda).

Molecular methods

Southern blot analysis

Southern blot analysis to detect Cre-mediated deletion of *Meis1*$^{fl/fl}$ was carried out using previously described procedures (Pawliuk *et al*., 1994). In brief, bone marrow cells from *Meis1*$^{fl/+}$mice were infected with MSCV-CRE-PURO retrovirus and treated with puromycin at 0, 1.6 or 3.6 μg/ml in vitro for 48-hours. Genomic DNA was extracted using DNAzol Reagent (Life Technologies). 10 μg of genomic DNA was digested with either

HindIII , EcoRI or BglII for 16 hrs at 37˚C and electrophoresed at 30V on a 1.0 % agarose/TAE gel. Gels were treated with 0.1 M HCl for 8 minutes, rinsed with deionized H_2O, treated with 1.5M NaCl/ 0.5N NaOH for 30 minutes and capillary transferred to ZetaProbe-GT (Bio-Rad) with 10x SSC for 16 hrs. DNA was fixed to membranes by treating @ 80˚C for 1 hour. Membranes were prehybridized 2 hours at 65˚C in buffer containing 0.8% skim milk, 8% Dextran Sulfate, 5X SSC, 8% Formamide, 0.8% SDS, 1.6 mM EDTA pH 8.0, and 400 µg/ml sheared and boiled Salmon Sperm DNA.

DNA probes were synthesized by PCR and gel purified prior to labeling. Probes and anticipated hybridization bands are outlined in Table 2.3**.** DNA probes were labeled by random priming and incorporation with ^{32}P dCTP , denatured and added to the pre-hybridization buffer with the membrane, incubated for 16 hrs at 65˚C, then washed 3 times at 65˚C (0.3X SSC, 0.1%SDS, 0.1% Tetra-Sodium Pyrophosphate). The hybridized membranes were then exposed to a phosphor –imaging screen for 24 hours. The phosphor screen was scanned by STORM Phosphorimager (Molecular Dynamics, Sunnyvale, CA, USA) and analyzed with ImageQuant 5.2 software (GE Lifesciences).

Table 2.4: Probes and anticipated hybridization sizes

Probe	**Position**	**Forward**	**Reverse**
Internal	5’ of the 3’ LoxP site	5’-gatttgatgctcttgcgaca-3’	5’-gaagttattaggtggatccaagct-3’
External	5’ of the 5’ LoxP site	5’-ccgtggttctccaagtttgt-3’	5’- tccatctcaaacccccttcag-3’
Probe	**Digest**	**WT hybridization**	**MUT allele hybridization**
Internal	HindIII	7.4 kbp	2.3 kbp
Internal	EcoRI	3 kbp	2.1 kpb/no band with Cre
External	BglII	2.3 kbp	2.4 kbp/3.8kbp with Cre

PCR detection of the 5' LoxP site

As described in Chapter 3, Southern blot analysis indicated that the second LoxP site was 3' of exon 8. Primers specific for extending regions of Intron 7 were used in concert with a reverse primer specific to the LoxP site 5' of exon 8 in an attempt to amplify the region of the mutant allele containing both LoxP sites. Detailed description of the rationale and primers are presented in Chapter 3. PCR amplification was performed with HiFi Platinum Taq Polymerase (Life Technologies).

RT-PCR cloning of the 5' LoxP site and truncated transcript

To confirm the positioning of the LoxP sites, the product of PCR amplification of with primer sets described in Chapter 3 were TOPO TA cloned into the PCR2.1 vector (Life Technologies) and sequenced by McGill University Sequencing Service. The presence and position of both LoxP sites were confirmed in the non-deleted mutant allele by sequence analysis, as well as and the deletion of genomic sequence containing exon 8 between these LoxP sites leaving a single remaining LoxP site.

In order to establish if a truncated transcript was generated following *in vivo* Cre-mediated *Meis1* deletion, splenocytes were isolated from *ERTCre/Meis1*$^{fl/fl}$, *ERTCre/Meis1*$^{+/fl}$, and *ERTCre/Meis1*$^{+/+}$ mice following *in vivo* Cre induction by 4-OHT. Cells were lysed in TRIZOL reagent (Life Technologies), and total RNA extracted as per recommended procedure. RNA was reverse transcribed with Superscript Vilo cDNA synthesis kit (Life Technologies) and amplified with Platinum Taq Polymerase (Life Technologies) with primers specific for *Meis1* exon7 (5'-TCCACTCGTTCAGGAGGAAC-3') and *Meis1* exon 11(5'-TGCTGACCGTCCATTACAAA-3'). Predicted sizes of amplicons were obtained (428bp, intact exon 8; 282 bp deleted exon 8), gel purified and TOPO-TA cloned into PCR 2.1 Vector (Life Technologies). Individual clones were

sequenced by McGill University Sequencing service with M13Forward and M13Reverse sequencing primers.

Western blot analysis of MEIS1 protein following* in vitro *deletion in MN1-overexpressing cells

pSF91-MN1-GFP transduced *ERTCre/Meis1*$^{fl/fl}$ or *ERTCre/Meis1*$^{fl/+}$ BM cells were cultured for 48 hours in 1μM 4-OHT. $1x10^6$ cells were harvested, spun, and rinsed twice in 2% PBS. The resulting cell pellets were re-suspended in 50μL 1x phosphate solubilization buffer (PSB – 50mM HEPES, 100nM sodium fluoride, 10mM tetrasodium phosphate, 2mM sodium vanadate, 4mM EDTA, 2mM sodium molybdate) and then diluted with 1x RIPA cell lysis buffer (2x: PSB, 1% sodium deoxycholate, 1% NP-40, 5x protease inhibitor cocktail (Roche, Penzberg, Germany)) for a total volume of 100μL. The cell pellet was sonicated for 5x 30 second intervals to homogenize the solution. Samples were prepared according to the NuPAGE Bis-Tris mini-gel kit instructions (Life Technologies) and 20μL loaded onto a 10-well 4-12% Bis-Tris Gel with SeeBlue Plus2 ladder (Life Technologies). Gels were run with MES buffer at 150V for roughly 1 hour. The gel was transferred to nitrocellulose membrane according to with the XCell II blot module according to manufacturers protocol (Life Technologies).

The nitrocellulose membrane was blocked in 5% skim milk powder in 0.1% TBS-T (150mM sodium chloride, 10mM Tris-HCl pH 8, 0.1% tween 20) for 1 hour at room temperature. Rabbit polyclonal to MEIS1 antibody (ab19867, AbCam, Cambridge, UK) was added at a 1:1000 dilution in 5mL fresh 5% skim milk powder in TBS-T (0.3μg/mL) and incubated overnight at 4^{o}C with gentle agitation. The membrane was rinsed 3 times for 15 minutes in TBS-T to remove excess primary antibody. The membrane was then incubated for 1 hour at room temperature with biotinylated goat anti-rabbit IgG (Vector, Burlington, ON,

CAN) at a 1:10 000 dilution (150ng/mL). Following three 15 minute washes in TBS-T, the membrane was incubated for one hour with horseradish peroxidase conjugated streptavidin (SA-HRP, Jackson ImmunoResearch, West Grove, PA) at a 1:10 000 dilution (150ng/mL). The membrane was again washed three times for 15 minutes in TBS-T with a final 15-minute rinse in PBS. Immun-Star HRP chemiluminescence reagents (Bio-Rad, Berkeley, CA, USA) were used to visualize protein levels with light-sensitive film (Kodak, Rochester, NY, USA). The membrane was then stripped with Re-Probe (GBiosciences, St. Louis, MO, USA) to asses equivalent cell loading using GAPDH. The above protocol was repeated using mouse α-GAPDH at a 1:15 000 dilution (Jackson ImmunoResearch, 100ng/mL) and donkey α-mouse-HRP at 1:10 000 (Jackson ImmunoResearch, 150ng/mL) as a secondary antibody.

Histology

The sternum, spleen and, in some cases, the tibia, of mice were isolated and placed directly into 4% paraformaldehyde solution. These specimens were fixed and mounted onto slides by the Provincial Health Services Authority Histology Laboratory (Vancouver, BC, CAN). Slides were stained with hematoxylin and eosin (H&E), anti-CD45R (RA3-62B, BD Pharmingen) or anti-Ter119 antibodies (TER-119, BD Pharmingen) using the Ventana Discovery XT (Roche) machine and protocols. Both anti-CD45R and anti-Ter119 antibodies were used at a 1:50 dilution and linked to anti-rabbit HRP using a rabbit anti-rat antibody (Jackson Immuno Research) secondary at 1:500 dilution.

Q-PCR & Q-RT-PCR

Genomic DNA purification from mouse bone marrow and peripheral blood for $<10^6$ cells was performed with PureLink^{TM} Genomic DNA Mini Kit (Life Technologies). For bone marrow samples of $>10^6$ cells, purification was performed with DNAzol Reagent (Life

Technologies). DNA concentration was quantified by NanoDrop and 25 ng DNA template used per reaction. Q-PCR was performed with the 7900HT Real-Time PCR System (Applied Biosystems) with FastStart Universal SYBR Green MasterMix (Roche). Table 2.4 lists the primer sets used for Q-PCR detection of genomic deletion of the floxed *Meis1* alleles. Primer set NDF (non-deleted floxed) is located between the LoxP sequences and anchored in the 3' LoxP site and is used to detect the non-deleted floxed *Meis1* allele. Primer set DF (deleted floxed) has the forward primer 5' of the 5'LoxP site and the reverse in the targeting vector sequence 3' of the 3' LoxP site such that only the collapsed floxed *Meis1* allele is detected. Control primers sets were used to normalize and confirm genotype. Primer set Floxed CTL uses the 3' targeting vector sequence to detect the floxed allele regardless of collapse wheras the Exon 7 CTL set detects both wild-type and floxed *Meis1* alleles. Control *MxCre/Meis1*$^{-/-}$ and *MxCre/Meis1*$^{fl/fl}$ genomic DNA samples confirmed by Southern Blot analysis to be 100% and 0% collapsed, respectively, were used as calibrator samples in Relative Quantification Analysis using RQ Manager version 2.1 software (Applied Biosystems, Foster City, CA, USA).

For Q-RT-PCR, RNA from the sorted populations listed above (LSK for Affymetrix gene expression analysis, described below) and sorted progenitor/mature populations for *Meis* family expression) was extracted using RNaqueous-Micro Kit (Ambion/Life Technologies) as per manufacturers instructions due to the limiting cell numbers. Approximately 10ng of total RNA was reverse-trancscribed with Superscript®Vilo cDNA Synthesis kit (Life Technologies). Prior to RT-PCR, cDNA was pre-amplified 14 cycles with Taqman PreAmp Mastermix (Applied Biosytems) with the relevant primer sets (Table 2.5) diluted to 1:100 for global amplification of the genes of interest. RT-PCR was performed on

pre-amplified cDNA (0.125 µl per reaction) with Universal Taqman Mastermix (Applied Biosytems) and 6-FAM/ZEN/IBFQ PrimeTime® Assays (Integrated DNA Technologies, Coralville, IA, USA) on a 7900HT Fast Real-Time PCR System (Applied Biosystems). Relative quantification analysis was performed using ABL1 as endogenous control and *MxCre/Meis1*$^{-/-}$ expression was compared to *MxCre/Meis1*$^{-/+}$ expression for each target using RQ Manager version 1.2 Software (Applied Biosystems).

Table 2.5: Primer sets for Q-PCR detection of *Meis1*$^{fl/fl}$ genomic collapse

Name	Detects	Forward	Reverse
NDF	Non-deleted floxed	5' - agcttcatttgaagttccctattg-3'	5'- tattaggtggatccaagcttcatt-3'
DF	Deleted floxed	5'- ctggactttctcctttagttggat-3'	5'- ggaacttcatcagtcaggtacata-3'
Floxed CTL	Floxed (regardless of deletion)	5'-tatgtacctgactgatgaagttcc -3'	5'- gcgtcacttggaaaagcaat-3'
Exon 7 CTL	Endogenous CTL	5'- ttggaatagagaccatgatgacac-3'	5'- gttatccccactgtgtgaagtatg-3'

Table 2.6: Primetime Q-RT-PCR Assays

Primetime Assays	IDT Assay ID
mABL1	Mm.PT.42.14158394
mMeis1	Mm.PT.42.14235881
mMeis2	Mm.PT.45.7421202
mMeis3	Mm.PT.42.9683604
mGata1	Mm.PT.45.10444529
mGata2	Mm.PT.45.13913016.g
mGata3	Mm.PT.45.11120670.g
mPrep1	Mm.PT.45.16285104
mPrep2	Mm.PT.45.14033370
mNotch1	Mm.PT.45.10390781
mIL7r	Mm.PT.45.14297778
mIL18r	Mm.PT.45.11896127
mHbb-b1	Mm.PT.42.10942091
mHbb-b2	Mm.PT.45.10154419
mHlf	Mm.PT.45.15839543
mMpo	Mm.PT.45.15839547
mMsi2	Mm.PT.45.17224408
mPcgf5	Mm.PT.45.10726269
mSelp	Mm.PT.45.16240531
mSenp8	Mm.PT.45.12425187.g
mTyrobp	Mm.PT.45.11022459
mVamp5	Mm.PT.45.5620876
mAurkb	Mm.PT.47.5154422
mCcna2	Mm.PT.47.1386893
mCcnb2	Mm.PT.47.17484650
mCcnd1	Mm.PT.47.12022381
mClec12a	Mm.PT.47.8638109
mDdx4	Mm.PT.47.16947842
mDgat1	Mm.PT.47.12387218
mE2f8	Mm.PT.47.7043043
mFlt3	Mm.PT.47.10501150
mGria3	Mm.PT.47.14084255
mGstm5	Mm.PT.47.11429296
mHes1	Mm.PT.47.8454373.g
mHoxA6	Mm.PT.47.13073650
mPtpn5	Mm.PT.47.10380131.g
mRassf4	Mm.PT.47.15971865
mSfpi1	Mm.PT.47.7508177
mSnx31	Mm.PT.47.15894188
mHIF1α	Mm.PT.47.8983770
mHIF2α	Mm.PT.47.7593249
mP16Ink4a	Mm.PT.47.9881334
mP19Arf	Mm.PT.47.5632963

Affymetrix mRNA array and analysis

RNA was extracted from LSK sorted bone marrow from induced *MxCre*$^{+}$*/Meis1*$^{fl/fl}$ and *MxCre*$^{+}$*/Meis1*$^{+/fl}$ mice with Rnaqueous-Micro Kit (Ambion) as per manufacturers recommended procedure. RNA was concentrated by ultra-centrifugation, amplified and hybridized to the Affymetrix Mouse Exon ST 1.0 Array (Affymetrix, Santa Clara CA, USA) by the BC Cancer Agency Centre for Translational and Applied Genomics (CTAG) using the Ovation Pico WTA System (NuGEN) according to manufacturer's instructions. For the quality control, 100 ng of each amplified cDNA product was tested in two separate runs by Bioanalyzer on an RNA 6000 Nano LapChip (Agilent): 1) before fragmentation and labeling (100 ng of each sample) and 2) after fragmentation and labeling. Input samples passed both the Bioanalyzer trace test for fragment size (>80% less than 200bp) and concentration and purity measurements by A320, A260 and A280 absorbance.

Affymetrix Expression Console software was used for the initial exon- and gene-based probe set signal normalization and log2 summarization. Our analysis was restricted to the well-annotated "core" exons and genes. Data were further adjusted using ComBat (Johnson, Rabinovic, & Li, 2007) to remove batch effects attributable to litter-to-litter variability rather than *Meis1* status. We confirmed that the loss of Meis1 exon 8 was reflected in the exon-based signal intensity. To identify differentially regulated genes, samples were compared by two-tailed T-tests with unequal variance followed by Benjamini-Hochberg correction for multiple hypothesis testing (Benjamini & Hochberg, 1997). The R statistical computing environment was used for batch correction and expression analysis (R Development Core Team, 2009)).

Statistical Analysis

Unpaired, unequal variance, two-tailed, Student's T-tests were perfomed to determined statistical significance between *Meis1*$^{-/-}$ and control samples in Vet Analyzer samples, all semi-solid colony forming assays (CFC & CFU-Mk), RT-PCR, Q-RT-PCR and FACS analyses. Unpaired, unequal variance, two-tailed Student's T-tests were also used to compare the peripheral blood engraftment between *MxCre/Meis1*$^{fl/+}$ and *MxCre/Meis1*$^{fl/fl}$ mice prior to and following PolyI:C induction. LTRC and LTC-IC frequency and testing for significant differences between groups was performed using the Extreme Limiting Dilution Analysis (ELDA) online tool (http://bioinf.wehi.edu.au/software/elda), which utilizes Poission distribution analysis (Szilvassy *et al.*, 1990). As described above, for the Affymetrix expression analysis, data were first normalized and summarized using the Affymetrix Expression Console software then adjusted using ComBat (Johnson, Rabinovic, & Li, 2007) to remove batch effects attributable to litter-to-litter variability rather than *Meis1* status. Samples were compared by two-tailed T-tests with unequal variance followed by Benjamini-Hochberg correction for multiple hypothesis testing (Benjamini & Hochberg, 1999)

Chapter 3 : Validation of Conditional *Meis1* Knock-Out Models

Introduction

The development of knockout mouse models has revolutionized gene function studies in the mammalian system. Such models have been instrumental in understanding the role of a wide range of genes critical for normal and leukemic hematopoiesis. Previous *Meis1* knockout models were limited by embryonic lethality. Hisa *et al.* disrupted embryonic expression of *Meis1* using a βgeo gene trap cassette into exon 8 of *Meis1,* which allowed monitoring of embryonic stage and cell type specific expression of *Meis1* through β-galactosidase expression (Hisa *et al*., 2004). This study showed that in the absence of *Meis1*, embryos do not survive past 14.5 days post coitus (dpc) and display massive hemorrhaging due to an absence of megakaryocytes. In addition, the embryos lack well-formed capillaries and have smaller lenses and partially duplicated retinas in the eye. The key results of this study were confirmed by Azcoitia *et al.*, (Azcoitia *et al.*, 2005) who attempted to generate an inducible model of Meis1 protein function by generating a fusion gene between *Meis1* and ER^{TM}. Theoretically, this protein should be sequestered to the cytoplasm in the absence of the synthetic estrogen-receptor ligand, tamoxifen, however, rescue experiments failed to correct embryonic lethality with *in vivo* tamoxifen administration to pregnant mice. Strikingly, both studies in analysis of fetal liver of $Meis1^{-/-}$ mice found a reduction of primitive hematopoietic cell number (KSL cells) as assessed by FACS (Azoitia et al, 2005) or loss of repopulation capacity as assessed by transplantation (Hisa et al., 2004) suggestive of a significant impairment in the number and/or function of HSC. However, these available models left

unanswered important questions concerning the role of Meis1 in later stages of ontogeny and in adult life.

Increasing evidence points to major differences in the properties and regulation of primitive hematopoietic cells in early ontogeny/embryonic versus post embryonic and adult stages of life. Around the time of birth, HSC activity moves from the fetal liver to bone marrow (Reviewed in Orkin & Zon, 2008). Both fetal liver and bone marrow HSC are termed to be "definitive", that is, they can give rise to the full spectrum of mature blood cell types when transplanted into lethally irradiated recipients (Müller *et al.,* 1994). Differences between fetal liver and bone marrow definitive HSC have been noted, however, as well as differences in bone marrow HSC in the peri-natal period compared to that of the adult. Fetal liver HSC show higher engraftment and mature cell output as well as self-renewal *in vivo* compared to adult bone marrow (Rebel *et al.*, 1996). Bone marrow HSC isolated in the first three weeks after birth demonstrate similar reconstitution and expression profiles to fetal liver HSC (Bowie *et al.*, 2007), suggesting that there are substantial differences between adult and fetal HSC.

Further support for differences in gene regulation between adult and fetal HSC comes from knock-out studies where a gene triggering embryonic lethality post-HSC development is not required in the adult. For example, loss of *Aml1* (*Runx1*) is embryonic by 12.5dpc and results in a complete absence of definitive hematopoiesis (Okuda *et al.*, 1996). In the adult however, absence of AML-1 results in a far subtler phenotype, with relatively normal engraftment with the exception of megakaryocyte, T -and B- cell maturation following transplantation (Ichikawa *et al.*, 2004). Disparities in the requirement between embryonic

and adult hematopoiesis have also been observed with *Scl(Tal), Mll* and *Tel/Etv6* (Mikkola *et al.,* 2003; McMahon *et al.*, 2007; Hock *et al*., 2004).

A conditional model of *Meis1* deletion would also be of use in the study of leukemogenesis. Several lines of evidence highlighted in the introduction of this thesis suggest a pivotal role for *Meis1* in the development of both *Hox* and non-*Hox* leukemias. For instance, it has been established that the oncogenicity of various *Mll* fusions is linked to the extent to which *Meis1* expression is up-regulated (Wong *et al.*, 2007) and that sh-RNA knock-down of *Meis1* triggers cell cycle arrest and delays the establishment of leukemia *in vivo* (Kumar *et al.*, 2009). It remains unknown, once a leukemia is established *in vivo,* if *Meis1* is required for the survival of the LSC clone or if loss of *Meis1* would have a significant impact on LSC number. The critical transcriptional networks controlled by *Meis1* expression are also not yet clear.

To overcome the embryonic lethality associated with previous knockout models and enable studies in the setting of adult hematopoiesis (normal and leukemic), efforts in our lab were directed towards developing a conditional knockout model for *Meis1*. Fortuitously at this same time, Dr. Nancy Jenkins and Dr. Neal Copeland in personal communication revealed that they had successfully generated a conditional knockout mouse line for *Meis1* based on the Cre/LoxP system. However, details of the nature of the targeting construct and resultant "floxed" region of the *Meis1* gene were not available beyond an understanding that "exon 8" had been targeted. Upon receipt of breeding pairs for this mouse line, initial efforts as described in this chapter were devoted to characterizing the precise nature of the floxed allele and subsequent validation and optimization of strategies for efficient induction of *Meis1* deletion both *in vivo* and *in vitro*. To these ends we first localized the position of the

two loxP sites flanking exon 8 and then validated the induction of Cre expression and subsequent floxed allele deletion *in vivo* using two inducible models of Cre expression (Mx-Cre and ERT-Cre, described below).

We confirmed the generation of a truncated RNA *Meis1* transcript and loss of protein expression following Cre expression. In addition, we developed Q-PCR tools to monitor in a quantitative manner the extent of genomic collapse and related changes in *Meis1* RNA expression. In order to focus our future investigations using the model we surveyed *Meis* family expression in the hematopoietic hierarchy in purified HSC, progenitor and differentiated cell enriched populations.

Results and Discussion

Identification of LoxP sites flanking Meis1 *in* B6-Meis1$^{tgLoxP/+}$ *mice*

Male *B6-Meis1*$^{tgLoxP/+}$ (*B6-Meis1*$^{fl/+}$) mice were a generous gift from Drs N. Jenkins and N. Copeland. The mice had been engineered with LoxP sites flanking exon 8 of *Meis1*, however for a variety of reasons, details on the exact position of the LoxP sites flanking exon 8 were not available when the mice were received in our lab. Based on the *Meis1* RefGene sequence and the sequence of the primers provided for genotyping, it was determined that one of the LoxP sites (and accompanying targeting vector sequence) was positioned 3' of exon 8 in intron 8 (anti-sense strand chromosome 11, 18 941 409; Dec. 2011(GRCm38/mm10 assembly))**.** With one site fixed, we used *in vitro* Cre expression by retrovirus, followed by Southern blot analysis to determine the collapsed fragment size, and thus likely location.

B6-Meis1$^{+/fl}$ bone marrow was infected with MSCV-CRE-PURO retrovirus (as described in the methods and materials) and selected for 4 days with 0, 1.6 or 3.2 µg/mL puromycin. DNA from the selected cells was digested with HindIII and EcoRI for Southern blot analysis. Probes specific to *Meis1* genomic regions flanking the known LoxP site 3' to exon 8 were generated by PCR. Compared to the size of the anticipated wild-type band, an additional hybridization band was detected using a probe 5' to exon 8 in *B6-Meis1*$^{+/fl}$ bone marrow. This band disappeared upon expression of Cre recombinase, supporting the presence of the second LoxP site 5' of exon 8. (Figure 3.1, Table 2.1).

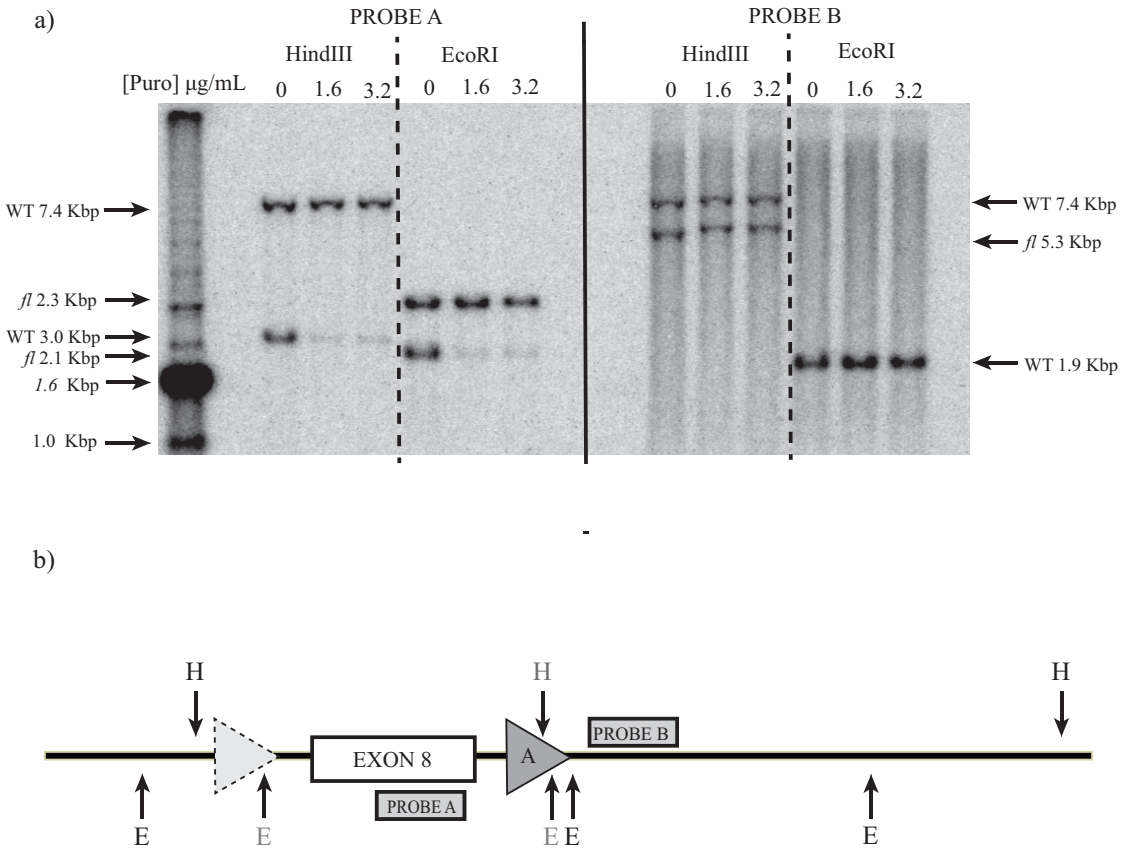

Figure 3.1: Southern blot analysis to localize the second LoxP site 3' or 5' to the known site.
a) Southern blot of Meisfl/+ 5-FU bone marrow infected with MSCV-Cre-Puro following selection with 0, 1.6 or 3.2 μg/mL puromycin and digested with HindIII or EcoRI. Probe A was designed to detect a change in hybridization signal if the second LoxP site was 5' to the known site (LoxP-A), whereas probe B was designed to detect a LoxP 3' to the known site. Following selection for Cre expressing cells, there is a loss in the HindIII and EcoRI hybridization signal with probe A, indicating the unknown LoxP site is 5' to LoxP-A. No change is seen with probe B. b) Schematic representation of the Meis1fl loci around Exon 8. The LoxP-A is represented as grey triangle "A". For clarity the determined position of the unknown LoxP site is included as a dashed triangle. H represents HindIII sites. E represents EcoRI sites. Restriction sites in the wild-type allele are in black type while sites introduced by the targeting vector are in grey.

The location of the LoxP sites flanking exon 8 were confirmed using a series of sequence specific primers for extending regions of intron 7 (Table 3.1, Figure 3.2). These were used in concert with 2 reverse primers in an attempt to amplify the region of the mutant allele containing both LoxP sites. MeisCKO Rev1 is anchored to the known LoxP site 3' of exon 8 and was designed to detect the targeted and uncollapsed allele as deletion of exon 8 by Cre recombinase will eliminate the site. MeisCKO Rev2 is located 3' of the 3' LoxP site in wild-type genomic DNA and remains intact regardless of exon 8 excision by Cre. The PCR analysis was performed on DNA from both selected and unselected *B6-Meis1*$^{+/fl}$ bone marrow infected with MSCV-CRE-PURO. The combination of Rev2/Intron 7 primer 3 revealed a significant size difference from the anticipated wild-type band, suggesting that the second LoxP site was 3' of this primer and captured in the Rev2/Intron 7 amplicon. This material and from Intron7 Primer 3/MeisCKO Rev1 was cloned into the TOPO TA PCR2.1 vector and sent for sequencing. Sequencing confirmed the presence of the 5' LoxP site (anti-sense strand chromosome 11 18943409; Dec. 2011(GRCm38/mm10 assembly))**.**

The presence and position of both LoxP sites was confirmed in the non-deleted mutant allele by sequence analysis. Additionally, the deletion of genomic sequence

containing exon 8 between these LoxP sites leaving a single remaining LoxP site was confirmed. Cre-mediated deletion of the *Meis1*$^{fl/fl}$ allele results in a loss of 2104bp in the targeted Meis1 locus (1998 of wild-type *Meis1* locus). Collapse of the LoxP sites following Cre expression should result in a frame-shift and premature stop codon 15 bases into exon 9 in the processed RNA sequence (Figure 3.3)

Table 3.1: "Walking" Intron 7 primers sequence and anticipated fragment sizes.
Sequence tethered in the LoxP site is highlighted in bold.

Name	Sequence	Anticipated size with Meis CKO rev1 (no Cre expression)	Anticipated size with MeisCKO rev1 (Cre expression)	Anticipated size with MeisCKO rev2 (no Cre expression)	Anticipated size with MeisCKO rev2 (Cre expression)
MeisCKO Rev1	5'- **GAA GTT ATT** AGG TGG ATC CAA GCT -3'	n/a	n/a	n/a	n/a
MeisCKO Rev2	5'- AGC GTC ACT TGG AAA AGC AAT GAT-3'	n/a	n/a	n/a	n/a
Intron7 Primer1	5' – GAT TTG ATG CTC TTG CGA CA – 3'	~1, 000 bp	**0**	~1, 100 bp	**0**
Intron7 Primer2	5'- GCC GTG TAA CTG CCA TAG GT -3'	~1, 700 bp	0	~1, 800 bp	0
Intron 7 Primer3	5'-TCT GAA GGG GTT TGA GAT GG -3'	~2, 500 bp	0	~2, 600 bp	0

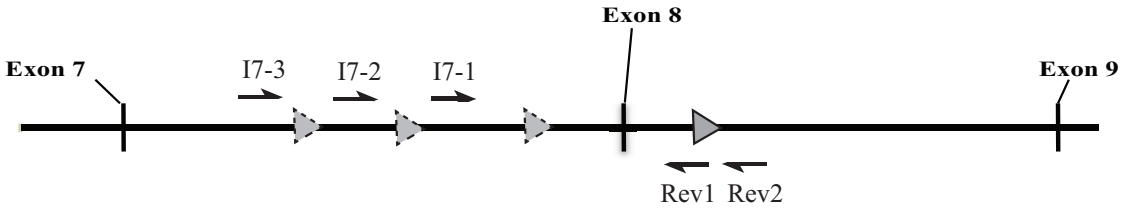

Figure 3.2: Schematic representation of Intron 7 primers to narrow the position of the second LoxP site.
I7-1: Intron 7 primer1. I7-2: Intron 7 primer 2. I7-3: Intron 7 primer 3. Rev1: MeisCKO Rev1. Rev2: MeisCKO Rev2. Primer sequences found in Table 3.1. LoxP-A site is denoted

as a solid grey triangle. The putative locations that the Intron 7 primers would detect are represented as dashed triangles. The primers were designed such that when Cre expression was introduced, presence of an amplification product with Rev2 and the intron 7 primers would indicate the presence of the LoxP site between the primer binding sequences. For example, if the second LoxP site was located between I7-2 and I7-3, with Cre expression, there would be no amplification product with I7-1 and Rev2 as the primer binding site would be lost with LoxP site collapse. I7-2 and Rev2 would generate an amplification product whose size would help narrow the position of the second LoxP site. Sequencing of the amplification products confirmed the location of the second LoxP site (LoxP-B) beteween primers I7-3 and I7-2.

```
18943465    CCATGTGACA CTGAAAATCT GGACTTTCTC CTTTAGTTGG ATGGGCTGAT GGCTTTAGGG
            ATCCCCTCGA GGGACCTAAT AACTTCGTAT AGCATACATT ATACGAAGTT ATATTATTAA
            GGGTTATTGA ATATGATCGG AATTGGGCTG CAGGAATTCG ATATCTGTGT TGGGGTCTTC
18943395    GTAATCTTTT CTAGAAAGAA CTCAGTCTAT GAGCCCAGGA AACCTTCATG ACTTATATAG
18943335    ATATTAAATG CACTAAACTT ATTATAGATG TTTTATAAAA GTTTACATTA CAAGAAGCTC
18943275    TGCCAAAACT CATGGTGGTA TAGCTCTACT AACAGTCGAA ATGTTGGAAT CCATCTGCTC
18943215    CTGACTAGAA GGAGTTTATC TCTGAACACA TTAAGACAAG TGAAAGCCAG CAGGGGTCAC
18943155    TTTTCACATG CCACAAGGGT GGGGCATGAG TTTCCTGATA CAATAGTTGT GAACAATTGA
18943095    AGATCTGCCG TGTAACTGCC ATAGGTTACT AGAATGAATG AAATCCAACT AGCAACCCTT
18943035    GTTGCACTGA GGACTTAGAG TAGCAACAAG TGATGGAAGA AGTGAAGCCA TGGACGAAAG
18942975    TCTAATGGGA GTACCAATAG GTAGTAGCCA TCGGGGAAGT GTACTAGCAA AGTGTCCAGT
18942915    TCTTAGGACC ATAGGTTCCC AATGACTTTA GTGGGATGAG GGTGCCCTGG GGTGTGGTTG
18942855    CTACCGCACG TTGAAGCCTG GCTATTGTAG CTTTTCATTC TGGGCCCAGA TCAATCAGTC
18942795    CATTTCCCTG ATAAGACGTG TCAGAGCACA GCTGCTGATC AGGATAGTGG GTTTAGTCCA
18942735    TTGTTATTTG TCCTTTGACT TTGGTGCAAA GATCAAAAAT AGGTATTTCT AATGTAGGTC
18942675    TTGATATATA TTACATGGGT AACTTTTTCT CATCTTATCA TATATGGCAT TATTACAGTA
18942615    ATACTGTATT ATCTTTTTAC TGAGTTACAG AGATCAAGTA TTTCCTAAAA TAAGCAACTC
18942555    AAGTGTTTAT AACAAATGCC AGTAGAAAAA TTGGATCCTT TAGGAATATG TTACCAGGTG
18942495    ACCTCTCAGT GAGTGATCCT TGAAGAAAAA AATGTAGAAA CTGCCCAGGT TATTAGTGAG
18942435    ATGCAATTCT AACATTACTT TATTTTACTT CAATTGCAAT TATTTTGTAA TTAAAAACTA
18942375    TGTCAGGGGG TTTCCCTTAC TGGATTTGAT GCTCTTGCGA CACTAAGCAA AATTATATCT
18942315    CTCCTTTGAA GCATTCCATG ACAAATTGCT TATGTGATGG ATTGCCTGCA GTTTCCCATG
18942255    CTGCTCCCAC CCCCACCAGT CTGAAGATAG ATCACCTGTG GCAGCAGTTG CTGTATTAAA
18942195    TGCATCTTCT TACCAGTTGA CGTCAGTGAC TTTATATGGA GTTCAAATAC TCAGAGACCC
18942135    CCACTAACCA TGTCACCACA CTGAACTCCC CAGTAGAGGT ATTACATATA CTGAAATAAT
18942075    TACCATGGCA ACAAAGCCAC TCAAGAGATG GATATTTCCC TCCAGTCCTT TTGCCTTTAT
18942015    TACTGATCTT TGAAAGATTT TTTTTATAG GCATGATTAT TTTTTAGTTG AGACCTTGTT
18941955    CTTTCTCTTT GTCTTGGAAT TTAAAAAAAG TACCAAAGAA ACTACTAATC CTTTAATTGA
18941895    TCTTTTGGTT TTGTTTGTAT CCAAAGGCAT TCTATTTGAA TAAAGCATGT TAAGGTAGCA
18941835    TCAGTCAAAA TTTGATTCAC TATATTTGCA G***GTGATGGCT TGGACAACAG TGTAGCTTCC***
18941775    ***CCCAGCACAG GTGACGATGA TGACCCTGAT AAGGACAAAA AGCGTCACAA AAAGCGTGGC***
18941715    ***ATCTTTCCCA AAGTAGCCAC CAATATCATG AGGGCGTGGC TGTTCCAGCA TCTAACA***GTA
18941655    AGTGGATTCT AAATGACATA TGTAAACTAA ATATGGACAA TGAACCAGTT TTGATAGAGA
18941595    AAAAAACGAT CCCTCTGCGC TTCCTACATC ACTGTGTTCC CCATTTTTAA CCAAGGGTTA
18941535    GCACTTATTT TCTAGACCCA TACCCTAAAA ATCAGGAGCT TCATTTGAAG TTCCCTATTG
18941475    TAATTGTGTT AATTTTCAAA AGTTATAAGG CTCGGGAGTC CATGTGTACT TGTGCTTTTA
18941415    TGAATGAAGC TTGGATCCAC CTAATAACTT CGTATAGCAT ACATTATACG AAGTTATATT
            ATGTACCTGA CTGATGAAGT TCCTATACTT TCTAGAGAAT AGGAACTTCG GAATTCTATG
18941405    TTAATATCAT TGCTTTTCCA AGTGACGCTG AAGTGCTTCC AGCTAGTTAC TAAACTTTCT
18941345    AAAAGGAAAG TAAAACCCTT CCTCGAGATG GTAACTGGAG TGAGCACTGC AGTGGACCCT
```

Figure 3.3: Sequence of targeted Meis1 allele.
The sequence is numbered according to the wild-type sequence on the antisense strand of chromosome 11 according to the Dec. 2011 (GRCm38/mm10) sequence from the Mouse Genome Reference Consortium. Non-wild-type sequence introduced by the targeting vector

is underlined while the LoxP sites are highlighted in grey. Exon 8 is denoted in italicized-bold type.

*Breeding of B6-***Meis1$^{fl/fl}$***/ B6;129*Gt(ROSA)26Sor$^{tm1(cre/ERT)Nat}$*/J and B6-*Meis1$^{fl/fl}$*/ B6.Cg-Tg(Mx1-cre)1Cgn/J mice***

The Mx-Cre (Kühn *et al.*, 1995) and ERT-Cre (Hayashi and McMahon, 2002) mouse lines were used to generate an inducible model of *Meis1* deletion in adult B6-*Meis1$^{fl/fl}$* mice. The Mx-Cre mouse line allows for induction of interferon inducible Cre expression using polyinosinic-polycytidylic acid (Poly:IC), a synthetic double stranded RNA that mimics viral infection (Kühn *et al.*, 1995). In the case of the ER^{TM}-Cre (ERT-Cre) line, *Rosa26* driven Cre expression is controlled at the level of cellular localization of the fusion protein consisting of a mutant form of the estrogen receptor (ER^{TM}), which cannot bind it's natural ligand 17β-estradiol and Cre recombinase. In the absence of the synthetic ligand 4-hydroxy-tamoxifen (4-OHT), ER^{TM}-Cre is sequestered in the cellular cytoplasm. Upon IP delivery of 4-OHT to the mouse, ER^{TM}-Cre moves to the nucleus to promote efficient Cre-LoxP excision in many tissues, including bone marrow (Badea *et al.,* 2003; Jo *et al.*, 2011).

B6-*Meis$^{+/fl}$* mice were bred onto the B6;129*Gt(ROSA)26Sor$^{tm1(cre/ERT)Nat}$*/J background (generous gift from A. Weng), for 4-OHT responsive gene deletion, and the B6.Cg-Tg(Mx1-cre)1Cgn/J background (Jackson Laboratories) for Poly:IC induced deletion. Progeny from these pairing were interbred to generate B6-*Meis1$^{fl/fl}$*/ B6;129*Gt(ROSA)26Sor$^{tm1(cre/ERT)Nat}$*/J (*ERTCre/Meis1$^{fl/fl}$*) and B6-*Meis1$^{fl/fl}$*/ B6.Cg-Tg(Mx1-cre)1Cgn/J mice (*MxCre/Meis1$^{fl/fl}$*). Mice from both strains were born in expected numbers and appropriate frequencies, suggesting that there was no selection against untreated *MxCre/Meis1$^{fl/fl}$* or *ERTCre/Meis1$^{fl/fl}$* germ cells or embryos *in vivo*.

Induction regimen of* MxCre/Meis1$^{fl/fl}$ *and* ERTCre/Meis1$^{fl/fl}$ *mice* in vivo *and generation of tools to quantitatively measure* Meis1$^{fl/fl}$ *deletion

A variety of induction schemes for both the *MxCre* and *ERTCre* models have been reported in the literature. For example, in the *MxCre* model, three to nine intraperitoneal injections of Poly:IC at 10μg/g every other day have been reported to be required for complete collapse of the target of interest in hematopoietic cells (Shinnick *et al*., 2010; Lieu & Reddy, 2009). Single monthly injections to consecutive daily injections for 5 days of 130 to 200μg/g of 4-hydroxytamoxifen (4-OHT) have been reported in the *ERTCre* and *ERT2Cre* models (Jo *et al.,* 2011; Gan *et al.*, 2008; Gurumurthy *et al.*, 2010).

Starting with the *MxCre/Meis1* model, we first tested three 300μg Poly:IC injections spaced 48 hours apart and measured *Meis1$^{fl/fl}$* deletion by Southern blot analysis. In these mice the deletion was variable with as little as 46% deletion in spleen and 86% in bone marrow (Figure 3.4, panel a). An increase in dosing to 9 injections at the same 48 hour interval resulted in >98% deletion of the floxed *Meis1* allele in bone marrow as measured by Southern blot (Figure 3.4, panel B). Based on these results, an induction regimen for *MxCre/Meis1* of 9 injections of 300μg Poly:IC every 48 hours) was selected for future experiments.

The induction scheme for *ERTCre/Meis1* (1mg 4-OHT/mouse every 48 hours for 6 injections) was initially chosen based on published reports (Gurumurthy *et al.*, 2010) and the experience of personnel using the strain in another lab. This scheme also yielded >98% deletion of the floxed *Meis1* allele in bone marrow as measured by Southern blot (Figure 3.4, panel b).

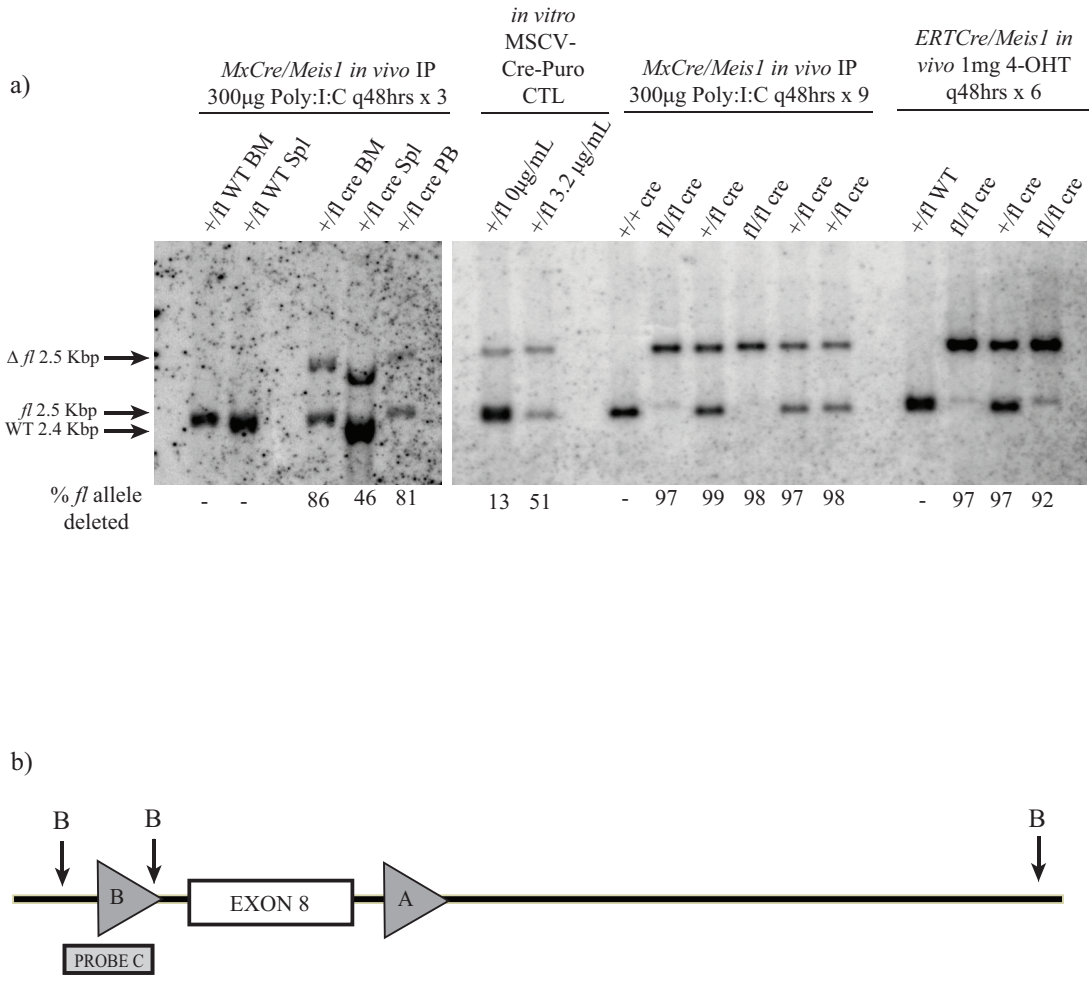

Figure 3.4: Southern blot analysis to localize the second LoxP site to 3' or 5' to the known site

a) Southern blot of loxP targeted *Meis1* tissues using various induction schemes for in vivo induction of Cre expression in *MxCre/Meis1*^{tg} and *ERTCre/Meis1*^{tg} mice. Tissue-derived DNA was digested with BamHI and probed in the region anchored in loxP-B. Percent deletion of the floxed *Meis1* allele was calculated using densitometry software (ImageQuant, GE). One of each *Meis1*$^{+/fl}$ and *MxCre/Meis1*$^{+/fl}$ mice were used in the first 3 injection induction experiment whereas a total of 6 *MxCre/Meis1*$^{+/+}$, *MxCre/Meis1*$^{fl/+}$ and *MxCre/Meis1*$^{fl/fl}$ mice were used in the second attempt. 2 *ERTCre/Meis1*$^{fl/fl}$ mice were compared to a *ERTCre/Meis1*$^{fl/+}$and *Meis1*$^{fl/fl}$ mouse. Mice were assessed 2 days after the last IP injection. b) Schematic representation of the *Meis1*^{fl} loci around Exon 8 with BglIII restriction endonuclease sites (B) and Southern probe location.

As key populations of interest in our studies such as HSC represent a small portion (0.0001%) of the total bone marrow, we also sought a method applicable to small cell numbers for accurately measuring the extent of *Meis1* deletion at the level of DNA and the reduction in *Meis1* expression at the RNA level. To accomplish this we generated Q-PCR primer sets that would allow quantitative detection of both the floxed intact and collapsed alleles using SYBR reagent with floxed and endogenous controls (Figure 3.5, Table 3.2). Primer set NDF (non-deleted floxed) amplifies the region between exon 8 and the 3' loxP site (LoxP-A). The reverse primer is anchored in the 5'region of LoxP-A such that only intact, $Meis1^{fl}$ alleles are amplified. Primer set DF (deleted floxed) uses sequences 5' of the LoxP-A site and 3' of LoxP-B site in targeting vector sequence such that a product is only efficiently generated following Cre mediated collapse of the loxP sites. The floxed CTL primers detect the floxed allele regardless of collapse due to positioning of the forward primer in the 3' of region of LoxP-A in the targeting vector sequence and the reverse primer in endogenous *Meis1* sequence. Primer set exon 7 CTL is a control for levels of both wild-type and targeted *Meis1* alleles. By comparing the CT values between the primer sets using the spleen DNA controls described below, it is possible to both confirm the genotype of the mice in the sample as well as the degree of collapse between the loxP sequences.

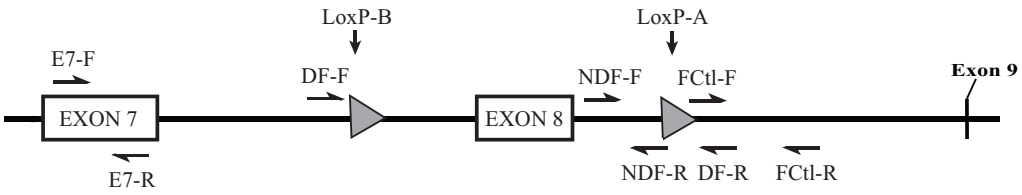

Figure 3.5: Schematic representation of Q-PCR primers for quantitative determination of Meis1^{fl} deletion.
These 4 sets of Q-PCR primers allow the quantitation of the floxed allele in a sample, regardless of deletion (FCtl), as well as non-deleted and deleted Meis1fl alleles (NDR and DF, respectively). Exon 7 (E7) primers serve as a control for the quantity of Meis1 DNA in the sample, be it wild-type or floxed.

Table 3.2: QPCR Primers for Genotyping and Detection of *Meis1^{fl}* Deletion

Name	Detects	Forward	Reverse
NDF	Non-deleted floxed	5'-agcttcatttgaagttccctattg-3'	5'-tattaggtggatccaagcttcatt-3'
DF	Deleted floxed	5'-ctggactttctcctttagttggat-3'	5'-ggaacttcatcagtcaggtacata-3'
Floxed CTL (FCtl)	Floxed (regardless of deletion)	5'-tatagtacctgactgatgaagttcc-3'	5'-gcgtcacttggaaaagcaat-3'
Exon 7 CTL (E7)	Endogenous control	5'-ttggaatagagaccatgatgacac-3'	5'-gttatccccactgtgtgaagtatg-3'

Spleen DNA from a *MxWT/Meis1$^{fl/fl}$* (C0) mouse and a *MxCre/Meis1$^{-/-}$* (C100) mouse that were 0% and >98% deleted as assessed by Southern blot were used to determine optimal primer sets in terms of efficiency and accuracy for a given percent genomic DNA collapse. Primer set efficiencies were tested by a series of five 2-fold serial dilutions from 25ng of DNA against appropriate samples for the primer sets. When plotted on a log2 scale, the slope of the CT values against the DNA dilution fell between 1.0 and 1.1, suggesting the efficiencies of all 4 primer sets are within the acceptable range and roughly equivalent. Varying proportions of C0 and C100 DNA were mixed to determine the accuracy of each primer set at a given deletion threshold. For example, when an allele is approaching 75-100% collapse, sample comparison to C0 using primer set NDF (detects the remaining intact floxed allele) is more accurate due to a larger ΔCT between the samples. We also used intron spanning RT-PCR primers to measure the amount of *Meis1* transcript containing exon 8 remaining (IDT PrimeTime Mm.PT.42.14235881). When the loss of exon 8 at the level of

DNA is >98% in a *Meis*$^{fl/fl}$ mouse, the loss of transcript is consistently >500-fold compared to a *Meis1*$^{-/+}$ control.

Confirmation of truncated transcript and protein expression in* ERTCre/Meis1 *mice

With *in vivo* induction schemes established for both the *ERTCre/Meis1* and *MxCre/Meis1* mouse models, we wanted to determine if collapse of the floxed exon 8 resulted in the expression of a Meis1 transcript and detectable truncated protein product. We first investigated whether there was expression of an exon 8 collapsed RNA transcript in *in vivo* treated mice by isolating splenocytes from *ERTCre/Meis1* mice treated every other day with 1mg/mouse 4-OHT as per the established induction scheme (*ERTCre/Meis1*$^{-/-}$, *ERTCre/Meis1*$^{-/+}$, and *ERTCre/Meis1*$^{+/+}$ mice). Total RNA was extracted and *Meis1* exon 7 and 11 primers used to amplify the segment of interest following reverse transcription. The amplified fragment was then cloned into the TOPO-TA vector and individual clones sent for sequencing. Sequencing results revealed that the expected sequence, with a frameshift mutation and premature stop codon in exon 9, was produced in treated *ERTCre/Meis1*$^{-/-}$ and *ERTCre/Meis1*$^{-/+}$ mice (Figure 3.6).

Figure 3.6: Sequencing results confirming introduction of premature stop codon in exon 9 of *Meis1*^{fl} with expression of Cre recombinase.
cDNA from *ERTCre/Meis1*$^{-/+}$, *ERTCre/Meis1*$^{-/-}$, and *ERTCre/Meis1*$^{+/+}$ splenocytes was amplified using primers in exon 7 and exon 11 and cloned into the TOPO-TA vector for sequencing. Sequencing of the clones confirmed generation of the predicted transcipt with a premature stop codon in exon 9 following Cre recombinase expression.

As a mutant RNA transcript was expressed in these mice, we went on to perform western blot analysis to confirm loss of full-length MEIS1 protein and investigate the possibility of expression of a truncated mutant protein (Figure 3.7a). As a large number of cells is required for western blotting and due to the limited cell populations in which *Meis1* is expressed, we chose to use *ERTCre/Meis1*$^{fl/fl}$ marrow expanded by retroviral expression of the oncogene *MN1* (Heuser *et al*., 2007). *ERTCre/Meis1*$^{fl/fl}$ marrow cells were infected, sorted for *MN1* expression based on co-expression of green fluorescence protein (GFP) by FACS, expanded in culture for 20 days and then treated with either 4-OHT or the carrier control (EtOH) *in vitro* for 48 hours. The Western blot was probed for MEIS1 using a polyclonal rabbit αMEIS1 antibody raised against residues 200-300 of MEIS1, as well as GAPDH as a loading control. Developed blots from the EtOH treated cells showed a band at the expected size for MEIS1a at 43KDa. An additional band at roughly 28KDa was detected which may correspond to *MEIS1D,* an isoform of *Meis1* previously reported in colorectal cancer (Crist *et al.*, 2011). Following 4-OHT induction, the band at 43KDa is completely absent, suggesting no wild-type MEIS1 protein is produced following *Meis1* exon 8 deletion. The 28KDa band present in the EtOH treated cells is also fainter and a stronger band at 27KDa is seen (Figure 3.7b). The band at 27KDa may represent expression of a truncated MEIS1 protein generated with the loss of exon 8 and premature stop in exon 9 (MEIS251) as it is at the expected molecular weight.

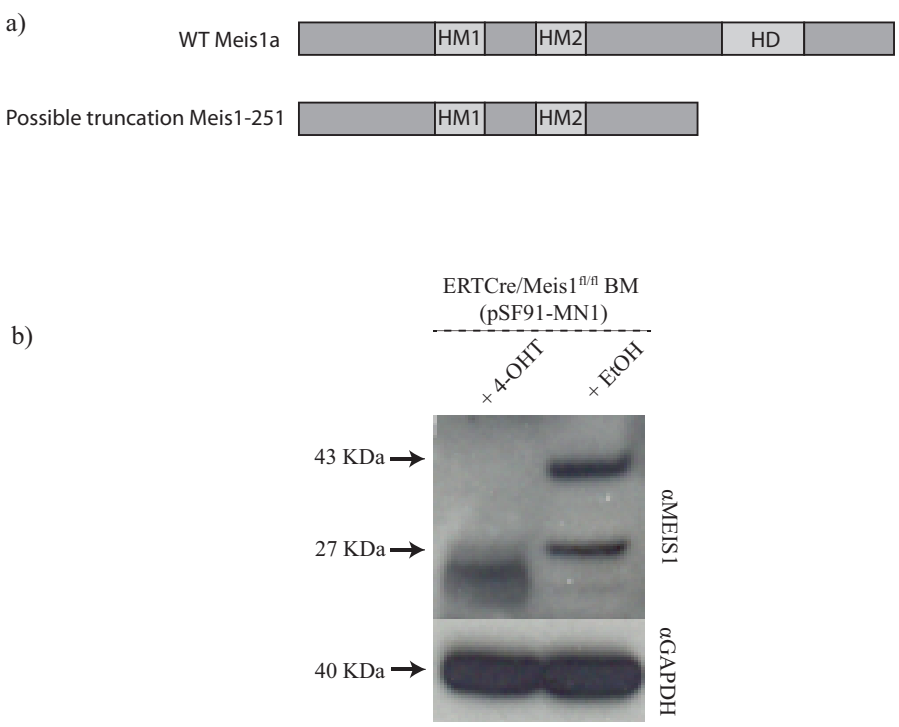

Figure 3.7: Western blot analysis confirming loss of MEIS1 protein following in vitro induction of Cre expression in mouse bone marrow expanded with pSF91-MN1 retrovirus.
a) Schematic representation of wild-type (WT) and possible truncated (MEIS251) protein due to Meis1fl/fl deletion by Cre-recombinase b) Due to the low level of MEIS1 expression in bulk marrow and the cell number required for Western blot analysis, bone marrow from 5-FU pre-treated *ERTCre/Meis1$^{fl/fl}$* mice was infected with a retrovirus to cause overexpression of the oncogene MN1 to expand a primitive population of MEIS1 expressing cells. Following induction of Cre expression with 4-OHT, there is loss of full-length MEIS1A protein as expected. The blots were stripped and re-probed with GAPDH antibody as a loading control.

Overexpression of a truncated protein does not interfere with CFC potential or re-plating

As MEIS251 retains PBX interaction motifs and may be expressed in our knock-out model, we wanted to investigate the possibility that MEIS251 could serve as a double mutation eg. serving as a dominant negative form of Meis1 by interfering with PBX1

availability by binding PBX protein and interfering with DNA binding. To do this, we chose to use a NUP98-HOXD13(ND13) model of overexpression in bone marrow progenitors and monitor the impact of MEIS251 on serial re-plating as compared to MEIS1A. Co-expression of Meis1 with ND13 has been shown in our lab to enhance the colony-forming frequency in semi-solid media in these cells (Pineault *et al.*, 2005), thus we reasoned that if MEIS251 served as a dominant negative, a negative impact on serial plating would be seen in isolation or in combination with ND13.

5-FU pre-treated bone marrow from a C57Bl6/J mouse was harvested and infected by producer co-culture with retrovirus expressing ND13-GFP, MEIS1A-YFP, MEIS1B-YFP, MEIS251-YFP or a combination of ND13 + MEIS. Cells were isolated, pre-stimulated, infected and sorted as described in Chapter 2. The retrovirally-transduced cells were plated into methycellulose cultures 2 days following sorting (9 days from harvest) grown for 7 days, counted, harvested and re-plated for a total of 3 platings. This was performed in triplicate. No significant differences in re-plating were seen in MEIS251 compared to MEIS1a cultures or ND13+MEIS251 or ND13+MEIS1a cultures (Figure 3.8). There was a significant difference between ND13+MEIS1/MEIS251 cultures and the MEIS1/MEIS251 culture alone ($p<0.05$).

This argues against a strong dominant negative effect of the truncated MEIS251 protein if it is expressed in significant amounts. There remains the possibility, however, that the truncated protein could exert an effect on a *Meis1* knockout background that was not evaluated in these experiments. A lack of dominant negative effect on a *Meis1* knock-out background is suggested by Hisa *et al.* (Hisa *et al.*, 2004) and their *Meis1-βgal* gene trap knock-out. The resultant truncation protein in their model is similar to ours, however, no differences were observed between heterozygous and wild-type littermates, arguing against a

strong dominant negative effect of the truncation (Hisa *et al.*, 2004). In several early experiments reported in Chapter 4, we included Cre-expressing *Meis1*$^{+/+}$ mice on the ERT-Cre and Mx-Cre background and found no significant differences between these mice and mice heterozygous for *Meis1*$^{-/+}$. This may not be surprising as other MEIS family members such as PREP1, MEIS2 and MEIS3 also induce nuclear accumulation of PBX1 when over-expressed (Saleh *et al.*, 2000).

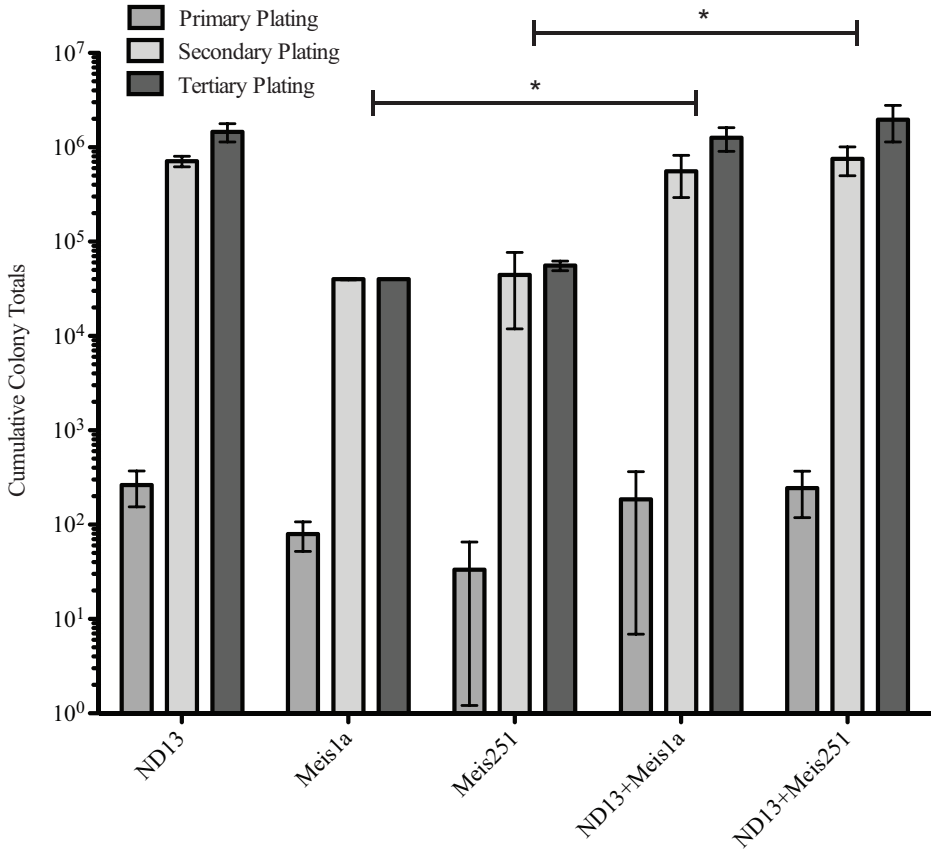

Figure 3.8: Serial re-plating of methylcellulose cultures over-expressing ND13, MEIS1A, MEIS251, ND13+MEIS1A or ND13+MEIS251.
Retroviral constructs over-expressing ND13, MEIS1A, MEIS251, ND13+MEIS1A or ND13+MEIS251 were introduced into wild-type 5-FU pre-treated mouse bone marrow. Following colony counts, the entire contents of the dish were harvested and used to re-initiate methylcellulose cultures. There was no significant difference in plating between MEIS251 or MEIS1A culture and ND13+MEIS251 or ND13+MEIS1A cultures, suggesting that MEIS251 does not exert a dominant negative effect on regulation of MEIS1 targets.

There was a significant difference between MEIS1A and ND13+MEIS1A cultures (p=0.05) at the third replating as well as between MEIS251 and ND13+MEIS251 cultures (p=0.04), corroborating the synergy between MEIS and HOX expression. Three replicates with duplicate methycellulose cultures were performed.

Meis family member expression in sorted wild-type mouse bone marrow populations

To gain a better appreciation of hematopoietic cell types most likely to be affected by Meis1 deletion, a series of experiments were carried out to assess the level of Meis1 expression by Q-RT-PCR in highly purified sub-populations spanning very primitive, HSC enriched to late lineage positive cells. These analyses were also extended to Meis1 family members including Meis2, Meis3, Prep1 and Prep2.

Wild-type, 8 week-old B6.SJL-*Ptprc*^{a} *Pepc*^{b}/BoyJ (Peb3b) mice were sacrificed and stained according to Table 2.2. Individual mice were used for each of the progenitor cell populations (ESLAM HSC, LSK HSC, CMP/MEP/GMP, CLP and MkP) to obtain sufficient cell numbers whereas the mature cell populations (B-cells, T-cell, granulocytes, granulocyte progenitors, and maturing erythroid) were possible to isolate from the same mouse for sufficient cell numbers. Mature MkP RNA from individual mice were a gift from the lab of Dr. S. Nilsson. The gating strategies for each population are outlined in Table 2.3**.** Following pre-amplification, Meis family member expression was assessed (Figure 3.10) in addition to several key genes that would allow confirmation of the sorted populations (Table 2.3).

Relative to *mAbl*, *Meis1* is expressed at high levels in purified HSC populations (ESLAM HSC, LSK HSC) and down-regulated as cells undergo lineage commitment in common myeloid and lymphoid progenitors (Figure 3.9). *Meis1* levels are similar in megakaryocyte progenitors (MkP) to HSCs, which is consistent with platelet defects seen in the embryonic knock-outs (Hisa *et al.*, 2004; Azcoita *et al.*, 2005). *Meis1* is minimally expressed in the mature cell populations examined. Both *Meis2* and *Prep2* are expressed at

very low levels in all the populations examined, suggesting a negligible role in hematopoiesis. *Meis3* seems to be expressed at a relatively consistent level across the populations but appears to be down-regulated in LSK HSCs, CMPs and GMPs as well as $Mac1^{+}$ cells. Higher levels of expression in ESLAM HSCs, MkPs and maturing erythroid cells may suggest a role in these cells. To date, little is known of the function of *Meis3* in the hematopoietic system, although overexpression in $Icsbp^{-/-}$ mice has a similar effect to *Meis1* overexpression (Hara *et al.*, 2008). *Prep1* is also expressed at the highest level in granulocyte progenitors ($Gr1^{+}Mac1^{+}$) and escalating levels in subsequent steps of erythroid maturation. A role for *Prep1* in these cell types have yet to be described, however a role as a tumor suppressor has been recently suggested as *Prep1* deficiency predisposes mice to lymphomas and carinomas and transplanted fetal liver cells deficient in *Prep1* induce lymphomas (Longobardi *et al.*, 2010). ALL samples, however, have higher levels of both *PREP1* and *MEIS1*, and etoposide-resistant cells up-regulate *PREP1* expression, suggesting a potential oncogenic role (Rosales-Aviña *et al.*, 2011). Overall these results support focused examination of the HSC and megakaryocyte lineages in $Meis1^{-/-}$ marrow as this is where the highest levels of expression are found.

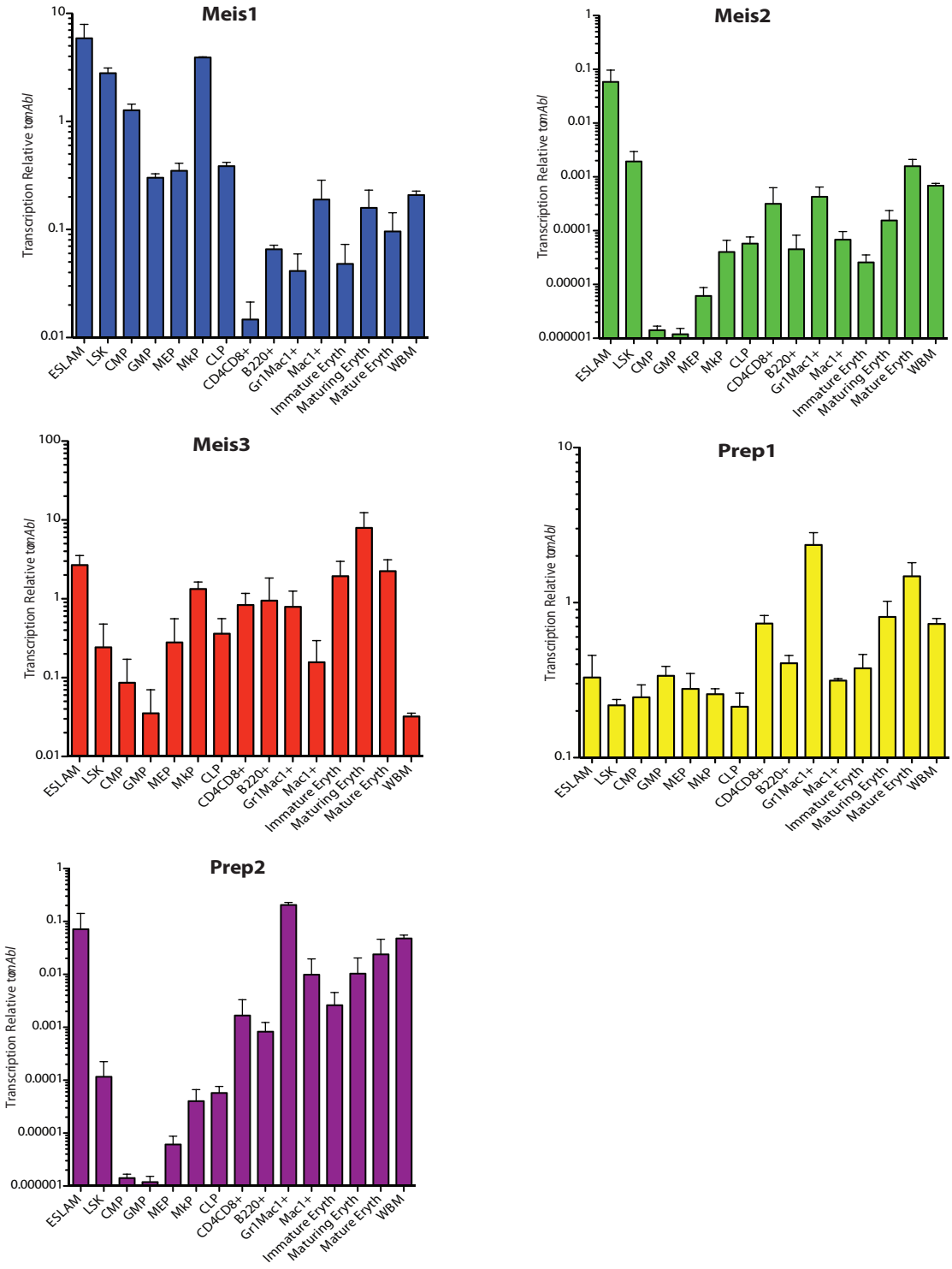

Figure 3.9: MEIS family expression in purified hematopoietic subsets.
Populations enriched for certain hematopoietc subsets were sorted by FACS. MEIS family expression was interrogated in these subsets using Q-RT-PCR following a gene-specific pre-amplification. n=3 for each of the cell lineages studied.

Summary

In this chapter we describe results validating two conditional models for *in vivo* deletion of *Meis1* in the adult. Following identification of the two loxP sites flanking exon 8 in the *Meis1* gene, we crossed the strain onto the Poly:IC inducible *MxCre* and 4-OHT inducible *ERTCre* strains. We validated *in vivo* induction of Cre expression and subsequent collapse of the loxP sequences in both models and developed a robust quantitative PCR based method for measuring the efficiency of deletion applicable to even small cell numbers. We also confirmed the generation of a loxP-collapsed *Meis1* transcript that results in the introduction of a premature stop codon in exon 9. Western blot analysis of MN1-expanded bone marrow cells following *in vitro* induction of Cre expression confirmed loss of the full length *Meis1a* protein in *Meis1*$^{-/-}$ mice. We additionally surveyed expression of *Meis* family members in a panel of purified cell populations ranging from populations highly enriched for HSCs (ESLAM HSCs) to terminally differentiated lymphoid, myeloid and erythroid populations ($CD4^+CD8^+$, $B220^+$, $Gr1^-Mac1^+$, $Gr1^+Mac1^+$ and $Ter119^+CD71^{+/mid/lo}$). Overall, these studies provide confidence to the validity of the inducible *Meis1*-deletion models and provide clues into populations potentially impacted by loss of *Meis1* expression.

Chapter 4 : Meis1 is required for hematopoietic stem cell maintenance and erythroid/megakaryocytic potential

Introduction

The Hox cofactor *Meis1* has been identified as an important transcription factor regulator in both normal and leukemic hematopoiesis. As reviewed in detail in Chapter 1, over-expression of *Meis1* is seen in a large proportion of human leukemias. In experimental models engineered overexpression of *Meis1* and *Hox* is highly leukemogenic and *Meis1* expression has been shown to be critical for leukemogenicity of a range of *MLL*-translocation oncogenes (Wong *et al.*, 2007). In non-*MLL* models of leukemia, the levels of *Meis1* appear to influence the target of transformation (Heuser *et al.*, 2011) as well as the expansion capacity of populations enriched for LSC activity (Woolthuis *et al.*, 2012). The critical players in initiating and maintaining transformation are likely to be oncogene and context specific and the critical genes and molecular pathways affected by *Meis1* expression largely remain to be determined.

In the context of normal hematopoiesis, our recent studies along with those of others previously reported reveal that *Meis1* expression is highest in populations enriched for HSC potential. *Meis1* expression diminishes with differentiation, with the exception of megakaryocyte progenitors where there is a resurgence of expression. Two previous studies using embryonic *Meis1* loss of expression point to a key role for *Meis1* in the maintenance of fetal HSC and megakaryocyte potential (Hisa *et al.*, 2004; Azcoitia *et al.*, 2005). More recently, a pair of studies published at the time of writing of this thesis with the same *Meis1*$^{fl/fl}$ mouse provided new evidence of a role for *Meis1* in adult hematopoiesis. Most strikingly, with induction of Meis1 deletion, there was a marked reduction in HSC as assessed at the level of phenotype and function, alterations that could, at least in part be

linked to the roles of *Meis1* in ROS pathways and cell cycle (Kocabas *et al.*2012; Unnisa *et al*, 2012).

Conflicting lines of evidence in several different experimental models exist for a role for *Meis1* in erythropoiesis and megakaryopoieis. During mouse development, in the absence of *Meis1*, megakaryocytes fail to form and erythroid colony numbers are reduced in the fetal liver (Hisa *et al.*, 2004; Azcoitia *et al.*, 2005). In zebrafish, *Meis1* knock-down results in loss of erythroid progenitors in mature fish (Cvejic *et al.*, 2010), although a recent study using ES derived hematopoietic cells suggests *Meis1* represses erythroid development at the MEP stage in favor of megakaryocyte development (Cai *et al.* 2012). The more recent studies of *Meis1* deletion in adult mice did not reveal any megakaryocytic or erythroid anomalies (Kocabas *et al.*2012; Unnisa *et al*, 2012), and thus suggested *Meis1's* role in these lineages are restricted to embryonic development.

In this chapter we describe the effects of loss of *Meis1* on adult hematopoiesis and additionally explore transcription programs influenced by *Meis1* through expression profiling. We confirmed a role for *Meis1* in maintaining HSC number and self-renewal in the adult mammalian system and obtained evidence of two novel effectors of *Meis1* function in the HSC compartment that have been previously implicated in leukemia. Additionally, our findings highlight important roles for *Meis1* in adult megakaryopoesis and erythropoiesis.

Results

Loss of Meis1 in adult mice perturbs peripheral blood composition in MxCre/Meis1$^{-/-}$ *and* ERTCre/ Meis1$^{-/-}$ *models*

As described in Chapter 3, our studies exploited a mouse line carrying a *Meis1* allele in which Exon 8 is flanked by loxP sites, thus allowing for inducible deletion upon Cre

expression. Two different inducible models were used: *MxCre/Meis1*$^{fl/fl}$ and *ERTCre/Meis1*$^{fl/fl}$, allowing for induction of Cre expression upon exposure to Poly:IC or Tamoxifen respectively. For all in vivo studies described, the induction regimens were as optimized and validated previously (see Chapter 3); these consistently yielded >95% deletion as measured 2 to 7 days following the end of the induction regimen.

A first series of experiments focused on identifying early effects of *Meis1* deletion (Figure 4.1). *ERTCre/Meis1* mice were bled two days after the last of six 4-OHT injections. At this time, 3 of 13 *ERTCre/Meis1*$^{-/-}$ mice were found to be moribund and euthanized along with litter matched Cre-expressing control mice. *ERTCre/Meis1*$^{-/+}$ and *ERTCre/Meis1*$^{+/+}$ mice are clustered in this analysis as no significant difference was found between the groups and both had significant differences compared to *ERTCre/Meis1*$^{-/-}$ mice when compared individually. The peripheral blood of all mice was analyzed on the basis of cellular composition using both an automated differential cell counter and flow cytometer for immunophenotyping. The spleen and sternum of the euthanized moribund and control mice were fixed in paraformaldehyde and sent for histological analysis on the basis of H&E staining and the cell surface markers B220 and Ter119.

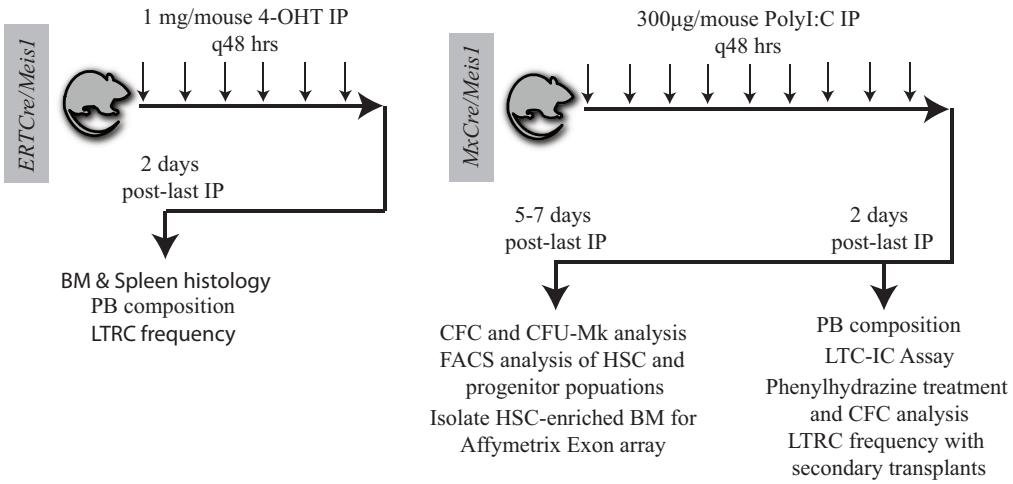

Figure 4.1: Cre expression induction schemes and summary of experiments performed with *ERTCre/Meis1* and *MxCre/Meis1* mouse models

Bone marrow from *ERTCreMeis1*$^{-/-}$ moribund mice (n=3) showed a marked reduction in cellularity, with less than $1.3x10^6$ nucleated cells per trunk (2 femurs, 2 tibias and 2 iliac crests) compared to $1.9x10^7$ nucleated cells in controls ($p<0.04$), fatty replacement of bone marrow (Figure 4.2, panel a) and a marked reduction in nucleated erythroid progenitors as demonstrated by Ter119 staining on fixed tissues (Figure 4.2, panel a). Although there was no significant reduction in BM nucleated cell counts for the remaining 10 surviving *ERTCreMeis1*$^{-/-}$, there was a significant reduction of the average number red blood cells (RBC) in the peripheral blood of *ERTCre/Meis1*$^{-/-}$ mice, even when moribund mice were excluded from the analysis (Figure 4.2, panel b). The distribution of mature nucleated cell types remained largely unchanged (Figure 4.2, panel e). Overall, there was also a significant reduction in the number of platelets in the peripheral blood of *ERTCre/Meis1*$^{-/-}$ mice compared to controls (Figure 4.2, panel d). Together these results reveal that deletion of *Meis1* in an adult mouse results in a rapid and marked decrease in RBC and platelet numbers

and in at least some mice an extreme situation of BM hypoplasia, notably in early erythroid and megakaryocytic cells.

A similar early time course study was also carried out using the *MxCre/Meis1*$^{fl/fl}$ model. In contrast to the *ERTCre/Meis1*$^{fl/fl}$ model, no early morbidity was detected for *MxCre/Meis1*$^{-/-}$ mice and marrow and spleen cellularity and histology remained unchanged compared to controls (data not shown) as assessed 2 days after induction. There were however significant reductions in WBC and platelet numbers (Figure 4.2, panel c, d). Thus in both the *MxCre/Meis1*$^{-/-}$ and *ERTCre/Meis1*$^{-/-}$ mouse models, loss of Meis1 was associated with a rapid decrease in late erythroid and/or megakaryocytic/platelet numbers strongly suggestive of a role for *Meis1* at the late progenitor stage of hematopoiesis in these lineages.

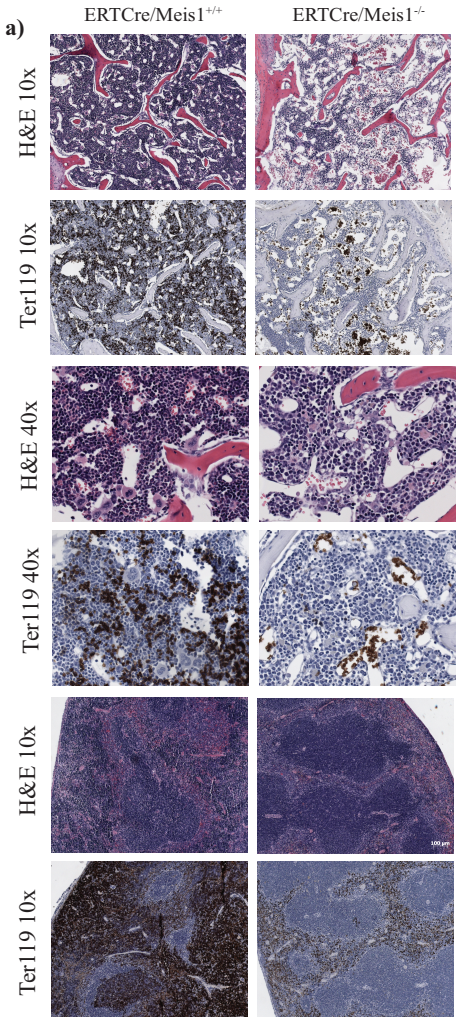
a)
ERTCre/Meis1+/+
ERTCre/Meis1-/-
H&E 10x
Ter119 10x
H&E 40x
Ter119 40x
H&E 10x
Ter119 10x

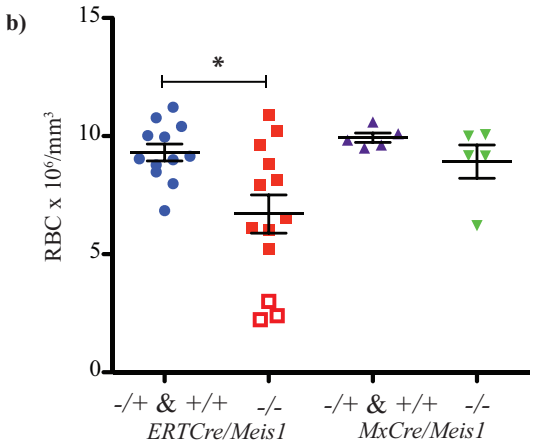
b)
RBC x 10⁶/mm³
15
10
5
0
*
-/+ & +/+
-/-
-/+ & +/+
-/-
ERTCre/Meis1
MxCre/Meis1

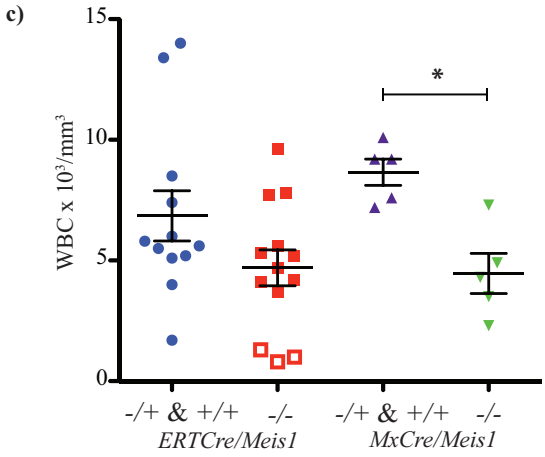
c)
WBC x 10³/mm³
15
10
5
0
*
-/+ & +/+
-/-
-/+ & +/+
-/-
ERTCre/Meis1
MxCre/Meis1

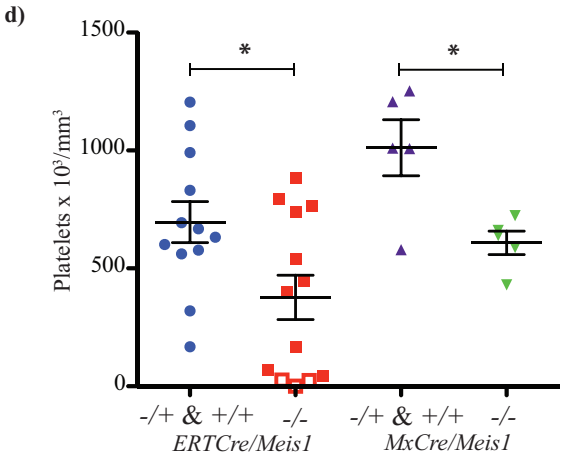
d)
Platelets x 10³/mm³
1500
1000
500
0
*
*
-/+ & +/+
-/-
-/+ & +/+
-/-
ERTCre/Meis1
MxCre/Meis1

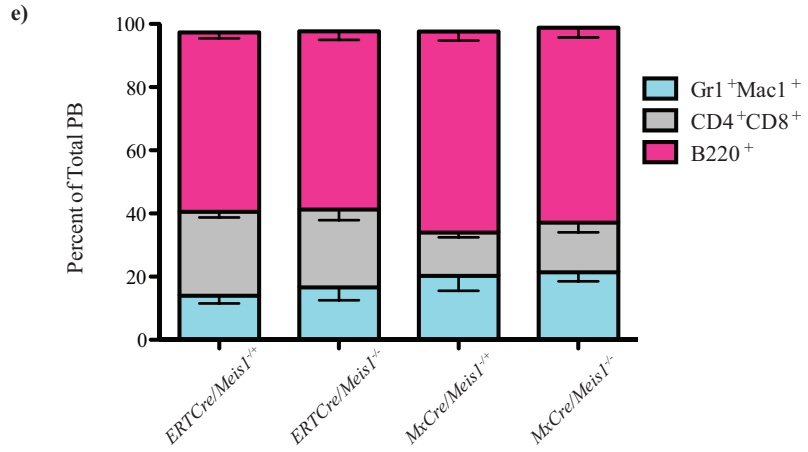

Figure 4.2: Loss of *Meis1* is associated with gross marrow and peripheral blood changes in *ERTCre/Meis1* and *MxCre/Meis1* mice.
a) Bone marrow and spleen cross-sections of moribund *ERTCre/Meis1*$^{-/-}$ mice stained with hematoxylin & eosin (H&E) and anti-Ter119 antibody, compared to *ERTCre/Meis*$^{-/+}$ control. **b)** Loss of *Meis1 in vivo* results in a significant decrease in red blood cells in the peripheral blood in *Meis1* $^{-/-}$ mice. *ERTCre/Meis1* $^{-/-}$ (n=13) compared to *ERTCre/Meis1*$^{-/+ \& +/+}$ (p=0.01; *ERTCre/Meis1*$^{+/+}$ n=3; *ERTCre/Meis1*$^{-/fl}$ n=10). The three *ERTCre/Meis1*$^{-/-}$ mice with the lowest RBC counts were euthanized due to pallor and lethargy and had profound reductions in bone marrow cellularity, that is, less than 1.3x10^6 nucleated cells per trunk (2x femur, 2x iliac crest, 2x tibia). Moribund mice are represented as hollow squares on the graph. *MxCre/Meis1*$^{-/-}$ mice (n=5) show no such reduction when compared to *MxCre/Meis1*$^{+/+}$(n=2) and *MxCre/Meis1*$^{-/+}$ (n=3) mice. **c)** Loss of *Meis1* results in a reduction of white blood cells (WBC) in *MxCre/Meis1* $^{-/-}$ mice compared to *MxCre/Meis1* $^{-/+ \& +/+}$ (p=0.004, n=5) 2 days after the final PolyI:C injection. **d)** Loss of *Meis1* results in a reduction of peripheral platelets (PLT) in *MxCre/Meis1* $^{-/-}$ *ERTCre*$^+$*/Meis1* $^{-/-}$ and mice compared to *MxCre*$^+$ and *ERTCre*$^+$ control mice 2 days after the final PolyI:C/4-OHT injection (p=0.02, and p=0.02, respectively). **e)** Lineage distribution in the peripheral blood of treated mice, 2 days following the last injection. No significant differences were found.

Generation of megakaryocyte and erythroid progenitors are impaired in MxCre/Meis1$^{-/-}$ *mice*

To gain further insight into the role of Meis1 at the level of erythroid and megakaryocytic progenitors, we assessed CFU-Mk numbers and proliferative potential from whole BM 7 days following the end of Poly:I:C induction in *MxCre/Meis1* mice (Figure 4.3, panel a). Loss of *Meis1* resulted in a reduction of total CFU-Mk (p=0.007, n=7) compared to

MxCre/Meis1$^{-/+}$ mouse marrow. The reduction was largely due to a 6-fold reduction in CFU-Mk with high proliferative potential that form colonies composed of >10 cell clusters (p=0.01, n=7, Figure 4.3, panel a). This loss of CFU-Mk is consistent with the drop in platelet number seen in the peripheral blood of *MxCre/Meis1*$^{-/-}$.

To examine if this reduction in progenitor number was exclusive to the megakaryocytic lineage or extended to less differentiated myeloid parent populations and their progeny, bone marrow CFC assays were carried out on *MxCre/Meis1*$^{-/-}$ BM cells 5 days after the end of induction. Compared to *MxCre/Meis1*$^{-/+}$ controls, the total colony number was not significantly reduced in *MxCre/Meis1*$^{-/-}$ bone marrow, but there was a 4-fold reduction in the number of large BFU-E derived erythroid colonies (p=0.04, n=7) and a 7-fold reduction in the number of multi-lineage colonies derived from CFU-GEMM (p=0.05, n=7) (Figure 4.3, panel b). The reduction in the erythroid progenitor population was even more evident when methylcellulose media optimized to support BFU-E colony formation was used (Figure 4.3, panel c). In this case, while total BFU-E colony number was unchanged compared to control, large colonies of greater than 16 cell clusters indicative of colonies derived from more primitive progenitors were reduced by 32-fold (n=7, p=0.003). The significant reduction in large BFU-E and CFU-Mk colonies in *MxCre/Meis1*$^{-/-}$ mice suggests a role for *Meis1* in the proliferative potential of these progenitors, although it is unclear if it is at the level of a shared megakaryocyte-erythroid progenitor (MEP) or in the individual erythroid (EP) and megakaryocyte lineages (MkP).

To further investigate the erythroid defect seen in these mice, we used an *in vivo* model of hemolytic anemia induced by phenylhydrazine (PHZ) to generate a proliferative stress on erythroid progenitors. Forty-eight hours after the last of 9 Poly:I:C injections,

MxCre/Meis1 mice were given an IP injection of PHZ (60mg/Kg) and euthanized 4 days later. Mice were assessed on the basis of bone marrow cellularity, spleen weight and the ability of bone marrow and spleen cells to form BFU-E in erythroid-supportive methylcellulose media. While spleen and marrow cellularity were comparable between treated control and *MxCre/Meis1*$^{-/-}$ (data not shown), erythroid colony numbers were greatly reduced in *Meis1*$^{-/-}$ mice following PHZ treatment. Again, this was particularly evident for large erythroid colonies for which there was a 73-fold reduction in number from spleens of *MxCre/Meis1*$^{-/-}$ mice compared to *MxCre/Meis1*$^{-/+}$ ($p=0.006$, $n=2$). Moreover, there were no colonies with greater than 16 clusters from the marrow of *Meis1* deficient mice, implying a greater than 2000-fold loss ($p=0.002$, $n=2$) (Figure 4.3, panel d). The BFU-E proliferation defect under normal and stress conditions demonstrates that *Meis1* is required for efficient erythropoieisis. While no loss of nucleated Ter119^{+} cells was seen in the spleen or marrow of these mice by immunohistochemistry in our first round of experiments, in contrast to the *ERTCre*$^{+}$*/Meis1*$^{-/-}$ model, there is clearly a large change in the potential of progenitors that cannot be distinguished by histology.

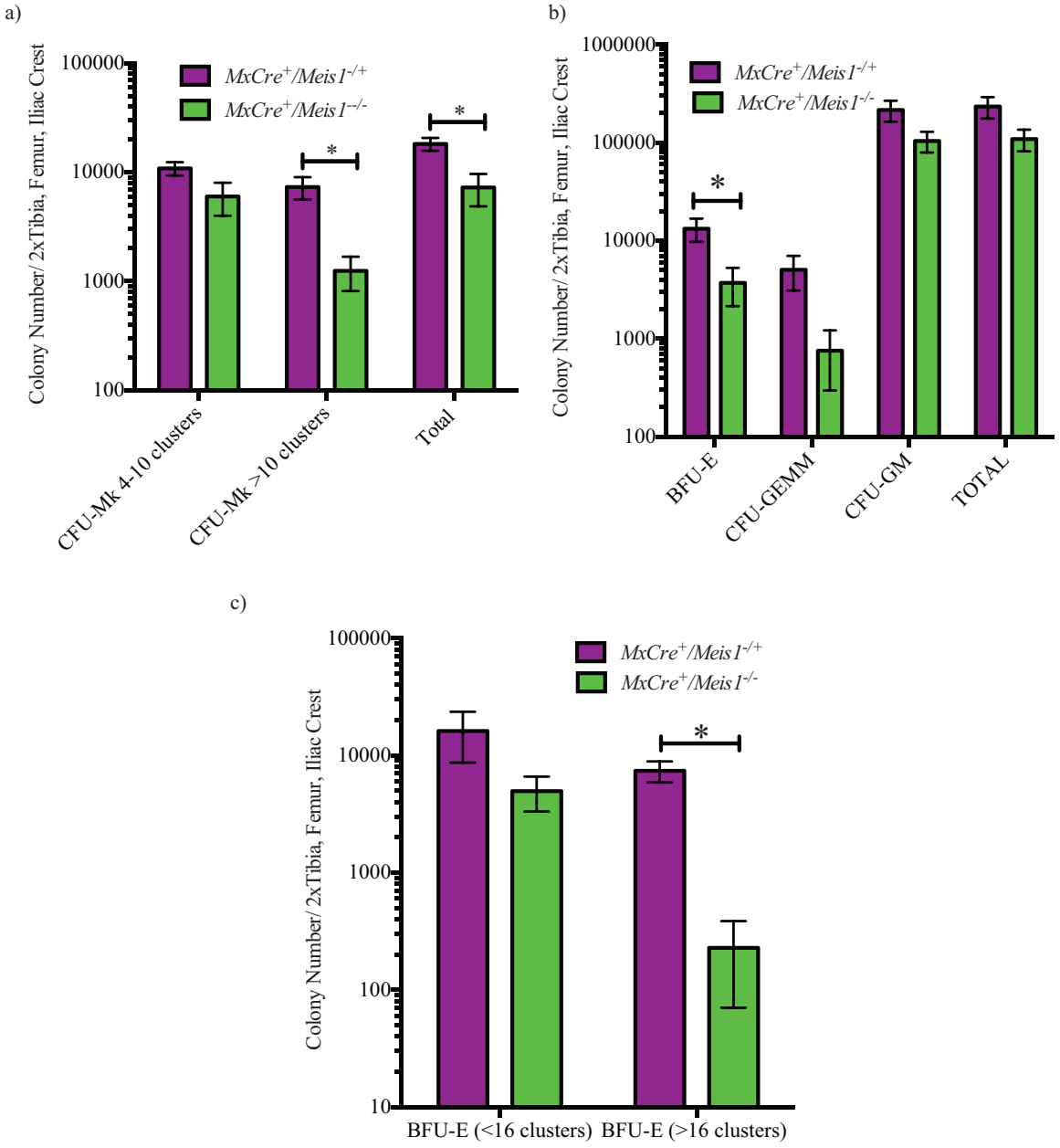
a)
Colony Number/ 2xTibia, Femur, Iliac Crest
100000
10000
1000
100
MxCre+/Meis1-/+
MxCre+/Meis1--/-
*
*
CFU-Mk 4-10 clusters
CFU-Mk >10 clusters
Total
b)
Colony Number/ 2xTibia, Femur, Iliac Crest
1000000
100000
10000
1000
100
MxCre+/Meis1-/+
MxCre+/Meis1-/-
*
BFU-E
CFU-GEMM
CFU-GM
TOTAL
c)
Colony Number/ 2xTibia, Femur, Iliac Crest
100000
10000
1000
100
10
MxCre+/Meis1-/+
MxCre+/Meis1-/-
*
BFU-E (<16 clusters)
BFU-E (>16 clusters)

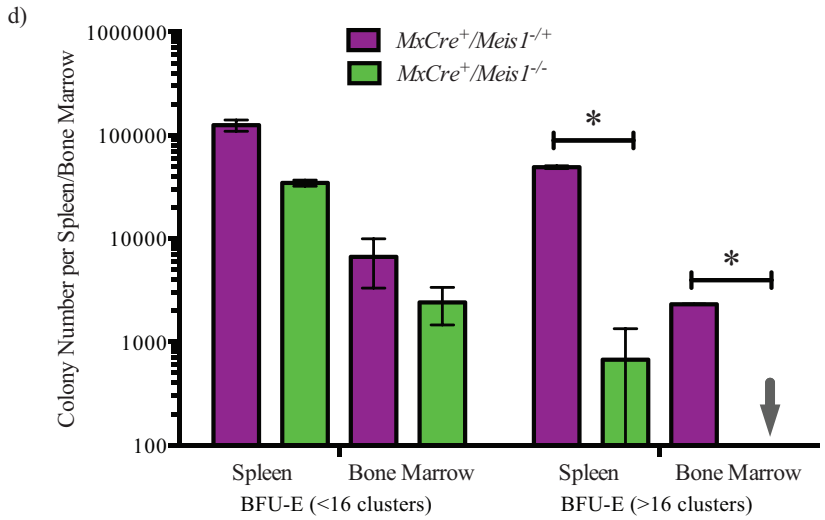

Figure 4.3: Colony forming cell (CFC) capacity is selectively reduced in the absence of *Meis1*.
a) CFU-megakaryocytic (CFU-Mk) collagen cultures demonstrate deficiency in the ability of *MxCre/Meis1*$^{-/-}$ bone marrow to generate CFU-Mk (p=0.007, n=7), most notably a 9-fold reduction in large CFU-Mk composed of >10 clusters per colony (p=0.01, n=7). **b)** Bone marrow from *MxCre/Meis1*$^{-/-}$ mice (n=7) have a 4-fold reduced capacity to form burst-forming erythroid (BFU-E, p=0.04), a 7-fold reduced CFU-granulocyte-erythrocyte-monocyte-megakaryocyte capacity (CFU-GEMM, p=0.05). **c)** BFU-E impairment in *MxCre/Meis1*$^{-/-}$ bone marrow is further demonstrated in erythroid-specific methylcellulose media. *MxCre/Meis1*$^{-/-}$ marrow 32-fold fewer BFU-E colonies with a potential of >16 clusters per colony (p=0.003, n=7). For both CFC and BFU-E assays, mice were euthanized and cells plated 5 days after the final PolyI:C injection. **d)** Phenylhydrazine treated *MxCre/Meis1*$^{-/-}$ spleen cells have a 73-fold reduced ability to form large(>16 clusters/colony) BFU-E (p=0.006, n=3) compared to *MxCre/Meis1*$^{-/+}$. Bone marrow showed a >2000-fold reduction in both small and large BFU-E colonies (p=0.002, n=3). Mice were euthanized 4 days after the phenylhydrazine and thus 6 days following the final PolyI:C injection in two replicate experiments.

To examine the possibility that erythroid progenitors, quantified by *in vitro* CFC assay from *MxCre/Meis1*$^{-/-}$ mice were derived from progenitors that escaped Cre-mediated *Meis1* deletion, individual BFU-E, CFU-GM and CFU-GEMM derived colonies were plucked and examined for *Meis1* deletion by PCR. All 40 colonies examined (Table 4.1) were collapsed around exon 8. This suggests that although the expansion of BFU-E and

multi-potential progenitors is impaired in the absence of *Meis1*, subsequent downstream proliferation and differentiation are not overtly impaired. Together these data point to a major if not absolute requirement for *Meis1* in the window of early erythroid and megakaryocytic progenitor (and possibly at the MEP stage) down to the intermediate stage of committed erythroid and late megakaryocytic development.

Table 4.1: PCR of individual CFC colonies for *Meis1* deletion.
(deleted/tested; NP = not possible; ND = not done)

	BFU-E	CFU-GM	CFU-GEMM
7-days post induction	ND	18/18	2/2
From LTC-IC	NP	7/15	NP
From Phenylhydrazine	20/20	20/20	NP

Meis1$^{-/-}$ *results in a loss of hematopoietic stem cells, common myeloid progenitors and megakaryocyte progenitors*

As an initial approach to examine the immediate impact of *Meis1* deletion on a broader spectrum of hematopoietic cells including the most primitive HSC populations, BM cells were subjected to detailed immunophenotype analyses 5 to 7 days after induction in *MxCre/Meis1*$^{-/-}$ mice and compared to *MxCre/Meis1*$^{-/+}$ controls. An immunophenotyping strategy as employed for isolation of subpopulatioins used for Meis expression profiling was used (see Chapters 2 and 3) with the exception that the LSKCD150^{+}CD48^{-} immunophenotype was used to identify primitive HSC at an estimated purity of 1 in 2 to 1 in 5 (Kiel *et al*., 2005) (Table 2.2). These analyses carried out in 5 experiments with a total of 7 mice per group, revealed significant decreases in absolute numbers per mouse of several of the progenitor populations (representative plots Figure 4.4, panel a; summary Figure 4.4,

panel b), despite normal numbers of nucleated cells and differentiated lineage distribution in the marrow. Consistent with our earlier results from progenitor assays, there was an 11-fold decrease in the number of phenotypically defined megakaryocytic progenitors (MkP) in the marrow of *MxCre/Meis1*$^{-/-}$ mice (p=0.02, n=7). Also consistent with our CFC results there was a 6-fold decrease in the number of megakaryocytic-erythroid progenitors (MEP) (p=0.05, n=7). This reduction in progenitors was also seen for the most primitive common myeloid progenitor (CMP) compartment, with a 9-fold reduction (p=0.04, n=7), which is consistent with the decrease observed in number of BFU-E and CFU-GEMM in CFC assays. No decrease was observed in the GMP subpopulaton. Together these data point to a requirement for *Meis1* in the CMP, MEP and MkP compartments but limited or no requirement at the stage of GMP and later. For the most primitive subpopulations assessed by immnophenotype analysis, there was no significant difference in the number of LSK cells (HSC frequency of ~1/50). However, in the more highly purified HSC subpopulation (LSKCD150^{+}CD48^{-}) there was a 5-fold reduction (p=0.005, n=7) in *MxCre/Meis1*$^{-/-}$ mice compared to *MxCre/Meis1*$^{-/+}$ mice.

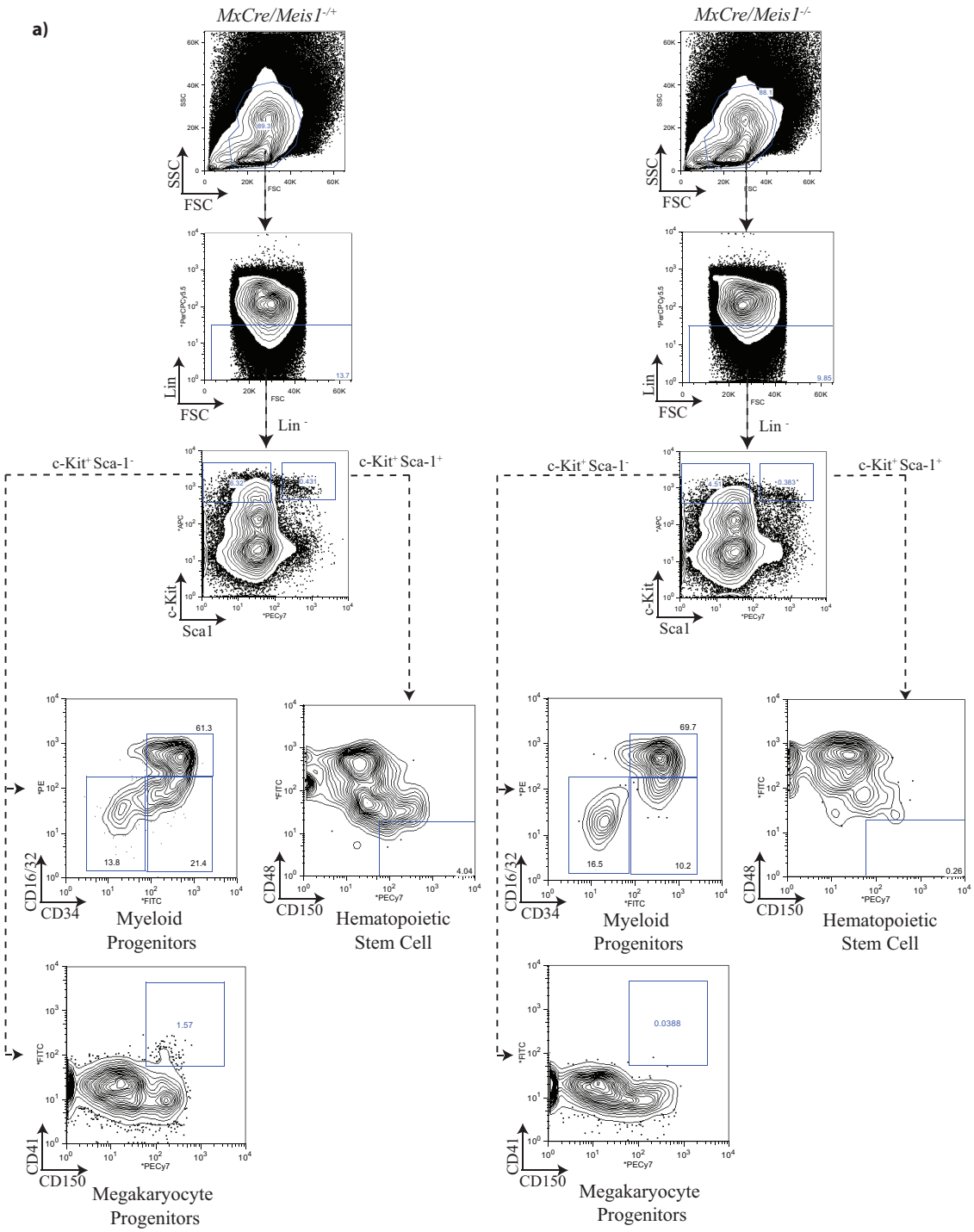
a)
MxCre/Meis1-/+
MxCre/Meis1-/-
SSC
FSC
Lin
Lin -
c-Kit
Sca1
c-Kit+ Sca-1-
c-Kit+ Sca-1+
CD16/32
CD34
Myeloid
Progenitors
CD48
CD150
Hematopoietic
Stem Cell
CD41
Megakaryocyte
Progenitors
61.3
13.8
21.4
4.04
1.57
69.7
16.5
10.2
0.26
0.0388

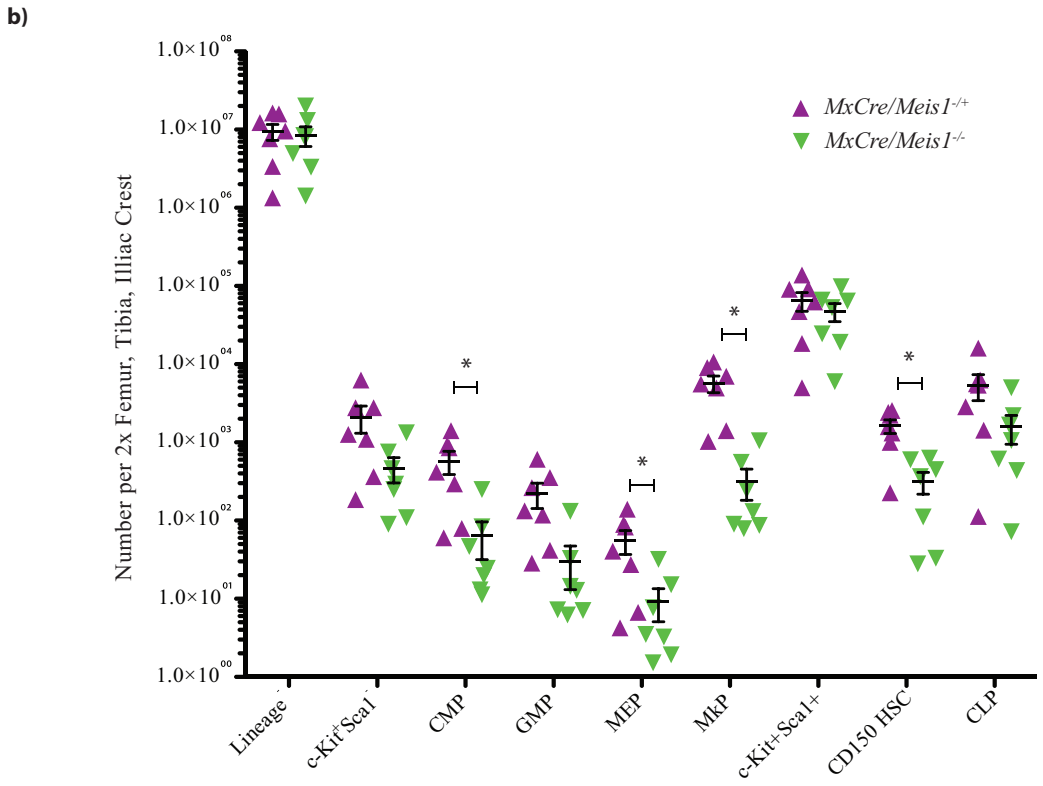

Figure 4.4: Loss of *Meis1* results in profound phenotypic changes in mouse bone marrow.
a) Gating strategy and representative plots for myeloid progenitors, HSCs and MkP from *MxCre/Meis1*$^{-/-}$ and *MxCre/Meis1*$^{-/+}$ bone marrow. **b)** Absolute number of phenotypically defined populations in the bone marrow of *MxCre/Meis1*$^{-/-}$ and *MxCre/Meis1*$^{-/+}$ mice. There was a 9-fold reduction in CMP (p=0.04, n=7), 6-fold reduction in MEP (p=0.05, n=7), 11-fold reduction in MkP (p=0.02, n=7) and 5-fold reduction in HSC (p=0.005, n=7) enriched populations.

Meis1 *is required for the maintenance of primitive cell populations capable of long-term hematopoiesis* in vitro *and* in vivo

To assess the impact of Meis1 deletion on functionally defined primitive hematopoietic cells, *in vitro* LTC-IC and *in vivo* competitive repopulation assays were performed. The frequency and calculated absolute number of LTC-IC as assessed by limit dilution assay was reduced by 6-fold in the BM of *MxCre/Meis1*$^{-/-}$ mice compared to

MxCre/Meis1$^{-/+}$ (assays initiated 2 days post end of induction) (Table 4.2). Interestingly only ~50% of CFC derived from LTC-IC assays of *MxCre/Meis1*$^{-/-}$ BM showed complete *Meis1* deletion (Table 4.1). This result is consistent with a near obligate requirement for *Meis1* at the stage of LTC-IC and early downstream progeny.

Table 4.2: LTC-IC frequency in *MxCre/Meis1*$^{-/-}$ bone marrow

4 week LTC-IC	1 in X	Upper 95% CI	Lower 95% CI
MxCre/Meis1$^{-/+}$	26 283	18 774	36 796
MxCre/Meis1$^{-/-}$	157 683	78 858	315 299

To further examine the requirement for *Meis1* in the most primitive hematopoietic compartment, limit dilution assays for competitive repopulating cells were carried out. Both *MxCre/Meis1*$^{-/-}$ and *MxCre/Meis1*$^{+/-}$ (Figure 4.5, panel a) and *ERTCre/Meis1*$^{-/-}$ *ERTCre/Meis1*$^{+/-}$ (Figure 4.5, panel b) bulk bone marrow cells were transplanted at different doses with competitor recipient type bone marrow cells (100,000 cells). Donor cell contributions to the peripheral blood of recipient mice were then serially assessed at 4 week intervals to 16 weeks post-transplantation. Limit dilution analysis revealed a 10.7-fold and 19-fold reduction in the frequency of HSC in *MxCre/Meis1*$^{-/-}$ (Figure 4.5, panel c) and *ERTCre/Meis1*$^{-/-}$ (Figure 4.5, panel b) mice, respectively, when compared to *MxCre/Meis1*$^{-/+}$ or *ERTCre/Meis1*$^{-/+}$ mice (Table 4.3). Expressed in absolute numbers of HSC per mouse, given that there is no difference in the total bone marrow cellularity between *Meis1*$^{-/-}$ and *Meis1*$^{-/+}$ mice in either the *ERTCre* or *MxCre* model, there is an average of 2900 HSC per *MxCre/Meis1*$^{-/+}$ compared to only 270 in the *MxCre/Meis1*$^{-/-}$ mouse. The reduction is similar

in the *ERTCre* model whereby there are roughly 5000 HSC in *ERTCre/Meis1*$^{-/+}$ mice compared to 230 in *ERTCre/Meis1*$^{-/-}$ mice.

No differences were seen in the lineage distribution of donor-derived peripheral blood cells. At the time of transplantation, donor cells were confirmed to be >95% deleted for *Meis1* and Q-PCR analysis normalized for the *Meis1*^{fl} allele showed persistence of *Meis1*$^{-/-}$ cells in the donor compartment at >80% (data not shown) at 16-weeks. Thus while *Meis1* loss results in a rapid and marked reduction in HSC number, the presence of *Meis1* does not appear to be an absolute requirement for at least limited repopulation capacity of downstream progenitors. As differentiated cell output at the 16 week time point is from cells with HSC potential at the time of transplantation, if *Meis1* was an absolute requirement for HSC lineage restriction and differentiation, we would have expected a far greater proportion of non-deleted alleles at this late time point. In addition, recipients receiving 1 HSC equivalent from either *MxCre/Meis1*$^{-/+}$ or *MxCre/Meis1*$^{-/-}$ mice, the relative lineage contribution of donor cells in the peripheral blood was equivalent.

To examine more closely the importance of Meis1 for HSC function, secondary transplants were performed to assess HSC self-renewal and expansion in the absence of *Meis1* in the *MxCre*/*Meis1* model. In this experiment, 3 *MxCre/Meis1*$^{fl/fl}$ and 3 *McCre/Meis1*$^{fl/+}$ mice were treated with PolyI:C as per the established induction scheme. Limiting dilution analysis into irradiated primary recipients was then performed at $2x10^6$, $1x10^6$, $2x10^5$ and $2x10^4$ cells per replicate mouse with 100, 000 helper cells. Following 4 months *in vivo*, a cohort of 3 mice transplanted with $2x10^6$ cells were sacrificed, pooled and transplanted into irradiated secondary recipient mice (Figure 4.5, panel c) based on the percent donor contribution. That is, $1x10^7$, $1x10^6$ or $1x10^5$ CD45.2 cells were transplanted

into secondary recipients, without helper cells. Based on the percent reconstitution (8% from *MxCre/Meis1*$^{-/-}$, 53% from *MxCre/Meis1*$^{-/+}$), this meant that 6.6x more cells were transplanted per secondary recipient in the *MxCre/Meis1*$^{-/-}$ arm. The highest transplant dose of $1x10^7$ cells was expected to contain the progeny of roughly 5 HSC (minimum 2 HSC, maximum 12 HSC) in the *MxCre/Meis1*$^{-/-}$ arm, based on the limiting dilution results in primary recipients. Even at this dose, however, there was no detectable long-term repopulation in secondary recipients in the absence of *Meis1* (Figure 4.5, panel d). *MxCre/Meis1*$^{-/+}$ cells were, however, capable of minimum maintenance of the transplanted stem cell pool. This represents, at minimum, a 25-fold reduction in the ability of HSC lacking *Meis1* to contribute to long-term repopulation. This deficit was evident as early as 4-weeks post-transplantation into secondary recipients, suggesting HSC lacking *Meis1* are severely impaired in their ability generate progeny with even short-term repopulating potential.

a)

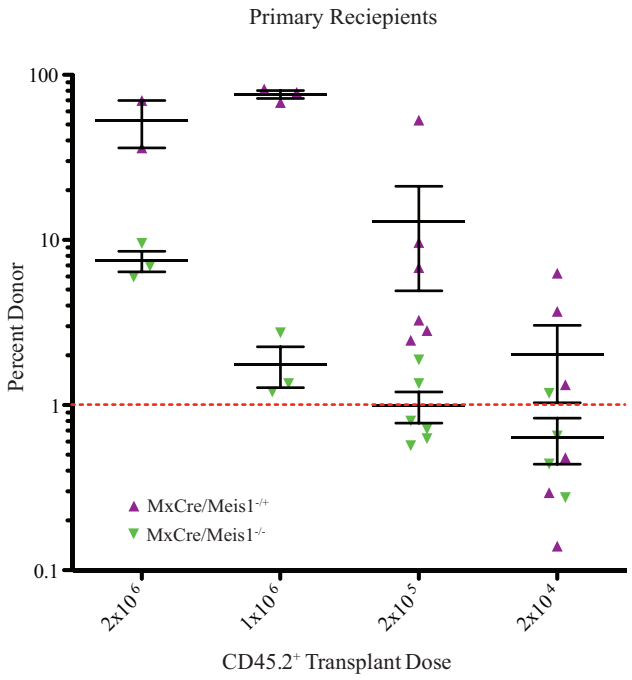
Primary Reciepients
100
10
1
0.1
Percent Donor
MxCre/Meis1-/+
MxCre/Meis1-/-
2x10 6
1x10 6
2x10 5
2x10 4
CD45.2+ Transplant Dose

b)

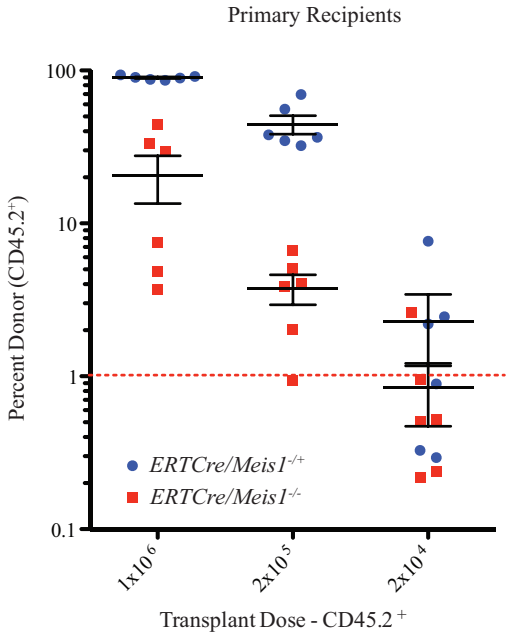
Primary Recipients
100
10
1
0.1
Percent Donor (CD45.2+)
ERTCre/Meis1-/+
ERTCre/Meis1-/-
1x10 6
2x10 5
2x10 4
Transplant Dose - CD45.2 +

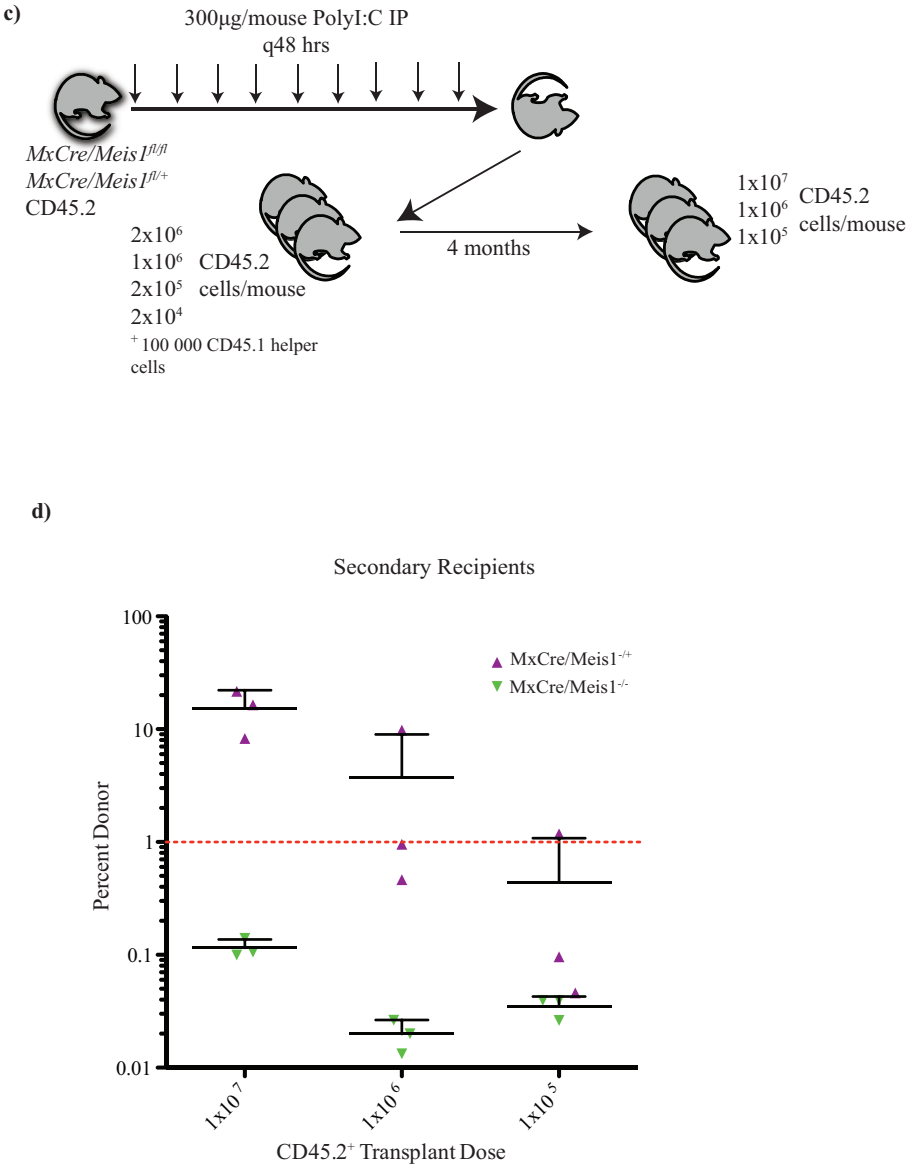

Figure 4.5: Loss of long-term repopulation and HSC self-renewal in the absence of *Meis1*.

a) Recipient CD45.2 engraftment 16 weeks post-transplant demonstrates a 10-fold reduction in HSC capacity in *MxCre/Meis1*$^{-/-}$ (n=2 donors into 3 recipients per cell dose at 2x10^6 and 1x10^6, with 1 failed injection at 2x10^6 cells. 6 recipient mice were used at 1x10^5 and 1x10^4 cells per mouse) bone marrow compared to *MxCre/Meis1*$^{-/+}$ (n=2 donors into 3 recipients per cell dose at 2x10^6 and 1x10^6. 6 recipient mice were used at 1x10^5 and 1x10^4 cells per mouse; p=0.009). Individual points represent individual mice from 2 independent experiments. **b)** Recipient CD45.2 engraftment 16 weeks post-transplant demonstrates a 10-fold reduction in LTRC capacity in *ERTCre/Meis1*$^{-/-}$ (n=2 donors into 6 recipients per cell dose) bone marrow compared to *ERTCre/Meis1*$^{-/+}$ (n=2 donors into 6 recipients per cell dose; p=0.00004). Individual points represent individual mice from 2 independent experiments. For both

ERTCre/Meis1 and *MxCre/Meis1* experiments, induced mice were euthanized and transplanted into donor mice 2 days following the final IP injection. **c)** Experimental outline of transplants into secondary recipients. **d)** Secondary recipients, 16 weeks following transplantation, demonstrate *MxCre/Meis1*$^{-/-}$ HSC are not maintained *in vivo*. *MxCre/Meis1*$^{-/-}$ (n=3 pooled donors into 3 recipient mice) bone marrow fails to engraft compared to *MxCre/Meis1*$^{-/+}$ (n=3 pooled donors into 3 recipient mice) at roughly equivalent HSC transplant doses.

Table 4.3: Reduction in HSC in *MxCre/Meis1*$^{-/-}$ and *ERTCre/Meis1*$^{-/-}$ mice

	Mouse	HSC Frequency	Upper 95% CI	Lower 95% CI
Primary	*MxCre/Meis1*$^{+/-}$	1/28 482	1/9 473	1/85 683
(*p*=0.009)	*MxCre/Meis1*$^{-/-}$	1/306 624	1/121 558	1/773 441
Primary	*ERTCre/Meis1*$^{+/-}$	1/18 199	1/6 509	1/50 887
(*p*=0.00004)	*ERTCre/Meis1*$^{-/-}$	1/345 174	1/151 649	1/785 665

The requirement for Meis1 for HSC is cell intrinsic

The decrease in HSC number detected following *Meis1* loss as assessed at the level of immunophenotype or functional repopulation could arise from cell HSC – intrinsic requirements for HSC function and maintenance, and/or from cell-extrinsic requirements, for example in the stem cell niche. To examine these possibilities, we transplanted $2x10^6$ *MxCre/Meis1*$^{fl/fl}$ (n=2 donor mice into 11 recipient mice) or *MxCre/Meis1*$^{+/fl}$ (n=2 donor mice into 11 recipient mice) cells with $1x10^6$ recipient-type cells into lethally irradiated wild-type recipients 4-weeks prior to induction of Cre expression (Figure 4.6, panel a). Both *MxCre/Meis1*$^{fl/fl}$ and *MxCre/Meis1*$^{+/fl}$ cells engrafted equivalently as read out in peripheral blood prior to Cre expression (Figure 4.6, panel b). Following PolyI:C treatment, there was a 17% decrease in *MxCre/Meis1*$^{-/-}$ contribution to peripheral blood 2 days after the final IP injection, whereas the levels of *MxCre/Meis1*$^{-/+}$ engraftment remained unchanged compared to control mice given PBS IP (p=0.0005, n=7 PolyI:C, n=4 PBS, Figure 4.6, panel c). The decrease in engraftment by *MxCre/Meis1*$^{-/-}$ was also evident in BM (38% decrease) while

again there was no difference between the engraftment of *MxCre/Meis1*$^{-/+}$ cells under PolyI:C treated or PBS conditions (p=6x10^{-6}, n=7 PolyI:C, n=4 PBS Figure 4.6, panel d).

In a first experiment to determine the HSC frequency following *Meis1* deletion, the 3 recipient PolyI:C-treated mice were euthanized 3 days after the final IP injection, BM pooled and transplanted into secondary recipients. In this initial experiment, BM cells were transplanted without separation such that there was a mixture of *MxCre/Meis1*-derived cells (CD45.2+) and recipient/competitor derived cells (CD45.1+). Cell doses were however adjusted so that equivalent numbers of *MxCre/Meis1*-derived cells were transplanted. In this setting, there was no detectable engraftment by *MxCre/Meis1*$^{-/-}$ cells in the peripheral blood at 16 weeks (3 recipient mice per cell dose, Figure 4.6, panel, Table 4.4) in contrast to readily detected engraftment by *MxCre/Meis1*$^{-/+}$ cells. As no mice were positive for engraftment in the *MxCre/Meis1*$^{-/-}$ arm, the HSC frequency could be only estimated to be <1 in 18 million compared to 1 in 140,000 for *MxCre/Meis1*$^{-/+}$ marrow and did not reach statistical significance of p<0.05.

By performing bulk transplants based on *MxCre/Meis1* cell number, however, *MxCre/Meis1*$^{-/-}$ HSC had to compete against a greater number of recipient wild-type cells than *MxCre/Meis1*$^{-/+}$ cells due to the reduction in engraftment following Poly:I:C treatment. The experiment was therefore repeated to compensate for increased competition by recipient cells by sorting for CD45.2^{+} bone marrow cells prior to transplantation into secondary recipients, thereby ensuring that *MxCre/Meis1*$^{-/-}$ and *MxCre/Meis1*$^{-/+}$ HSC were competing against equivalent numbers of wild-type HSC for engraftment. 4 PolyI:C-treated primary recipient mice were euthanized, pooled and sorted by CD45.2^{+} by FACS and transplanted into 3 secondary recipient mice per cell dose (the injection failed in one secondary recipient

mouse transplanted with $1.5x10^6$ *MxCre/Meis1*$^{-/+}$ cells). The decreased frequency of HSC in *MxCre/Meis1*$^{-/-}$ cells was maintained in the absence of greater competition and was indeed 7-fold lower than *MxCre/Meis1*$^{-/+}$ cells ($p<1x10^{-125}$, Table 4.4). These experiments demonstrate that the major requirement for *Meis1* in the maintenance of HSC number is likely cell intrinsic.

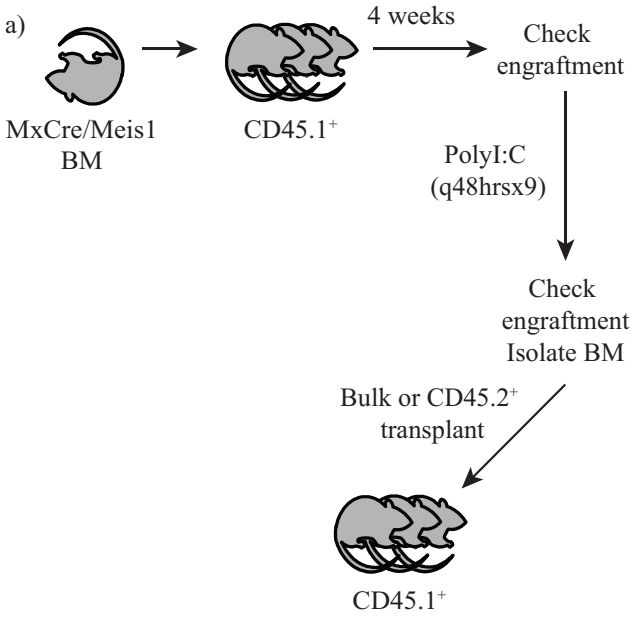
a)
MxCre/Meis1
BM
CD45.1+
4 weeks
Check
engraftment
PolyI:C
(q48hrsx9)
Check
engraftment
Isolate BM
Bulk or CD45.2+
transplant
CD45.1+

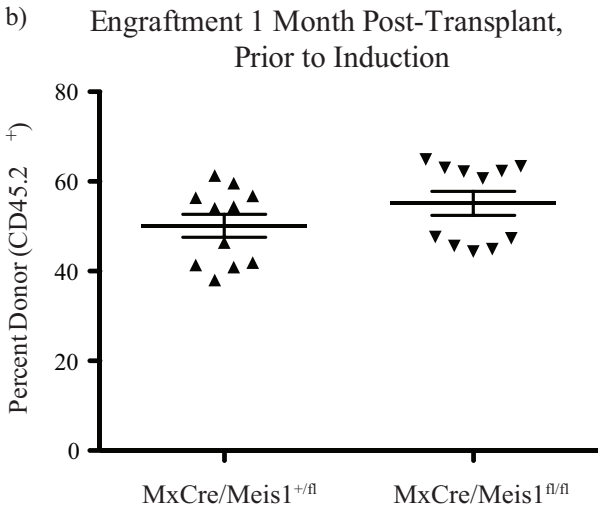
b)
Engraftment 1 Month Post-Transplant,
Prior to Induction
Percent Donor (CD45.2 +)
80
60
40
20
0
MxCre/Meis1+/fl
MxCre/Meis1fl/fl

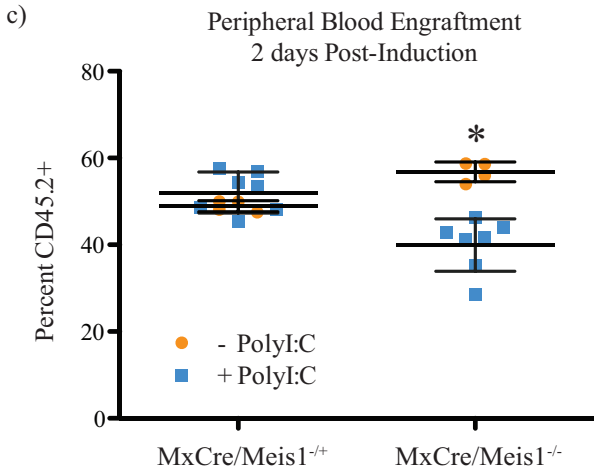
c)
Peripheral Blood Engraftment
2 days Post-Induction
Percent CD45.2+
80
60
40
20
0
*
- PolyI:C
+ PolyI:C
MxCre/Meis1-/+
MxCre/Meis1-/-

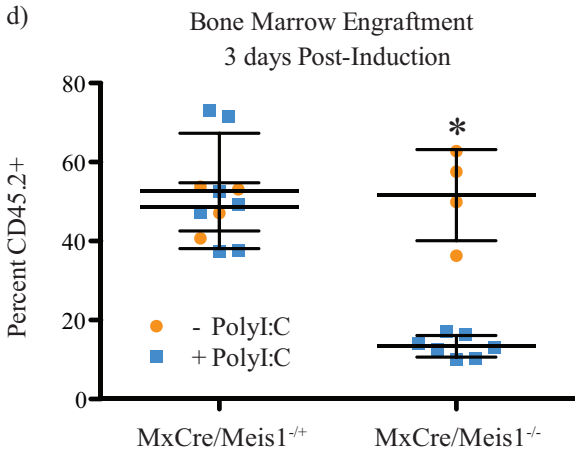
d)
Bone Marrow Engraftment
3 days Post-Induction
Percent CD45.2+
80
60
40
20
0
*
- PolyI:C
+ PolyI:C
MxCre/Meis1-/+
MxCre/Meis1-/-

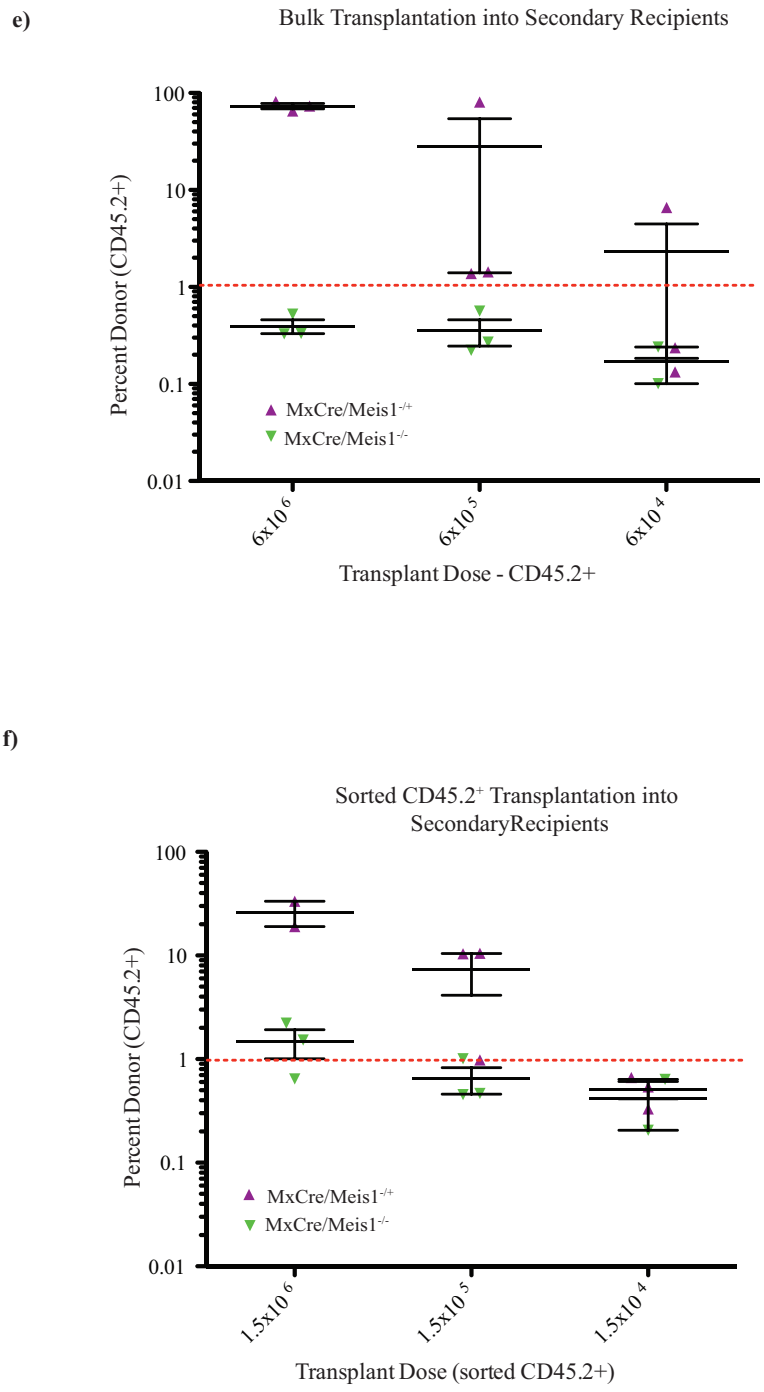

Figure 4.6: Loss of *Meis1* results in an intrinsic defect in LTRC.
a) Experimental plan to test the cell-intrinsic requirement for *Meis1* in HSCs. **b)** Peripheral blood engraftment of primary recipients 4 weeks after transplantation and prior to induction

shows no difference in engraftment (n=11). **c)** Peripheral blood engraftment of primary recipients 2 days following PolyI:C administration. *MxCre*$^{+}$*/Meis1*$^{-/-}$ (n=7) engraftment is reduced 17% compared to *MxCre/Meis1*$^{fl/fl}$ (n=4; p=0.0005). **d)** Bone marrow engraftment in primary recipients 3 days following PolyI:C administration. *MxCre*$^{+}$*/Meis1*$^{-/-}$ (n=7)_engraftment is reduced 38% compared to *MxCre/Meis1*$^{fl/fl}$ (n=4; p=6x10^{-6}). **e)** Engraftment of secondary recipients transplanted with bulk CD45.2 cells from primary mice with transplant dose based on the number of CD45.2 cells 24 weeks after transplantation. **f)** Engraftment of secondary recipients transplanted with sorted CD45.2 cells from primary mice 24 weeks after transplantation.

Table 4.4: HSC frequency following *in vivo* deletion of *Meis1* in primary recipients

	CD45.2^{+}	HSC Frequency	Upper 95% CI	Lower 95% CI
MxCre/Meis1$^{+/-}$	BULK	1/138 474	1/31 167	1/615 000
MxCre/Meis1$^{-/-}$	p<0.06	1/17 857 263	1/2 532 079	1/126 000 000
MxCre/Meis1$^{+/-}$	SORTED	1/160 806	1/39 986	1/646 690
MxCre/Meis1$^{-/-}$	p<1x10^{-125}	1/1 015 552	1/284 833	1/3 620 882

Gene expression changes following loss of* Meis1 *in an HSC-enriched population

To search for differentially regulated genes following Meis1 deletion, *Meis1* was deleted in *MxCre/Meis1* mice and the HSC-enriched LSK population isolated for mRNA extraction 7 days after the final PolyI:C injection. mRNA isolated from 3 individual *MxCre/Meis1*$^{-/-}$ and 3 *MxCre/Meis1*$^{-/+}$ mice was amplified and subjected to transcriptome analysis using the Affymetrix Exon ST array (Figure 4.7, panel a). Following normalization for hybridization, litter batch effects and multiple hypothesis testing as described in Chapter 2, 171 differentially expressed genes were identified using a 90% confidence interval (Table 4.5). Of these differentially expressed genes, 8 had a fold change expression greater than two-fold (Table 4.6).

These 8 genes and others of interest selected from previous studies of *Meis1* candidate targets were validated by RT-PCR on the original samples and an additional two

independent replicates (Figure 4.7, panel b). Of note, 2 genes implicated in leukemia, *Hlf* and *Msi2* (Andres-Aguayo, *et al.*, 2012, de Boer *et al.*, 2011) are down-regulated in response to the loss of *Meis1*. Msi2 has also been reported to be up-regulated in the context of Vp16/Meis1 (Wang *et al.*, 2006). ChIP-Seq data for Meis1 performed in our laboratory (Eric Yung *et al.*, unpublished) has also revealed MEIS1 binding sites in the body of *Msi2* and in both the body and transcription start site of *Hlf*. *Flt3* was also identified as direct target of MEIS1 in these experiments and was found to be differentially expressed by 1.5-fold between $MxCre^{+}/Meis1^{-/-}$ and $MxCre^{+}/Meis1^{-/+}$ LSK cells. *Flt3* has previously been shown to be induced by *Meis1* overexpression and is thought to be one of several pathways by which *Meis1* influences leukemic activity (Argiropoulos *et al.* 2008).

Leading edge Gene Set Enrichment Analysis (GSEA) of all differentially expressed genes showed enrichment in cell cycle genes, consistent with the proliferation defect seen in CFC studies and previous work in leukemia models (Figure 4.7, panel c, Argiropoulos *et al.,* 2010). We attempted to follow up with cell cycle analysis on $Meis1^{-/-}$ cells in both primary cells *in vitro* and *in vivo*. In the LSK subset *in vitro* and *in vivo* no differences were seen in bromodeoxyuridine (BrdU) incorporation, suggesting no major differences in the proportion of cells in Go/G1, S or G2/M in the LSK population (data not shown) of $Meis1^{-/-}$.

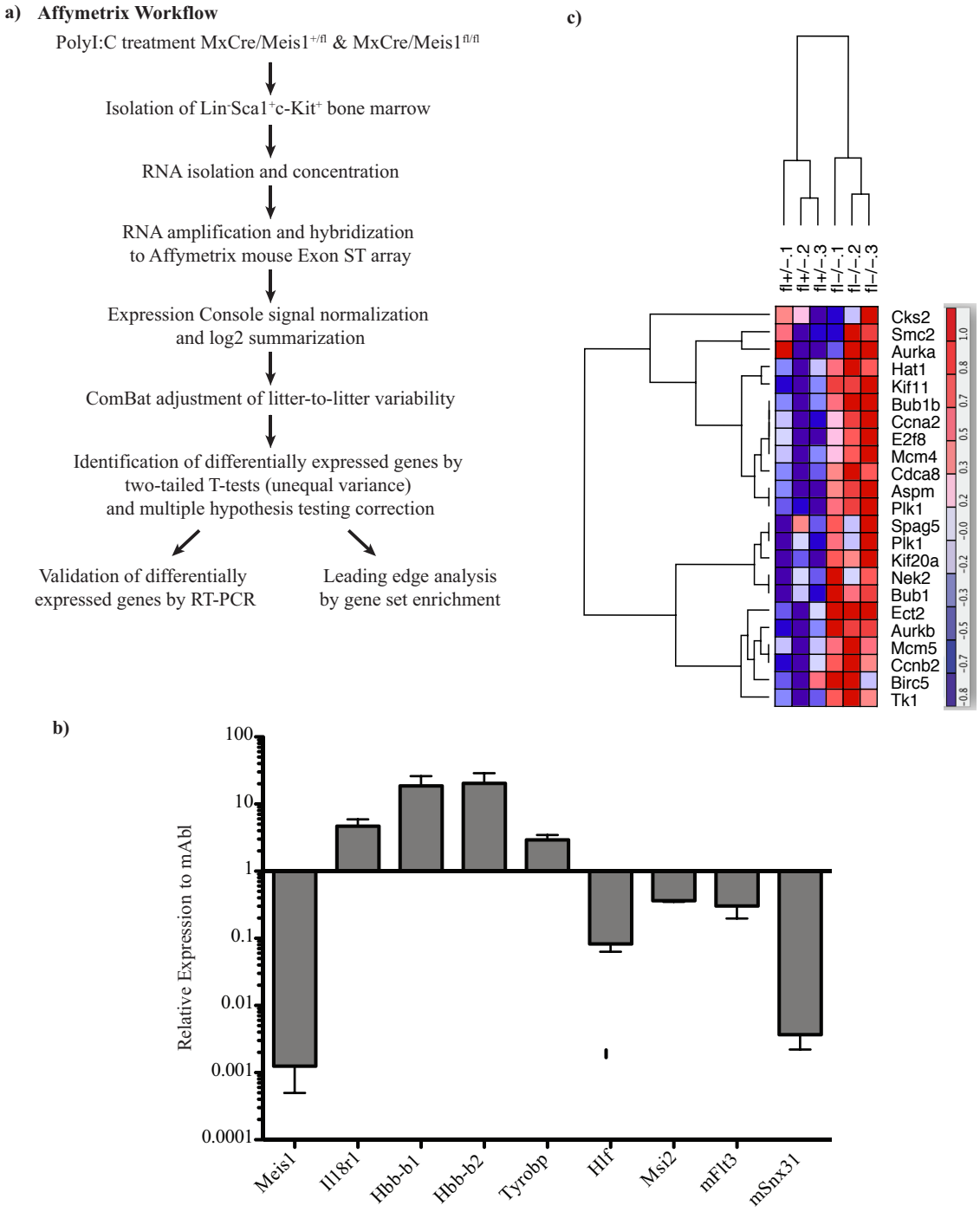

Figure 4.7: Affymetrix mouse Exon ST 1.0 analysis of gene expression changes as a result of loss of *Meis1* in an HSC-enriched population.

a) Experimental design. Individual, litter-matched *MxCre/Meis1*$^{fl/fl}$ and *MxCre/Meis1*$^{fl/+}$ mice were induced for *Meis1* deletion with PolyI:C every 48 hours for 18 days. 7 days following the final injection, mice were euthanized, bone marrow extracted and sorted for Lin$^-$ Sca-1$^+$

c-Kit^{+} cells by FACS. RNA was isolated from this HSC-enriched population and amplified prior to hybridization on an Affymetrix mouse Exon ST 1.0 gene expression array. Signal was normalized using Expression Console software and log2 summarization. Differentially expressed genes were identified using two-tailed t-test with multiple hypothesis correction. Changed pathways were interrogated by leading edge analysis. **b)** Validation of selected candidate target genes by Q-RT-PCR, using both sample RNA and two additional independent replicates. **c)** Leading edge gene-set enrichment analysis reveals enrichment of genes involved in cell cycle.

Table 4.5: Genes differentially expressed with deletion of *Meis1* as determined by Affymetrix analysis within a 90% adjusted confidence interval

Probe Name	Description	Adjusted t-Test	Fold decrease in *Meis1*$^{-/-}$
6836829	Dgat1	0.006761443	0.686689462
6817970	Nt5dc2	0.01133132	0.70196703
6828741	C1qtnf3	0.01148776	0.829957265
6790699	Hlf	0.01207463	3.180698125
6942692	Tmem184a	0.03904288	0.919683837
6835004	Snx31	0.03916838	1.214778913
6790621	Msi2	0.04223439	2.070406603
6871457	Incenp	0.04471138	0.867291904
6929828	Nat8l	0.04471138	0.791477701
6798334	Adam6b	0.05381157	1.562741704
6993465	Endod1	0.05650069	0.808002529
6993472	Fut4	0.05650069	0.671168355
6953607	Hoxa6	0.05650069	0.835739062
6808173	Irx2	0.05650069	0.903497659
6992172	Dusp7	0.07083209	0.709573183
6769213	Plk5	0.07433471	0.958082417
6769381	D10Wsu102e	0.07433471	0.799486601
6790046	Evi2b	0.07433471	0.754337234
6974010	Ing1	0.07433471	0.795613559
6992436	Ngp	0.07433471	0.686477168
6967109	Ptpn5	0.07433471	0.953819688
6820084	Reep4	0.07433471	0.750008593
6992178	Rrp9	0.07433471	0.876239425
6916748	Slc2a1	0.07433471	0.904081689
6883184	Slc2a10	0.07433471	0.85757217
6857885	Srbd1	0.07433471	0.75571711
6894253	Chrna4	0.07433471	1.044130276
6933084	D930016D06Rik	0.07433471	1.512825956
6782496	Dbil5	0.07433471	1.221825464
6869635	Entpd1	0.07433471	1.258515318
6900348	Gstm5	0.07433471	1.529539288
6962759	Kctd14	0.07433471	1.338515966
6964011	Scnn1g	0.07623116	0.878159125
6867632	Cabp2	0.07905712	0.92302027
6748889	Il18r1	0.07905712	0.487679618
6978369	Mmp15	0.07905712	0.946099273

Probe Name	Description	Adjusted t-Test	Fold decrease in *Meis1*$^{-/-}$
6805191	Olfr263-ps1	0.07905712	3.401042566
6789360	2810408A11Rik	0.08290535	0.859347092
6895915	Bhlhe22	0.08290535	0.907053702
6925562	Zbtb8b	0.08290535	0.91087139
6965893	Lypd4	0.08290535	1.055802188
6763295	Ralgps2	0.08290535	1.363438361
6982267	Wwc2	0.08290535	1.165781047
6846010	Cd96	0.09373904	0.655477699
6995384	Fam55b	0.09373904	0.77994938
6920609	Gja10	0.09373904	0.847973393
6969997	Hbb-b1	0.09373904	0.205045826
6852144	Lbh	0.09373904	0.742217798
6855706	Srf	0.09373904	0.796670523
6883261	Trp53rk	0.09373904	0.68789235
6815523	Naip5	0.09373904	1.459240896
6751349	Dgkd	0.09440419	1.271864279
6917813	Asap3	0.09593448	0.956210778
6767782	Lilrb4	0.09593448	0.217899404
6959584	Tyrobp	0.09593448	0.477594239
6858134	Nrxn1	0.09593448	1.52807978
6959536	Zfp30	0.09593448	1.163797528
6858910	Ttc39c	0.09641302	0.885682526
6802491	6430527G18Rik	0.09826282	0.822903471
6969016	9930013L23Rik	0.09826282	0.934908463
6775322	C030046I01Rik	0.09826282	0.914925308
6966490	C230052I12Rik	0.09826282	0.835897232
6972491	Ccnd1	0.09826282	0.78631627
6910126	Clca2	0.09826282	0.875813922
6818044	D830044D21Rik	0.09826282	0.881678297
6873363	Fgf8	0.09826282	0.839396182
6780332	Gabrb2	0.09826282	0.744622975
6927253	Gabrd	0.09826282	0.903307584
6785213	Galr2	0.09826282	0.817732162
6964600	Gpr26	0.09826282	0.804403471
6981099	Ido1	0.09826282	0.920582657
6838716	Itgb7	0.09826282	0.861326652
6789197	Ntn1	0.09826282	0.873434537
6863467	Osbpl1a	0.09826282	0.811192447
6751264	Psmd1	0.09826282	0.903584256
6917963	Rap1gap	0.09826282	0.922605325
6983163	Rfxank	0.09826282	0.922160403
6799645	Rps7	0.09826282	0.800539592
6801636	Rtn1	0.09826282	0.931952816
6865957	Slc6a7	0.09826282	0.923006603
6841739	Tomm70a	0.09826282	0.708964521
6977523	Anapc10	0.09826282	1.102988954
6775441	Atcay	0.09826282	1.093399049
6937253	Fam53a	0.09826282	1.289113157
6943142	Flt3	0.09826282	1.510209021

Probe Name	Description	Adjusted t-Test	Fold decrease in *Meis1*$^{-/-}$
6980568	Gas6	0.09826282	1.076483534
6791302	Gjd3	0.09826282	1.212372281
6866800	Katnal2	0.09826282	1.120357182
6755237	Kcnj10	0.09826282	1.080823042
6838695	Krt78	0.09826282	1.093853513
6936930	Lmbr1	0.09826282	1.268653264
6818858	Mudeng	0.09826282	1.298148084
6818523	Ptger2	0.09826282	1.153822817
6815382	Rgnef	0.09826282	1.080829635
6966041	Shkbp1	0.09826282	1.039448805
6799842	Slc26a4	0.09826282	1.065860955
6871139	Mtvr2	0.09826282	1.12901198
6864444	Stard4	0.09826282	1.188663435
6824195	Txndc16	0.09826282	1.185122457
6954615	Vamp5	0.09826282	5.77675678
6807209	Zfp346	0.09826282	1.258522896
6872206	1700028P14Rik	0.09871875	0.939795599
6867593	1810055G02Rik	0.09871875	0.858117949
6969429	4632434I11Rik	0.09871875	0.699203711
6899308	4933434E20Rik	0.09871875	0.886234308
6875832	Adamts13	0.09871875	0.949246684
6968126	Arrdc4	0.09871875	0.789476573
6784765	Axin2	0.09871875	0.909899641
6784329	BC030867	0.09871875	0.859150792
6790199	Ccl1	0.09871875	0.852827886
6773485	Cdc40	0.09871875	0.644957771
6950137	Clec12a	0.09871875	0.55226552
6748695	Cnga3	0.09871875	0.848009481
7016421	Cul4b	0.09871875	0.756217809
6861751	D18Ertd653e	0.09871875	0.859290586
6892580	D630003M21Rik	0.09871875	0.972298247
6871627	Dtx4	0.09871875	0.920747116
6959674	Gm6725	0.09871875	0.680986794
6935273	Eif3b	0.09871875	0.666257578
6953126	Fam131b	0.09871875	0.838222299
6947394	Mogs	0.09871875	0.884365136
6934506	Glt1d1	0.09871875	0.893948355
6941215	Gltp	0.09871875	0.880693101
6840400	Hes1	0.09871875	0.918382136
6762452	Igfn1	0.09871875	0.918880257
6784845	Kcnj2	0.09871875	0.869945205
6823849	Mapk8	0.09871875	0.689086426
6829297	March11	0.09871875	0.865598668
6850723	Mea1	0.09871875	0.810454696
6876010	Med27	0.09871875	0.816689095
6993272	Mmp1b	0.09871875	0.872917557
6850661	Mrpl14	0.09871875	0.782647265
6943387	N4bp2l1	0.09871875	0.789798996
6911925	Nbn	0.09871875	0.719175098

Probe Name	Description	Adjusted t-Test	Fold decrease in *Meis1*$^{-/-}$
6804893	Nid1	0.09871875	0.918265128
6832332	Nup50	0.09871875	0.795160585
6850345	Olfr130	0.09871875	0.917081849
6958995	Opa3	0.09871875	0.808539415
6919095	Pank4	0.09871875	0.869308084
6991358	Plscr1	0.09871875	0.858824362
6924882	Ptprf	0.09871875	0.954875573
6791534	Pyy	0.09871875	0.82370519
6956765	Rassf4	0.09871875	0.628405716
6789789	Rph3al	0.09871875	0.895808026
6797572	Serpina5	0.09871875	0.823835983
6762423	Shisa4	0.09871875	0.888228821
6768323	Slc25a16	0.09871875	0.888569833
6978937	Sntb2	0.09871875	0.87858046
6902192	Ssx2ip	0.09871875	0.966105003
6893057	Sulf2	0.09871875	0.927836986
6837318	Tob2	0.09871875	0.891491411
6971410	Prss53	0.09871875	0.733547615
6768898	Vpreb3	0.09871875	0.866078032
6888928	Accs	0.09871875	1.100261389
6972149	BC066028	0.09871875	1.126072063
6864520	Brd8	0.09871875	1.137338966
6968772	Cib1	0.09871875	1.279751569
6845159	Fbxo45	0.09871875	1.099376831
6934855	Gatsl2	0.09871875	1.407191182
6961012	Magel2	0.09871875	1.155860681
6907869	Mov10	0.09871875	1.303027043
6970037	Olfr649	0.09871875	1.128090383
6955066	Paip2b	0.09871875	1.161642402
6957178	Plekhg6	0.09871875	1.048243756
6857834	Prepl	0.09871875	1.156735331
6854460	Rab11fip3	0.09871875	1.075945323
6866862	Setbp1	0.09871875	1.044104365
6762355	Tmem183a	0.09871875	1.227058832
6859415	Zfp397	0.09871875	1.286213235
6862627	Zfp516	0.09871875	1.940285837
6753091	Elk4	0.09986983	1.358886916

Table 4.6: Genes with > 2-fold expression change associated with deletion of *Meis1* as determined by Affymetrix analysis

Probe Name	Description	Adjusted t-Test	Fold decrease in *Meis1*$^{-/-}$
6954615	VAMP5	0.0982	5.7767
6805191	OLFR4	0.0790	3.4010
6790699	HLF	0.0120	3.1807
6790621	MSI2	0.0422	2.0704
6748889	IL18R1	0.0790	0.4877
6959584	TYROBP	0.0959	0.4776
6767782	LILRB4	0.0959	0.2179
6969997	HBB-B1	0.0937	0.2050

A recent study using *Meis1* $^{-/-}$ Lin^{-} adult BM cells as input for the Affymetrix array (Unnisa *et al.*, 2012) revealed down-regulation of several gene sets up-regulated in response to hypoxia, including those regulated by *Hif1* α. This is consistent with recent reports by another group (Simsek *et al.*, 2010; Kocabas *et al.*, 2012) reporting direct regulation of *Hif1α* by *Meis1* in the HSC compartment. We were unable to find evidence of *Hif1α* loss of expression by RT-Q-PCR in our sorted KSL population. We also looked in the more highly HSC-enriched LSKCD150^{+}CD48^{-} population by Q-RT-PCR and found no difference in expression between *MxCre/Meis1*$^{-/-}$ and *MxCre/Meis*$^{-/+}$ in terns of *Hif1α* or *Hif2α* gene expression relative to *mAbl* (Figure 4.9, panel a).

***Treatment with N-acetyl-L-cysteine rescues some of the phenotypic abnormalities seen with loss of* Meis1**

Recent studies suggest that MEIS1 plays a role in regulation of *Hif1α* expression and resultant regulation of ROS. It is thus hypothesized that increased ROS levels and resultant damage to HSC may underlie the decrease in HSC number and function upon *Meis1* deletion

(Simsek *et al*., 2010; Kocabas *et al.*, 2012; Unnisa *et al.*, 2012). Support for this model has been derived from studies demonstrating phenotypic rescue with N-acetyl-L-cysteine (NAC), a ROS scavenger. Despite a lack of evidence of *Hif1α* dysregulation at the level of mRNA in our model, we tested whether *in vivo* administration of NAC could rescue deficits seen in the HSC, MkP and EP populations. PolyI:C mediated Cre expression was initiated in *MxCre/Meis1*$^{fl/fl}$ and *MxCre/Meis1*$^{fl/+}$ mice. On the third PolyI:C injection, daily subcutaneous NAC or PBS injections were initiated (Figure 4.8, panel a). Five days after the final subcutaneous injection of PBS or NAC, mice were euthanized and analyzed for level of *Meis1* deletion, phenotype, CFC capacity and gene expression in sorted HSC and MkP populations. Estimated *Meis1* deletion was comparable for control and NAC treated mice (97% versus 85% respectively). 3 mice per genotype and per arm were used, however one *MxCre/Meis1*$^{-/-}$ mouse treated with NAC died prior to completion of the regime. Thus the comparisons using *MxCre/Meis1*$^{-/-}$ +NAC are estimates of significance as opposed to a statistical comparison. More replicates would ideally be done. Phenotypic analysis of PBS treated mice replicated earlier experiments, that is, there was an 11-fold drop and 7-fold drop in HSC and MkP absolute numbers, respectively in *Meis1* deleted mice compared to controls (p=0.001, p=0.05; Figure 4.8, panel b). CMP and GMP numbers were also reduced (14.5-fold, p=0.008; 2.5-fold, p=0.03), however the loss of the MEP population was not seen in this experiment. Strikingly, delivery of NAC abolished any phenotypic differences by FACS between *MxCre/Meis*$^{-/-}$ and *MxCre/Meis1*$^{-/+}$ mice (Figure 4.8, panel c) with the exception of CMPs where there was still a 4.5-fold reduction in *MxCre/Meis1*$^{-/-}$ marrow (p=0.02).

CFC numbers, however, were not affected by NAC treatment as there was still a significant decrease in detectable CFU-GM (1.5x, p = 0.04) and CFU-GEMM (7.8x, p =

0.006) in *MxCre/Meis*$^{-/-}$ mice treated with NAC compared to *MxCre/Meis1*$^{-/+}$ mice, also treated with NAC, in myeloid biased media (Figure 4.8, panel d). Using erythroid supportive conditions, numbers of large BFU-E (>16 colonies) also were not rescued by NAC administration in *MxCre/Meis*$^{-/-}$ mice compared to *MxCre/Meis1*$^{-/+}$ (12.8x reduction, p = 0.03; Figure 4.8, panel e). Significant differences in these groups are based on duplicate methylcellulose cultures per mouse

We additionally sorted HSC (LSKCD150^{+}CD48^{-}) and MkPs from *MxCre/Meis*$^{-/-}$ and *MxCre/Meis1*$^{-/+}$ PBS and NAC treated mice 5 days after the final treatment. We wanted to confirm the targets we identified in a more highly HSC-enriched population, examine if NAC had any impact on these genes, as well as if any key expression changes may be relevant in the MkP population. These results confirmed that loss of *Meis1* in HSCs results in loss of expression of *Hlf* and *Msi2*, candidate genes identified in our earlier Affymetrix analysis. In the more highly enriched LSKCD150^{+}CD48^{-} population, there was a 21-fold drop in *Hlf* (p=0.03) compared to 3-fold in the LSK population (Figure 4.9, panel a). This enrichment is roughly proportional to the increase in HSC content between the two populations, arguing for a role of *Meis1* regulation of *Hlf* expression in the HSC. *Msi2* expression dropped 4.3-fold (p=0.01) in the more enriched HSC population with the loss of *Meis1*. This is 2-fold more than was identified in the Affymetrix screen, suggesting this gene also plays a role in the HSC population, but likely also as well in non-HSC cells in the LSK population. Neither *Msi2* nor *Hlf* expression was significantly altered in the MkP population, suggesting regulation of these genes is exclusive to HSC-enriched cell populations as opposed to *Meis1*-expressing cells in general. In the presence of NAC, there were still significant changes in *Hlf* and *Msi2* expression in the absence of *Meis1*, although the

magnitude of this change was blunted. That is, there was a 3-fold lower expression of *Hlf* (p=0.02) and a 2-fold loss of *Msi2* expression (p=0.03) in *MxCre/Meis1*$^{-/-}$ compared to *MxCre/Meis1*$^{-/+}$ HSC.

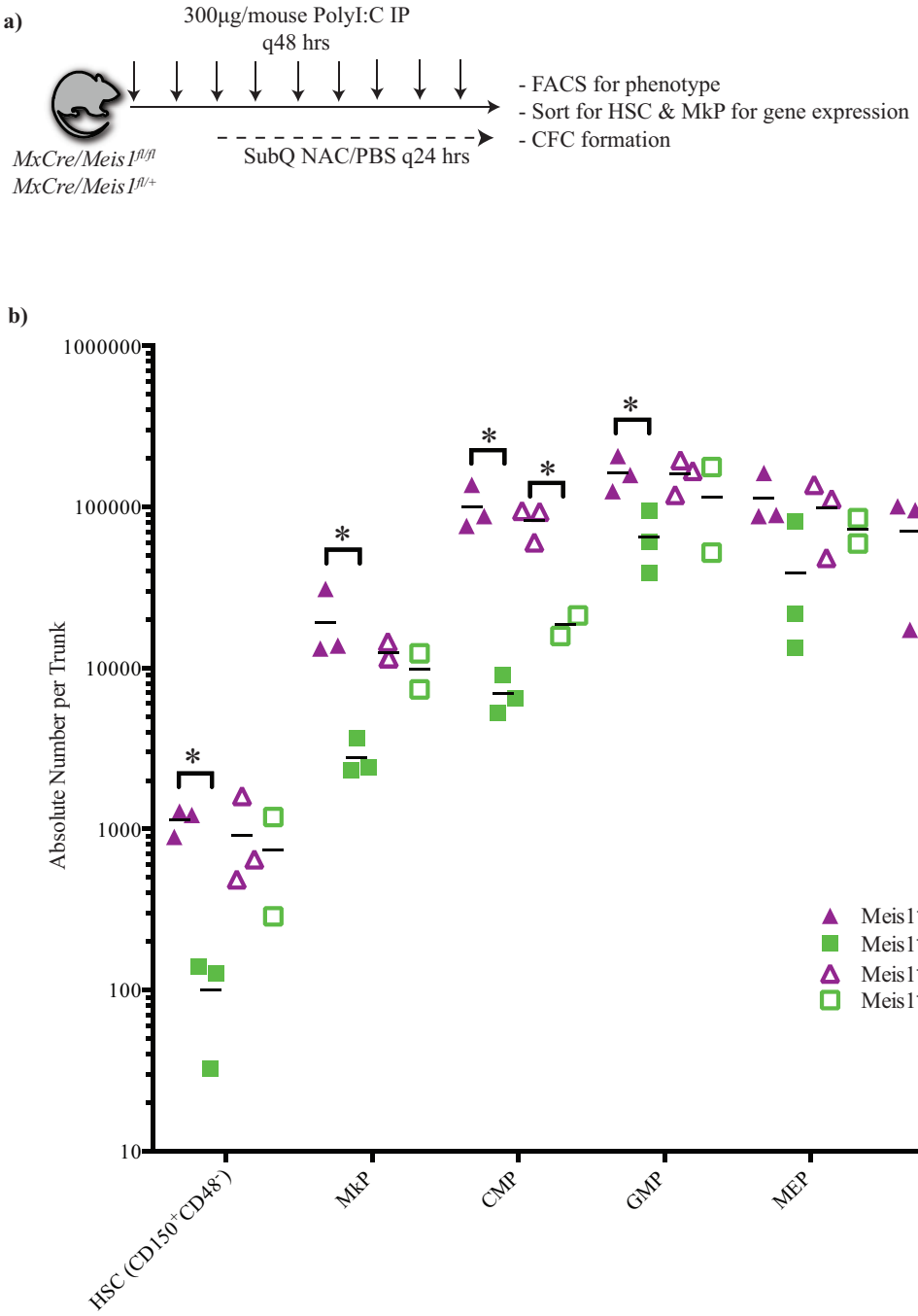
a)
300µg/mouse PolyI:C IP
q48 hrs
- FACS for phenotype
- Sort for HSC & MkP for gene expression
- CFC formation
SubQ NAC/PBS q24 hrs
MxCre/Meis1fl/fl
MxCre/Meis1fl/+
b)
Absolute Number per Trunk
1000000
100000
10000
1000
100
10
HSC (CD150+CD48-)
MkP
CMP
GMP
MEP
CLP
Meis1-/+ + PBS
Meis1-/- + PBS
Meis1-/+ + NAC
Meis1-/- + NAC

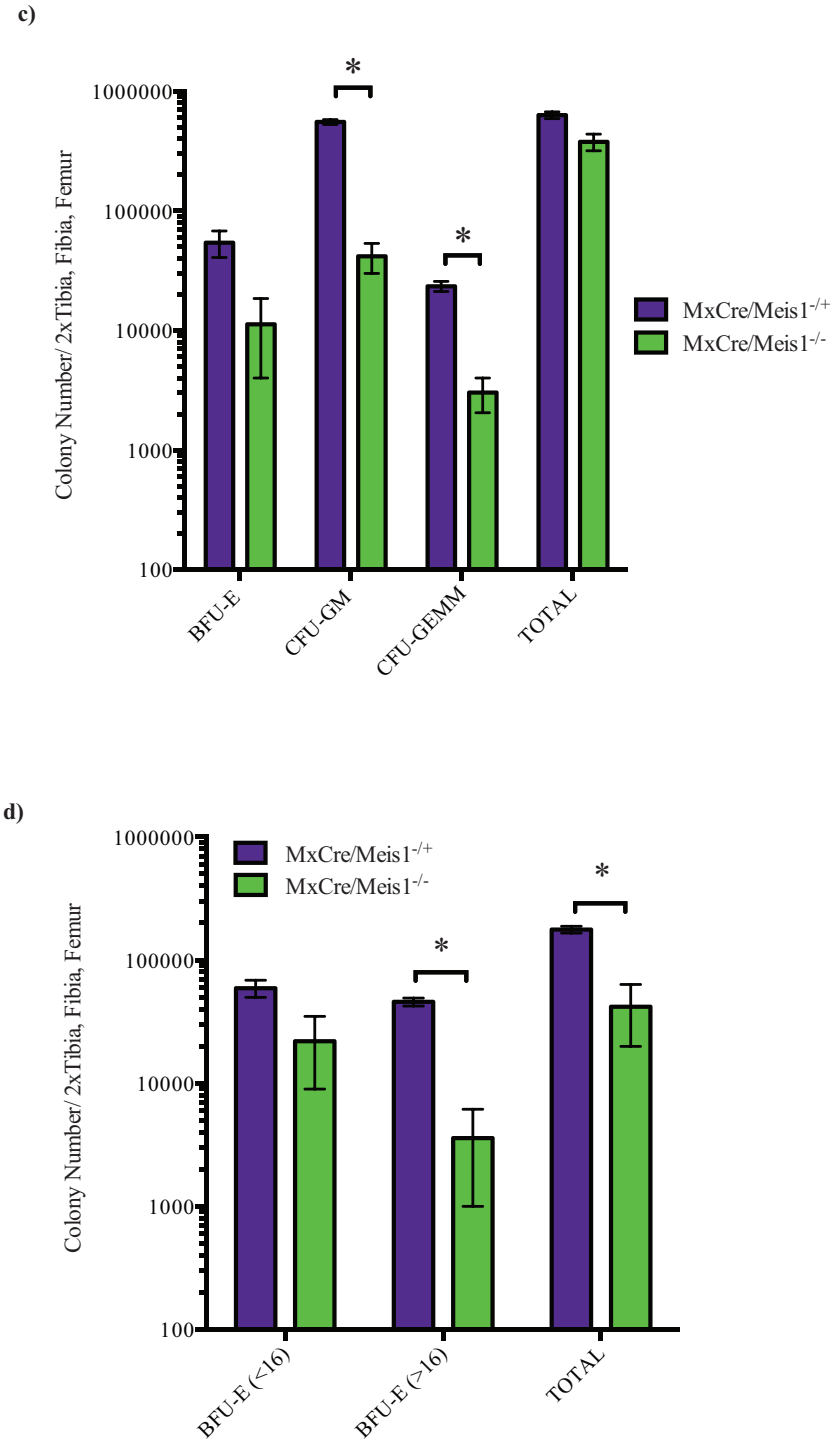

Figure 4.8: NAC treatment partially abolishes differences between *MxCre/Meis1*$^{-/-}$ and *MxCre/Meis1*$^{-/+}$ mice.

a) Experimental design. **b)** Phenotypic analysis of various cell populations by FACS between *MxCre/Meis1*$^{-/-}$ and *MxCre/Meis1*$^{-/+}$ mice treated with PBS and NAC. The differences

between *MxCre/Meis1*$^{-/-}$ and *MxCre/Meis1*$^{-/+}$ mice treated with PBS are consistent with those found in earlier experiments. Phenotypic differences between *MxCre/Meis1*$^{-/-}$ and *MxCre/Meis1*$^{-/+}$ mice were abolished with NAC treatment with the exception of maintenance of a 4.5-fold reduction in CMP numbers ($p = 0.02$). **c)** CFC formation in myeloid-supportive conditions continues to be impaired in *MxCre/Meis1*$^{-/-}$ mice following *in vivo* NAC administration. CFU-GM are reduced 1.5-fold ($p = 0.04$) and CFU-GEMM are reduced 7.8-fold ($p = 0.006$). **d)** NAC does not rescue the capacity for *MxCre/Meis1*$^{-/-}$ cells to form large BFU-E (>16 clusters/colony) in erythroid supportive media (12.8-fold reduction, $p = 0.03$). Both FACS data and colony numbers are expressed as absolute numbers isolated from the trunk of mice (2 femurs, 2 tibias, 2 iliac crests).

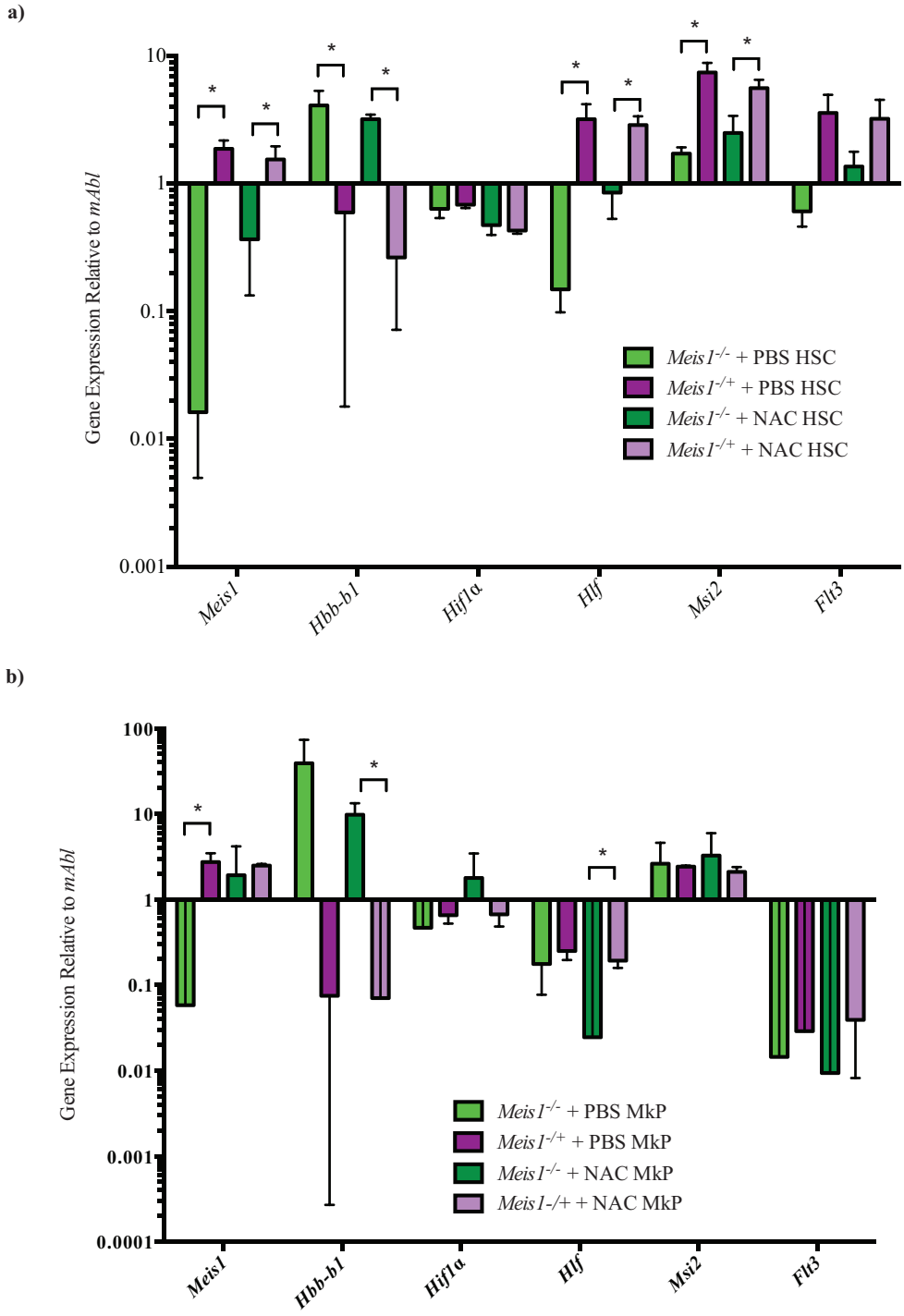

Figure 4.9: Gene expression changes as a result of NAC-treatment in sorted HSC and MkP populations

a) Gene expression changes as a result of loss of *Meis1* in the sorted HSC population treated with NAC or PBS. In PBS treated mice, there is a significant difference between *MxCre/Meis1*$^{-/-}$ mice and *MxCre/Meis1*$^{-/+}$ mice in the expression of *Meis1* (115-fold, *p*=

0.004), *Hlf* (21-fold, p=0.03), *Msi2* (4.3-fold**,** p=0.01) and *Hbb-b1*(8-fold gain, p= 0.02). These differences are maintained with NAC treatment: *Meis1* (4-fold, p= 0.04), *Hlf* (4-fold, p=0.02), *Msi2* (2-fold**,** p=0.03) and *Hbb-b1*(12-fold gain, p= 0.0007). No differences in expression of these genes were found between PBS and NAC treated *MxCre/Meis1*$^{-/-}$ mice. **b**) Very few significant gene expression changes were found between *MxCre/Meis1*$^{-/-}$ and *MxCre/Meis1*$^{-/+}$ treated MkP cells. In PBS treated mice, there was a 47-fold drop in *Meis1* expression (p=0.02) and in NAC treated mice, a 8-fold loss of *Hlf* (p=0.01) and 140-fold gain in *Hbb-b1* expression (p=0.01).

Discussion

The primary goal of the studies described in this chapter was a better understanding of the roles *Meis1* may play in adult hematopoiesis. To this end we have exploited mouse models in which *Meis1* can be conditionally deleted using two different Cre induction strategies. Four key findings emerge from these studies. First, *Meis1* is essential for the homeostatic maintenance and regenerative capacity of adult HSC. Second, *Meis1* has essential roles also in the early steps in the megakaryocytic and erythroid pathways. Third, our results of gene expression analyses point to novel putative effectors of *Meis1*'s activity. Fourth, the impact of *Meis1* deletion can be blunted using scavengers of reactive oxygen species and thus further implicating ROS regulation as a Meis1 functional pathway.

Meis1 *is required for HSC maintenance and self-renewal*

We founds that *Meis1* is required for the HSC maintenance by two lines of evidence. In the absence of *Meis1* there was a 5-fold reduction in the numbers of phenotypically defined HSC (LSKCD150^{+}CD48^{-}) in the *MxCre* model that correlates to a 10.7-fold reduction in functionally defined HSC by long-term repopulating assays. This is supported by a 19-fold reduction in HSC in long-term repopulating assays in the *ERTCre* model in the absence of *Meis1* compared to heterozygous controls. As total bone marrow cellularity is not impacted by loss of *Meis1* this corresponds to only 270 or 230 HSC per mouse in the *MxCre*

and *ERTCre* models, respectively. This is in contrast to *Meis1*$^{-/+}$ mice where there are roughly 3000 or 5000 HSC per mouse in the *MxCre* and *ERTCre* models, respectively. In a serial transplantation assay we show that *Meis1*$^{-/-}$ stem cells are almost devoid of self-renewal capacity as they fail to contribute to repopulation into secondary recipients. This is in comparison to *Meis1*$^{-/+}$ cells that are able to sustain long-term repopulation in secondary recipients. This represents, at minimum, a 25-fold reduction in self-renewal capacity between *Meis1*$^{-/-}$ and *Meis1*$^{-/+}$ HSC. We additionally show this deficit to be largely cell intrinsic as there is a 6.3-fold drop in HSC frequency in *Meis1*$^{-/-}$ cells compared to *Meis1*$^{-/+}$ transplanted into wild-type recipients prior to induction of allele deletion.

Overall our findings are consistent with two recently published studies using the same *Meis1* conditional knock-out allele (Kocabas *et al.*2012; Unnisa *et al*, 2012). While Unnisa *et al.* crossed mice onto the same *Rosa26ERTCre* strain as some of our studies, Kocobas *et al*. used the *SclERTCre* mouse where Cre expression is driven from the *Scl* promoter which is expressed in primitive hematopoietic, erythroid and megakaryocytic cells as well as in endothelium and specific neural tissues (Bockamp *et al*. 1995; Elefanty *et al.*, 1999). This is of interest since although our studies have utilized different induction schemes, there are some key similarities between our studies. Although Unnisa *et al.* also used the *ERTCre* model, they used 5 daily IP injections of 1mg 4-OHT or one large 4mg bolus. Of note, they used non-quantitative PCR to document allele deletion and achieved only a 50% reduction in *Meis1* mRNA as compared to our consistently >90% deletion. Unnisa *et* al. also confirmed loss of full-length *MEIS1a* by Western blotting, although only showed a narrow view of the blot, making a comparison to our study impossible. Kocabas *et al.* used daily IP injections of 1.2mg 4-OHT for 14 days, also used non-quantitative PCR to

document deletion and were able to achieve a similar 90% reduction in *Meis1* mRNA to our studies.

Studies by both Unnisa *et al.* and Kocabas *et al.* documented a loss of phenotypically and functionally defined HSC similar to our studies. Unnisa *et al.* used the same markers to our studies and found a 2.5-fold reduction in HSC numbers. Using bulk competitive transplants of $1x10^6$ cells from 4-OHT-treated transgenic mice, they were unable to show significant reconstitution by *Meis1*$^{-/-}$ cells in recipient mice 4 weeks following transplantation. Kocabas *et al.* used a similar competitive transplantation experiment using purified *Meis1*$^{-/-}$ LSKFlk2$^-$CD34$^-$ cells enriched for long-term HSC activity and were also unable to document long-term contribution to recipient mouse engraftment. Both groups were unable to detect a significant contribution to engraftment of *Meis1*$^{-/-}$, similar to our findings. Notably, in contrast to our studies of engraftment in primary and secondary recipients, neither group used limiting dilution assays and were thus unable to quantify HSC frequency in their studies. Also of note is that although Kocabas used a different marker subset to define HSC-enriched populations, their studies suggest that there are increased numbers of HSC that are cycling and fail to support long-term engraftment due to loss of quiescence and exhaustion.

Together our results robustly reveal a critical and indisputable role of *Meis1* in HSC function. Where our studies differ in terms of HSC function however is with respect to quantitation and interpretation of underlying mechanisms. Both Unnisa *et al.* and Kocabas *et al.* devote a number of experiments to documenting a role for ROS in the HSC compartment as well as increased cell cycling. Comparison of our ROS studies are discussed below. Both Unnisa *et al.* and Kocabas *et al.* found increased proportions of *Meis1*$^{-/-}$ cells in G_1+S-G^2-M

using Hoechst/Pyronin in their respective HSC-enriched compartments (LSKCD150^{+}CD48^{-} and LSKFlk2^{-}CD34^{-}, respectively). Unnisa *et al*. were also able to document a nearly 2-fold increase in bromodeoxyuridine (BrdU)-positive cells in the LSKCD150^{+}CD48^{-} HSC-enriched compartment using *in vivo* staining. We were unable to document this using *in vivo* or *in vitro* BrdU in our studies. This may be due to our practice of using treated *Meis1*$^{-/+}$ mice as controls in our studies. Unnisa *et al* used both non-Cre expressing and Cre expressing *Meis1*$^{fl/+}$ mice as controls, whereas Kocabas *et al.* also included *Meis1*$^{+/+}$ and *Meis1*$^{fl/+}$ non-Cre expressing and Cre expressing mice as controls. Inclusion of non-Cre expressing and *Meis1*$^{+/+}$ mice as controls does not account for cell cycle changes as a result of DNA damage and repair resultant from Cre-mediated deletion. Cre-mediated deletion of *Meis1*, involves DNA strand damage, Holliday quadruplex formation and DNA repair by homologous mechanisms (reviewed Craig, 1988). Even in the absence of LoxP sites, Cre expression in mammalian cells leads to reduced cell proliferation and accumulation in G_2/M in a Cre-dose dependent manner (Loonstra *et al.*, 2001). It is thus possible that differences in cell cycling in the Kocabas *et al.* and Unnisa *et al.* studies are due to a lack of Cre-mediated cell cycle depression in a significant proportion of their controls as opposed to a genuine influence of loss of *Meis1*. While the major finding of a loss of HSC potential remains consistent among the three studies, certain key differences highlight the need for further study.

Meis1 ***is required for megakaryopoiesis and erythropoiesis in the adult***

While *Meis1* expression had been previously implicated in fetal megakaryopoieis (Hisa *et al.*, 2004; Azcoitia *et al*, 2005), our studies are the first to show a critical role in

adult megakaryo- and erythropoiesis. We found a loss in platelets in both our models as well as reductions in RBC numbers in the *ERTCre* model. Reduced numbers of terminally differentiated mature cell types was supported by a 9-fold reduction in large CFU-Mk colonies and 11-fold loss of phenotypically defined megakaryocyte progenitors. A 6-fold reduction in phenotypically defined megakaryocytic-erythroid progenitors (MEP) was mirrored by a 4-fold reduction in BFU-E colonies in the bone marrow of *MxCre/Meis*$^{-/-}$ cells compared to *Meis1*$^{-/+}$ controls. The loss of erythroid potential in the absence of *Meis1* was exacerbated in the phenylhydrazine (PHZ) model of hemolytic anemia and stress erythropoiesis where the proliferative potential of *Meis1*$^{-/-}$ erythroid progenitors is severely blunted.

Kocabas *et al.* also documented a consistent reduction in RBC and platelet numbers in the peripheral blood of *Meis1*$^{-/-}$ mice and reduction in phenotypically defined CMP, GMP and MEPs. They did not examine lineage-restricted megakaryocytes either phenotypically or functionally and limited their examination of erythroid lineages to a similar finding of reduced BFU-E numbers in the bone marrow of treated mice. Their interpretation was of a pan-lineage reduction in myeloid progenitors due to a loss of primitive HSC. Our finding that *Meis1*$^{-/-}$ cells can be assayed as CFCs of myeloid, erythroid and mixed lineage may support a model whereby *Meis1* is dispensable for lineage-restricted progenitors. As GMP numbers are unchanged in our hands, however, our findings do not necessarily support this interpretation. Also at odds with this interpretation is a lack of lymphoid lineage perturbation in either of our studies. In addition, in our hands, peripheral blood platelet numbers in both the *MxCre* and *ERTCre* models normalize to normal levels 2 weeks after induction, despite persistence of the deleted *Meis1* allele, that is, outgrowth of *Meis1*$^{+}$ cells alone cannot

account for this phenomenon (data not shown). That *Meis1*$^{-/-}$ bone marrow cells fail to form large BFU-E colonies following PHZ treatment (73-fold reduction in *Meis1*$^{-/-}$ spleen cells) may support an alternative model whereby *Meis1* expression is required for proliferation of erythroid and megakaryocytic progenitors but is dispensable for differentiation along these lineages. Further studies are warranted to determine if the deficit in these lineages is due solely to a lack of upstream HSC or if lack of proliferation of megakaryocytic and erythroid progenitors plays a more predominant role in this phenotype.

In the *ERTCre*-model, we found a loss of mature megakaryocytes histologically in the bone marrow of moribund mice that was reflected in a loss of platelet numbers in the peripheral blood of these mice. Interestingly, in the *MxCre* model, no such loss of mature megakaryocytes was seen histologically, although there was a loss of phenotypically defined megakaryocytic progenitors, primitive colony-forming cells and mature platelets. This phenomenon of altered progenitor number without an apparent reduction of the mature cell type is reminiscent of the role of TGF-β1 in the erythroid population where expression serves to stimulate differentiation (Krystal *et al*., 1994). In these studies, TGF-β1 in culture lead to impaired expansion of immature progenitor cell types, likely due to early differentiation. Whereas at certain time points the mature cell output was identical between conditions, ultimately the loss of progenitors in culture lead to reductions in overall mature cell output. In other words, when examining a lineage of cells that mature along a progression of stages, where each stage has variable proliferative potential, the distribution of cell stages will be heavily influenced by the time at which you take your measurement. A similar phenomenon could account for the lack of evidence of mature megakaryocyte loss in the marrow of *MxCre/Meis1*$^{-/-}$ mice, despite reductions in mature platelets and progenitors. Although

primitive cell number and mature megakaryocyte platelet output is reduced, intermediary mature megakaryocyte number may appear grossly normal. Histological evaluation at a later time point or following forced expansion in response to stress may reveal a loss of mature megakaryocytes in *MxCre/Meis1*$^{-/-}$ mice, similar to *ERTCre/Meis1*$^{-/-}$ mice.

Hlf *and* Msi2 *are putative effectors of* Meis1 *function in adult hematopoiesis*

Overall, we identified loss of expression of 4 genes (*Hlf*, *Msi2*, *Olfr4-2* and *Vamp5*) and gain of expression of 4 genes (*Il18r1, Tyrobp, Lilrb4,* and *Hbb-b1*) in response to loss of *Meis1* that met both criteria of a >90% confidence interval and >2-fold change. *Meis1* has previously been shown to be a transcriptional activator, thus, up-regulated genes in this model do not likely represent direct Meis1 targets. Up-regulated genes in our data set are primarily implicated in cell maturation and immune response, and are likely reflective of the loss of potential in the population studied and expression of Cre recombinase.

Our screen did not identify *PF4* as a differentially expressed target in the LSK compartment using Affymetrix analysis (Okada *et al.*, 2003). This is likely due to the fact that cells with megakaryocytic potential are found within the Sca1^{-} compartment, which was not evaluated in this study. *Flt3*, a defined but dispensable target for *Meis1* activity in leukemia, was found to be less-expressed in the absence of *Meis1* by RT-Q-PCR in our study. This loss of signal was not apparent in the Affymetrix analysis however. This may be a function of the high litter-to-litter variability in sample replicates as a result of using individual mice for each sample as opposed to a pooled population. It would be of interest to perform additional individual mouse replicates to reduce the signal to noise ratio between changes as a result of individual variability and those as a result of true loss of expression of *Meis1*.

Olfr4-2 (re-designated *Olfr153* May 2005), which encodes an olfactory receptor, and *Vamp5*, a plasma membrane protein (Entrez Gene results) were found to have lower expression with loss of *Meis1* by Affymetrix analysis. Neither have been implicated in hematopoiesis to date. *Olfr4-2* is not expressed at appreciable levels in HSC-enriched tissues based on information from the Immunological Genome Project (www.immgen.org; Jojic *et al.*, 2013), whereas *Vamp5* is expressed at ~1/3 the level of *Meis1*. The olfactory receptors share high sequence similarity, but there is also some homology (77% identity over 211 base pairs) to segments of *Pdgfra* cDNA, which was also down-regulated in our screen in response to loss of *Meis1*, however it did not reach statistical significance. This highlights a limitation of Afffymetrix gene analysis, that is, differentially expressed genes are identified by virtue of concurrent changes in hybridization of segments along a gene. Thus, transcripts with high homology are difficult to differentiate, especially transcripts with relatively low abundance.

Detection of significant changes in expression of transcripts at low abundance is one of the main weaknesses of hybridization-based gene expression arrays. In response to this, leading-edge analysis of gene sets (Gene Set Enrichment Analysis/GSEA) was developed (Subramanian *et al.*, 2005) in which sets of genes with associated functions/pathways are linked together based on *a priori* knowledge. Although individual genes in the set may not reach statistical significance, consistent changes in a gene set with related function may provide clues into differentially regulated processes between samples. In our analysis, although no cell cycle genes reached statistical and fold-change significance in isolation, GSEA was significant for cell cycle data sets, supporting a role for *Meis1* in cell cycle.

Our Affymetrix analysis and RT-Q-PCR also identified *Hlf* as a possible effector of *Meis1* function in an HSC-enriched population. *HLF* has been previously implicated in leukemia as a fusion with *E2A* in B-precursor ALL (de Boer *et al.*, 2011) as well as direct target of *Meis1* in Hox-mediated transformation (Argiropoulos *et al.*, 2010). E2A-HLF translocations are also thought to mediate leukemogenesis via Hox-independent mechanisms (Ayton & Cleary, 2003), highlighting Hox-independent functions for *Meis1*-mediated leukemogenesis. *Hlf* is differentially methylated and silenced through differentiation (Ji *et al*, 2010) and expression is enriched in the HSC population (www.immgen.com), supporting a possible role in HSC maintenance. Evidence for direct binding and regulation of *Hlf* by *Meis1* in leukemia (Argirpoulos *et al*., 2010) and our work suggests that *Meis1* may mediate possible *Hlf* function in the HSC. Interestingly, *Lmo2*, a transcription factor required for hematopoietic development in the embyo, is thought to be regulated by both *Hox* and *Hlf* (de Boer *et al.*, 2011; Calero-Nieto *et al.*, 2013). This highlights the complex interplay between transcription factor regulation in the HSC.

Msi2 was also identified as differentially expressed in our screen of *Meis1* targets. *Msi2* has been gaining attention in recent years due to increasingly evident roles in the maintenance of HSC repopulation potential (Hope *et al*. 2010) and AML prognosis (Byers *et al*., 2011). *Msi2* was also identified as part of a gene signature characterized by persistent *Vp16-Meis* transactivation in *Hox* models of leukemia (Wang *et al.*, 2006). The gene was first characterized in *D. melagnoster* as a regulator of asymmetric cell fate and may be involved in maintaining HSC quiescence via regulation of *Hes1* expression, a downstream effector of Notch signaling. Regulation of *Msi2* may be partially responsible for the deficits in BFU-E expansion in our studies as *Msi2* selectively expressed in cycling LT-HSC and

down-regulated with differentiation, with the exception of re-expression in the BFU-E (Hope *et al.*, 2010).

Regulation of *Hlf* and *Msi* by *Meis1* is also supported by ChIP-Seq experiments in our lab using a *Hox-Meis1* overexpression model (Yung *et al*., unpublished data) that demonstrates MEIS1 binding in the body of *Msi2* and in the transcription start side of *Hlf*. We examined changes of *Hlf* and *Msi* expression in highly purified populations of HSCs (LSKCD150^{+}CD48^{-}) and MkPs**.** These genes were consistently changed with loss of *Meis1*-expression in the HSC population, but not the MkP population, supporting a key role for *Hlf* and *Msi2* as effectors of *Meis1* function in the HSC compartment**.**

Regulation of ROS may play a role in* Meis1 *function

Although ROS and relative hypoxia had been previously implicated in HSC function (reviewed in Sardina *et al.*, 2012**)**, it was while examining the metabolic state of LT-HSC (as defined as Lin^{-}Sca1^{-}c-Kit^{+}CD34^{-}Flk2^{-} in their studies), that Simsek *et al.* (2010) first drew a link between ROS and *Meis1*. In this work, they showed that LT-HSC could be enriched on the basis of low metabolic activity and that this fraction was enriched for Hif1α protein, a mediator of adaptation to low oxygen environments. In addition, they highlighted a conserved MEIS1 binding site in the promoter of *Hif1α* and demonstrated regulation of *HIf1α* expression by MEIS1 through luciferase and shRNA experiments. A role for *Meis1* in hypoxia tolerance was a novel discovery and triggered subsequent work looking at *Hif1α* expression and ROS regulation by *Meis1* in the HSC compartment (Kocabas *et al.*2012; Unnisa *et al*, 2012, this work).

Our studies show that treatment with the ROS scavenger N-acetyl-L-cysteine (NAC) abolished any phenotypic differences between *MxCre/Meis1*$^{-/-}$ and *MxCre/Meis1*$^{-/+}$ mice in

HSC and MkP-enriched populations. Differences in CMP numbers remained unchanged, however, consistent with the lack of CFC rescue *in vivo* in our studies. This is in contrast to rescue of CFC formation from Lin^- cells *in vitro* found by Unnisa *et al*. using *in vitro* NAC treatment and deletion of *Meis1*. Using this model of *in vitro* deletion, they also performed Affymetrix analysis to show down-regulation of hypoxia-related gene sets and loss of *Hif1α* at the mRNA and protein level. The differences in our results may be rooted in both the experimental conditions as well as interpretation of NAC activity exclusively due to alteration of ROS levels.

Hif1α dimerization to Hif1β is thought to trigger gene expression programs that allow adaptation to hypoxic environments. These programs are hypothesized to protect against the DNA damage caused by high ROS levels in the hypoxic environment that lead to HSC apoptosis. This theory has been supported by studies using NAC as an ROS scavenger. NAC provides a source of glutathione as a substrate for degradation reactions of peroxide (H_2O_2) into O_2 and H_2O and thus reduces ROS levels following cellular treatment. Several studies have used restoration of HSC function with NAC treatment to infer ROS scavenging rescues the deficient phenotype (Tothova *et al*. 2007; Kocabas *et al.*2012; Unnisa *et al*, 2012). This is problematic, however, as NAC activity is not isolated to this role. NAC has been shown to modify the activity of key cell signaling and cycle cascade members Raf-1, MEK and ERK1/2, independently of its effect on ROS scavenging to promote cell survival (Zhang *et al*., 2011). Thus it is difficult to interpret if rescue using NAC is a result of reduction of ROS species or stimulation of the survival and cycling cascades influenced by Raf-1, MEK and ERK1/2.

Interplay between ROS, the niche, cell signaling and differentiation may also be of import in megakaryocyte commitment and differentiation. Recent evidence suggests that ROS may be a signal for megakaryocyte lineage commitment and proliferation from the HSC progenitor through activation of the MEK-ERK1/2 pathway (reviewed in Chen *et al*., 2013). In our study with *in vivo* NAC treatment, NAC treatment abolished HSC and MkP differences between *Meis1*$^{-/+}$ and *Meis*$^{-/-}$ mice and perhaps increased HSC and MkP numbers in NAC *Meis*$^{-/-}$ mice compared to PBS treated controls. As both ROS and NAC treatment stimulate MEK-ERK1/2 in the MkP, it is difficult to infer whether *Meis1* regulation of *Hif1α* plays any role in the MkP homeostasis. In our analysis of gene expression in the MkP population, no significant differences in *Hif1α* or *Hif2α* expression was found with either PBS or NAC-treatment between *MxCre/Meis1*$^{-/-}$ and *MxCre/Meis1*$^{-/+}$mice.

It is of note that in our gene expression studies, *Hif1α* expression was found to be unchanged in our HSC-enriched LSK population by Affymetrix, nor by directed RT-Q-PCR with loss of *Meis1*. This could be due to a technical problem in our studies or low levels of *bona-fide* HSC in the KSL population. Most LSK cells (~49/50) are not HSCs. Thus, lack of a difference between *Meis*$^{-/+}$ and *Meis1*$^{-/-}$ LSK cells does not preclude the possibility of cell cycle differences in the HSC compartment that we are not able to detect in this design. RT-Q-PCR in the more highly enriched LSKCD150^{+}CD48^{-} population, however, also did not reveal changes in *Hif1α* expression.

It is possible that our studies failed to show *Hif1α* changes in response to *Meis1* levels due to sample heterogeneity. Our studies use individual mice as replicates, as opposed to pooled individuals. We additionally used Cre-expressing *Meis1*$^{-/+}$ mice as controls, whereas other studies looking at ROS and *Meis1* used a collection of *Cre*$^{+}$*/Meis*$^{+/+}$, *Cre*$^{+}$*/Meis1*$^{-/+}$ or

Cre^{-}*/Meis1*$^{fl/fl}$ mice, raising the possibility of gene dosage differences between *Meis1*$^{-/+}$ and *Meis1*$^{+/+}$ mice that blunts detection of differentially expressed genes. This may be especially true for genes expressed at relatively low levels. For example, *Hif1α* is expressed at 10x lower levels than *Meis1* in the LT-HSC (www.immgen.org). Unnisa *et al*. showed enrichment for hypoxia gene signature, however, this was in a bulk Lin^{-} population which is ~10x enriched for HSC in bulk marrow compared to ~2000x for the LSK population used in our study.

An intriguing possibility is that while *Meis1* may be able to trigger *Hif1α* expression in experimental models, this may be a coincident change but not a particularly physiologically relevant one. While phenotypic rescue by NAC may apparently support a role for *Meis1* in hypoxia regulation, the varied effects of NAC makes this a somewhat tenuous conclusion. Use of specific MEK and mTOR inhibitors that would isolate general ROS changes from ERK1/2 effects would be useful in this regard.

Summary

Overall, we have validated a conditional model of *Meis1* deletion in the adult mouse that has lead to greater understanding of roles for *Meis1* in the adult HSC and novel roles in adult megakaryopoiesis and erythropoiesis. We identified 2 novel effectors of *Meis1* in adult, HSC-enriched populations, that is *Msi2* and *Hlf*. While we demonstrate that NAC treatment *in vivo* is able to rescue of some of the phenotypic changes seen as a result loss of *Meis1*, the varied effects of NAC outside of ROS scavenging and lack of documented changes of *Hif1α* make it difficult to ascertain if this is due to a true influence of *Meis1* on ROS levels. Our studies demonstrate the power of the conditional model of *Meis1* deletion as hypothesis

generating as well as testing. Further studies using the model and complementary methods will be invaluable for future study of *Meis1* function and resolving remaining key questions for its role in defined hematopoietic subsets.

Chapter 5 : Discussion

Introduction

While up-regulation of *Meis1* is a relatively common occurrence in leukemia, previous to the generation and distribution of a conditional knock-out mouse (Drs Jenkins & Copeland), a role for *Meis1* in normal adult hematopoietic homeostasis remained unknown. The concurrent validation of the model by our group and others has lead to a significant advance into our understanding into *Meis1* function and revealed some surprising putative mechanisms, including possible regulation of ROS (Kocabas *et al.*2012; Unnisa *et al*, 2012). For our part, the evidence presented in this work validates a conditional knock-out model to study the role of *Meis1*. Our subsequent studies using this model support a key role for *Meis1* in HSC maintenance and revealed novel roles in the maintenance of adult megakaryopoiesis and stress erythropoiesis. We show that in the absence of *Meis1,* there is a dramatic loss of HSCs, CMPs, MEPs and MkP phenotypically. These losses were reflected functionally in a number of assays. The MkP defect was seen as a reduction in platelet numbers *in vivo* as well as a reduced numbers of CFU-Mk in the bone marrow of *MxCre/Meis1*$^{-/-}$ mice. There was a loss of RBC in the peripheral blood of *ERTCre/Meis1*$^{-/-}$ mice and in *MxCre/Meis1*$^{-/-}$ BFU-E numbers as well as proliferative potential in response to PHZ induced stress. HSC number and self-renewal capacity is all but obliterated in the absence of *Meis1* based on quantitative limiting dilution CRU assays. In addition, we have used microarray expression analysis as a hypothesis-generating tool to identify *Msi2* and *Hlf* as possible effectors of *Meis1* in adult hematopoiesis, roles that have not been previously appreciated for these genes. This highlights the power of a conditional model of *Meis1* deletion in order to appreciate its contribution to a number of processes including normal development, adult homeostasis and

leukemia. The following discussion highlights some of these unresolved mechanisms and proposes experimental models in which these questions could be studied. These are grouped into the study of leukemic processes, revision of the canonical hematopoietic hierarchy, resolution of the role of *Meis1* deficiency in cell cycle regulation, and *Meis1* regulation of ROS via *Hif1α*.

Future avenues for research using the model outside of normal adult hematopoiesis to delineate roles for *Meis1* in leukemia

Several lines of evidence suggest *Meis1* plays a significant role in the generation of leukemia. Notably, it is up-regulated at high frequency in human hematologic malignancies and overexpression in immature mouse hematopoietic cells, be it in conjunction with *Hox* or as an MLL fusion co-expression, invariably causes leukemia. It is thus of interest to determine at which stages of leukemogenesis *Meis1* expression is essential and if disruption of *Meis1*-regulated expression profiles has significant impact on the generation or maintenance of the leukemic population, most importantly in the LSC population.

Although not reported in this work, we were able to generate leukemic cell lines on both the *ERTCre/Meis1*$^{fl/fl}$ and *MxCre/Meis1*$^{fl/fl}$ backgrounds using retroviral overexpression of genes of interest in leukemia including *Nup98-Hox* fusions, *MN1* and *MLL-AF9*. We were able to demonstrate both *in vitro* and *in vivo* deletion of *Meis1* using these lines. Other lab members have gone on to optimize generation and *Meis1* deletion in these lines. Experiments that could be envisaged using this model include both qualitative and quantitative studies as well as regulation of gene expression in the leukemic context by *Meis1*. Depending on when the *Meis1* is deleted in the target cell relative to the introduction of the oncogenes of interest,

it could be elucidated whether *Meis1* is important for the generation or maintenance or both of leukemic potential using both *in vitro* assays, including serial re-plating of CFCs, and *in vivo* transplantation experiments. Other groups have had success enriching for LSC potential on the basis of immunophenotyping and FACS (Bonnet and Dick, 1997; Gibbs *et al.*, 2012). Current studies into *Meis1* in the leukemic setting rely on overexpression and analysis of bulk populations with leukemic potential. It would be exciting to enrich for the LSC on the basis of phenotype then delete *Meis1*. One could then examine the functional impact on the LSC following the loss of *Meis1* as well as identify gene targets in this population. One could also monitor possible compensatory changes in gene expression following the loss of *Meis1* that maintain leukemic potential. Although not reported in this work, preliminary *in vivo* experiments using *MN1*-overexpression demonstrated that leukemia could be maintained in the absence of *Meis1*, however these bulk populations showed increased expression of *Meis3* relative to the input population. This raises the possibility that other MEIS/PREP family members can compensate for loss of *Meis1* in some contexts, a possibility that bears investigation as it may limit the effectiveness of *Meis1* knock-down as a potential therapeutic target.

Erosion of regulation of cellular division is considered to be a key step in the generation of leukemia as the overgrowth of abnormal cells stifles normal cell function. Our Affymetrix expression profiling of *Meis1*$^{-/-}$ suggests upregulation of a subset of genes involved in cell cycle, although we could not measure any differences in cell cycle functionally. In a dominant-negative model of *Meis1* function in the context of *Hox*-overexpression, Argiropoulos *et al.*, showed cell cycle arrest in G_1 to S phase, in part due to loss of *cyclin D3* (Argiropoulos *et al.*, 2010). In contrast, studies using a conditional model

of *Meis1* deletion *in vivo*, loss of *Meis1* is associated with loss of quiescence and cell cycle entry (Kocabas *et al.*, 2012; Unnisa *et al.*, 2012). This raises the possibility of opposite functions of *Meis1* in cell cycle regulation depending on the context. Possible explanations for this are not readily apparent as the key effectors of both HSC and LSC potential, that is, *Hox* genes, are expressed at high levels in both contexts. Interestingly, although loss of *Meis1* is detrimental to the survival of both the LSC and the HSC, it does raise the possibility that this differential response to cell cycling could be exploited for therapeutic gain. For example, *Pten* deficiency leads to both the development of LSC and loss of HSC through increased cycling, however, treatment of cells with an inhibitor of the downstream pathway lead to selective preservation of the HSC population at the expense of the LSC (Yilmaz *et al.,* 2006). Identifying such a differentially expressed downstream target in the context of *Meis1*-associated leukemias could lead to the development of therapeutics with improved LSC kill with fewer adverse side-effects, such as neutropenia.

Power to delineate roles for* Meis1 *during mammalian development

One of the first studies using a conditional model for deletion of *Meis1* was performed by Azcoitia *et al*. (Azcoitia *et al.*, 2005) who used in-frame fusion of *Meis1* to the modified estrogen receptor ER^{T2}. Theoretically, in the absence of 4-OHT, the fusion protein would be sequestered in the cytoplasm and thus be inactive as a transcription factor. Using this model, they found similar results to previous work by Hisa *et* al. (Hisa *et al.*, 2004), that is, embryos homozygous for loss of *Meis1* died between day 11.5 and 14.5pc from hemorrhaging due to loss of megakaryocytes and vascular patterning deficits. Both studies also noted a reduction in HSC potential in the fetal liver of these mice, where HSC activity is localized at this developmental stage. For Azcoitia *et al.* administration of 4-OHT *in vivo* to

the pregnant mouse would in principle rescue the phenotype of these mice by permitting nuclear localization of the fusion *MEIS1* protein. The group was, however, unable to demonstrate nuclear localization of the protein nor phenotypic changes in response to 4-OHT, making further experiments into the specific developmental time points where *Meis1* is required for the various cell types unfeasible.

Our model systems provide the opportunity to further examine the time points at which *Meis1* is required for given cell types in further detail. *ERTCre* expression mice can be induced in gravid mice (Danielian *et al.*, 1998), thus administration of 4-OHT at different d.p.c. would allow determination at which d.p.c. is *Meis1* no longer required for proper vascular endothelial cell patterning, for example, which may be different than that required for HSC function. Also of note, the fetal liver between days 10.5 p.c. and birth is where the bulk of functionally complete HSC activity is found, that is, HSC that are able to give rise to the mature lymphoid and erythroid cell types that typify the organism at birth (Reviewed in Orkin and Zon, 2008). More immature HSC potential, however, is found in the aorta/gonad/mesonephros (AGM) region days 8.5 thru 11.5 p.c. and it is thought that these cells migrate to the fetal liver and mature into full HSCs. Previous studies were unable to distinguish if *Meis1* was essential for HSC development or maturation or both as *Meis1* was inactivated from conception. Using *ERTCre/Meis1*$^{fl/fl}$ mice, it would be possible to administer 4-OHT at time points such as day 5, 8.5 and 10.5 p.c. and measure HSC potential in both the AGM and fetal liver at day 12 p.c. to determine the relative influence of loss of *Meis1* on the populations. This information would contribute to the body of work concerning mouse development and gene expression profiles required in given cell types for the appropriate growth of the organism.

Insights gained and key topics for resolution highlighted for the role of *Meis1* in normal hematopoiesis by the model

Alternative models of the hematopoietic hierarchy

Recent studies have proposed alternative routes of differentiation of various hematopoietic cells from the HSC. These modifications suggest not all differentiated cell types arise from successively more committed progenitors, but may in fact, also or alternatively arise directly from extremely primitive progenitors (Adolfsson *et al*. 2005; Arinobu *et* al. 2007; Pronk *et al.,* 2007; Boyer *et al.*, 2012) (Figure 5.1b). Supporting the latter model is the maintenance of CD150 expression in the MkP compartment (Pronk, 2007) and significant overlap in concurrent hematopoietic and megakaryocytic defects in various mouse knock-out models such as c-mpl, SCL and Evi-1 (Murone *et al.*, 1998; Mikkola *et al.*, 2003, Goyama *et al.,* 2008). Another model additionally suggests a minimum of two distinct progenitor subsets with myeloid potential derived from the short-term HSC – one with traditional CMP potential and one with both GMP and CLP (the GMLP or LMPP) potential and the other with MEP and GMP potential (Adolfsson *et al.,* 2005) (Figure 5.1c).

The lack of gross lymphoid, monocytic and granulocytic perturbation in the absence of *Meis1* in our studies, in the face of significant impairments of megakaryocytic/erythroid potential and specific HSC defects may support these proposed changes to the dogma of the hematopoietic hierarchy. Our studies using inducible models of *Meis1* deletion hint at a minimum of 2 possible routes to generation of megakaryocytic and erythroid potential, one through the canonical CMP to GMP/MEP transition and the other directly from a HSC-like progenitor. Both CMP and MEP numbers were diminished in our studies while granulocytic/monocytic potential remained unchanged. This could be due to exclusive GMP

commitment from the CMP in the absence of *Meis1,* which supports both the canonical stepwise differentiation model and the possibility that MEPs can arise directly from the primitive HSC. Loss of *Meis1* in our model could impact several independent progenitor types from which cells with megakaryocytic and erythroid potential could be derived. Induction of Cre expression in sorted progenitor populations and subsequent *in vitro* differentiation and/or *in vivo* transplantation may help to resolve some of these questions.

Experimental evidence calling for revised models of the hierarchy have been criticized for using artificial *in vitro* models to draw conclusions about *in vivo* cellular behavior. Use of the conditional model of *Meis1* deletion in conjunction with lineage tracking mice, such as those that express a fluorescent marker upon promoter expression (Boyer *et al*. 2012) could help elucidate if there are multiple progenitor types from which megakaryocyte/erythroid potential can be derived, in contrast to the canonical model. For example, Boyer *et al*. used *Flk2/Flt3* driven Cre expression to demonstrate that nearly all platelet potential develops through progenitors that do not express *Flk2/Flt3*. This suggests that MkP are derived from a cell type closely related to the HSC and not through a CMP, which expresses *Flk2/Flt3*.

In our model, very few mice died in the absence of *Meis1*, platelet defects in the peripheral blood were transient (no difference 2 weeks after the final Cre induction dose, data not shown) and BFU-E formed in the absence of *Meis1* despite reduced erythroid and megakaryocytic potential. Given the magnitude of deficit for CFU-Mk and BFU-E in our model, one could argue that *in vivo,* pathways that bypass the *Flk2/Flt3*$^{+}$ CMP may be favored and that possibly this mechanism may not require *Meis1* expression. By deleting both *Meis1* and tracking progression through *Flk2/Flt3* progenitor stages, one will be able to

monitor if megakaryocyte and/or erythroid potential that remains in our deleted mice is due to progression through the CMP progenitor.

We additionally were not able to examine if the CFU-Mk were deleted for *Meis1* in our assays due to the fixation method required for enumeration. Thus, although both CFU-Mk and BFU-E potential and the phenotypic MEP were reduced in *Meis1*$^{-/-}$ mice, we could not confirm that CFU-Mk were deficient for *Meis1*. If MkP escaped Cre-mediated deletion, this could raise the possibility that in the adult *Meis1* is required for MkP generation from a HSC progenitor exclusively, while erythroid potential that depends on *Meis1* arises through the CMP and not the HSC. Future studies to examine this could be done whereby MkP are isolated from *Meis1*$^{-/-}$ mice, the percent deletion in the population examined and CFU-Mk per MkP examined. Alternatively, MEPs could be sorted from *Meis1*$^{fl/fl}$ mice, deleted *in vitro* and examined for CFU-E and CFU-Mk potential. This could be compared to CFU-E and CFU-Mk potential from *in vitro* deletion at the HSC stage. Failure to form either lineage in the given populations could provide clarity for cells of origin of these progenitors in the adult mouse. These studies could provide insight into the conflicting evidence from the ES and zebrafish models for the relative contribution of *Meis1* into each of these lineages as well (Cvejic *et al.*, 2010; Cai *et al*., 2012).

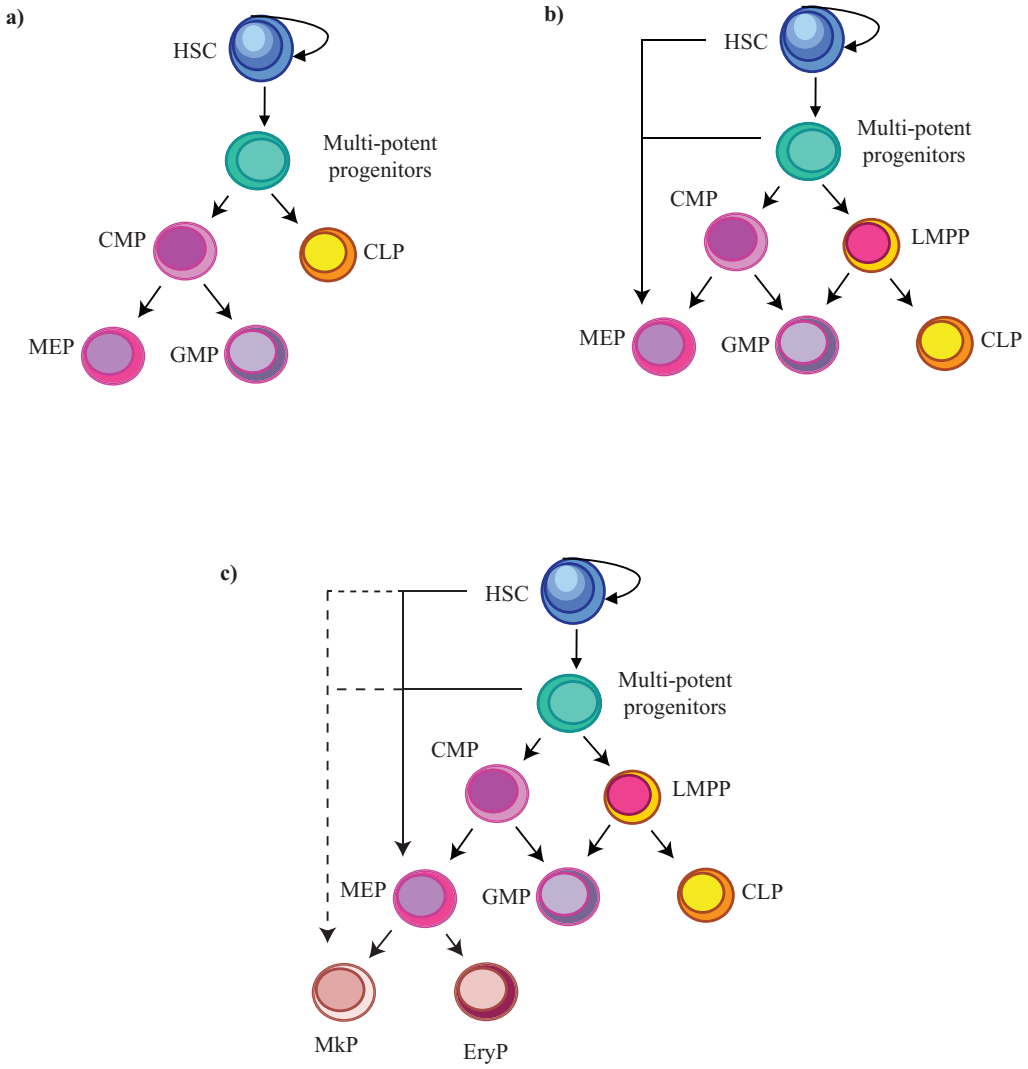

Figure 5.1: Alternative models of the hematopoietic hierarchy.
a) Canonical view of the hematopoietic hierarchy as a step-wise transition through progenitors to unique differentiated cell types. **b)** Update to canonical model postulated by Adolfsson *et al.* 2005, whereby a lymphoid-primed multipotent progenitor (LMPP) exists that retains both granulocytic/monocytic and lymphoid potential. An additional modification suggested by Pronk *et al*., 2007 that allows for derivation of MEP potential without sequential differentiation through the CMP. **c)** Possible revision to the model that could be tested experimentally using a combination of conditional *Meis1* mice and complementary methods, whereby MkP potential could be derived independently from the HSC or other primitive progenitor, bypassing the MEP and CMP stages.

Genetic programs underpinning cell fate decisions at the megakaryocytic-erythroid junction

Although *Meis1* had previously been thought to be important, at minimum during development, in the erythroid and megakaryocyte lineages, few effectors of *Meis1* function are known in these cells. Transcription and epigenetic regulation by *Lsd1/Gfi1/Gfi1b* complexes have been proposed as a mechanism for *Meis1* regulation in erythroid and megakaryocyte progenitors. Histone demethylase LSD1 interacts with repressive transcription factors GFI1 and GFI1B to inhibit expression of *Hoxa9*, *Pbx1* and *Meis1* in hematopoietic lineages (Horman *et al*., 2009; Sprüssel *et al.*, 2012; Chowdhury *et al.*, 2013). A recent model suggests than in combination with LSD1, GF1B regulates *Meis1* expression in the erythroid lineage, while Gfi1 does so at the CMP to GMP/MEP transition (Chowdhury *et al.*, 2013). This model is problematic, however, as it suggests that *Meis1* regulation does not impact the megakaryocyte lineage, in contrast to our experimental evidence. In addition, another study using LSD1 knock-down showed increased *Gfi1b* in both the megakaryocyte and erythroid populations and subsequent expansion of both populations (Sprüssel *et al.*, 2012). The inconsistency with the proposed model and various lines of evidence are likely as a result of the use of fetal liver primary cells and cell lines.

Our results support a role for *Meis1* in both megakaryocytic and erythroid progenitor potential. Of interest, our results do not necessarily refute the results of Chowhudry *et al.,* which suggests *Gfi1b* regulation of *Meis1* is not at play in the megakaryocyte, despite changes in expression of *Gfi1b* and megakaryocyte potential in response to knock-down of *Lsd1*. Regulation of *Meis1* expression in very likely specific to the cell type in question and it is increasingly thought that megakaryocytic potential can be derived from both HSC and MEP populations (discussed below). Although some common regulators may be present, it is

possible that differentiation to the megakaryocytic lineages from these populations employs a unique transcriptional cascade.

Role of* Meis1 *in normal cell cycle

Given the strong implication for *Meis1* in cell cycle regulation in leukemic contexts as well as in recent work using the same knock-out model, it was somewhat surprising we could not identify changes in cell-cycle *in vitro* or *in vivo*, with the exception of enrichment for cell cycle gene sets by Affymetrix. Technical issues could be at the root of this, as well as some key differences in leukemic overexpression studies and conditional models of *Meis1* excision. Leukemia models implicating *Meis1* in cell cycle come from over-expression or shRNA studies to determine dynamic changes in cell cycle. In addition, as discussed in chapter 4, Cre mediated deletion and associated DNA repair is associated with reduced cell proliferation and accumulation in G_2/M in a Cre-dose dependent manner (Loonstra *et al.*, 2001).

Both Unnisa *et al.* and Kocabas *et al*. demonstrated increased numbers of cells in the S-G_2-M compartments in *Meis1*$^{-/-}$ cells compared to controls. Their interpretation was loss of quiescence in the HSC compartments in the absence of Meis1, which is somewhat inconsistent with increased cell cycling found in *Meis1*-overexpressing cells. While context and cell specific regulation of cell cycling may be a play, a far more mundane explanation may account for the differences between our studies. Both groups used a combination of mouse genotypes as controls, including *Cre*$^{+}$*Meis1*$^{+/+}$, which would not be expected to have high levels of DNA damage and repair as there are no LoxP sites for targeted recombination. Thus, significant differences in cell cycle may be due to the relative level of DNA damage and repair between the two groups as a result of Cre excision, versus a genuine effect of loss

of *Meis1* expression. Further *in vivo* replicates comparing $Cre^{+}Meis1^{-/+}$ mice to $Cre^{+}Meis1^{-/-}$ mice would help resolve this, as would *in vitro* experiments with *ERTCre/Meis1* mice. Further work in our lab has validated *in vitro* Cre expression and deletion of *Meis1* in a titration series. Use of varying doses of 4-OHT and hence Cre expression using $ERTCre/Meis1^{fl/fl}$, $ERTCre/Meis1^{fl/+}$ and $ERTCre/Meis1^{+/+}$cells would allow one to investigate changes in cell cycle as a function of both *Meis1* expression and DNA damage as a result of Cre expression.

***Role of ROS and regulation of* Hif1α *regulation by* Meis1**

While strong evidence for regulation of *Hif1a* by *Meis1* has been shown recently with condition models of *Meis1* deletion (Simsek *et al.,* 2010; Kocabas *et al*, 2012; Unnisa *et al*., 2012), we were unable to show changes in *Hif1a* expression by RT-Q-PCR nor by gene set enrichment analysis from the Affymetrix array. This disparity may be, at least in part, due to the actions of NAC beyond providing a substrate for reduction of intracellular ROS species. In our hands, CFC formation was not rescued by NAC administration *in vivo*, whereas Unnisa *et al.* used *in vitro* deletion and found CFC formation capacity was restored by the addition of NAC to cultures. CFC formation from progenitors *in vitro* would not necessarily use a *Hif1α*- dependent pathway to minimize ROS as these assays occur in normoxic conditions. They were also able to show, however, rescue of CFC using sh-RNA against VHL1, which would be expected to increase *Hif1α* levels as VHL is a principle mediator of *Hif1α* degradation. In our experiments NAC is postulated to mimic the downstream effects of *Hif1α* activation, whereas sh-VHL would be expect to increase levels of *Hif1α* itself. Thus, while NAC may function to activate MEK/ERK1/2 both *in vitro* and *in vivo*, sh-VHL *in vitro* may activate *Hif1a* pathways and confer a survival benefit that is not related to levels of

ROS. In an experiment not shown in this thesis, we also attempted to rescue CFC formation in *Meis1*$^{-/-}$ cells by induction of HIF1α stabilization via culture in hypoxic 5% O_2 as opposed to normoxic 20% O_2. This condition would also be expected to positively influence HIF1α activity by preventing degradation by the 26S proteasome (Reviewed in Lindsey & Papoutsakis, 2012). In our hands, CFC formation in *Meis1*$^{-/-}$ was not rescued by culture in 5% O_2 conditions, regardless of the addition of NAC. This may be due to insufficient levels of hypoxia as although while 5% O_2 is considered to be hypoxic in some studies (Roy *et al.*, 2012), others use 2%, (Perry *et al.*, 2007) or 1% O_2 (Couseens *et al.*, 2010).

To clarify the link between actual ROS, *Hif1α* pathways and *Meis1*, it would be of interest to isolate HSC from *Cre*$^{+}$*/Meis1*$^{fl/fl}$ mice and introduce a plasmid expressing sh-VHL linked to fluorescent reporter gene. Following induction of Cre expression, the persistence of donor cells could be measured as a function of sh-VHL expression. Various donor cell fractions could then be isolated and the levels of ROS measured by dyes such as DCF-DA and correlated to CFC capacity. If shVHL and non-physiologic expression of *Hif1α* pathways conferred survival benefit in CFCs independently of ROS, one would expect increased CFC from committed progenitors in the absence of changes in ROS.

It is also difficult to resolve how *Meis1*$^{-/-}$ deficits could be rescued by administration of a compound following permanent deletion of a gene. For instance, Kocabas *et al.* completed their induction schemes before administering NAC *in vivo.* Both our work and that of the other groups support that a loss of *Meis1* results in loss of HSC numbers. If the HSC no longer exists in the organism, upon which cell does NAC work to restore function? Possibilities include reprogramming of a downstream progenitor or perhaps rescue of an incapacitated cell with remaining HSC potential. What is additionally possible is that NAC

provides an advantage to transient repopulating cells without true HSC potential. Both the work by Kocabas *et al.* and our own show phenotypic rescue of HSC numbers by FACS, however we attempted to rescue cells with true HSC potential by administering NAC concurrently with the Cre induction scheme. While both our population and that of Kocabas *et al*. are enriched for HSC potential, cells in the populations are not exclusively HSCs. So while we may have a phenotypic rescue, this does not guarantee true HSC function as defined as long-term (>16 weeks) multi-lineage engraftment. Kocabas *et al*. imply rescue of HSC function on the basis of donor cell engraftment at 4 weeks post transplant with no mention of lineage distribution.

As discussed in the previous chapter, NAC has impacts on both ROS scavenging and cell signaling and cycle cascade members Raf-1, MEK and ERK1/2, independently of its effect on ROS scavenging to promote cell survival (Zhang *et al*., 2011). ERK1/2 signaling has also been shown to be important for lineage commitment, differentiation and expansion of erythroid and megakaryocytic progenitors as well as expansion and survival of myeloid progenitors (reviewed in Geest & Coffer, 2009; Chen *et al.*, 2013). Loss of ERK1/2 in the adult mouse results in bone marrow aplasia, anemia, leukopenia, early lethality and loss of the LSK HSC-enriched compartment by FACS (Chan *et al.*, 2013). Other groups have postulated that loss of *Meis1* results in loss of *Hif1α* expression and thus an increase in aerobic metabolism and ROS production (Kocabas *et al.*, 2012; Unnisa *et al.*, 2012). It has been suggested then that ROS scavenging by NAC accounts for the phenotypic and functional rescue of some *Meis1*$^{-/-}$ deficits in their model system (Figure 5.2). As there is considerable overlap between Meis1 and ERK1/2 activity in the hematopoietic stem cell, megakaryopoiesis and erythropoiesis, it is also possible that the phenotypic rescue seen with

NAC in our model is a result of direct activation of ERK1/2 as opposed to elimination of ROS species. Further evaluation of the ERK1/2 knock-out mouse for the nature of the HSC deficit would be valuable, as would be experiments that examined functional and phenotypic rescue of the HSC, megakaryocyte and erythrocyte compartments using ROS scavenging compounds that do not modulate ERK1/2 activity, such as sodium pyruvate (Franco, Panayiotidis & Cidlowski, 2007).

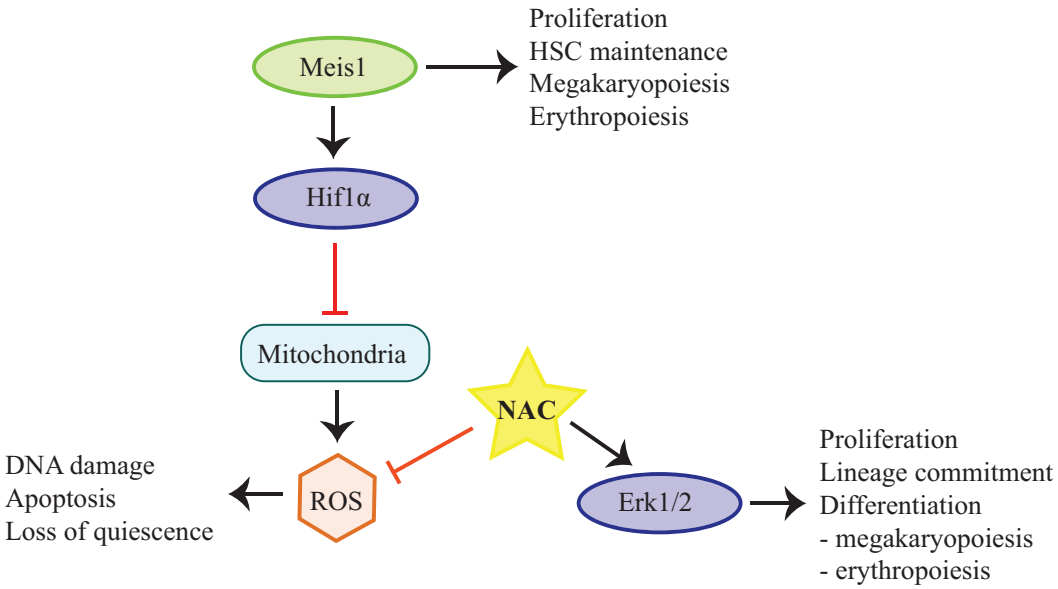

Figure 5.2: Model of NAC activity in the hematopoietic compartment.

Meis1 has been implicated in the regulation of *Hif1α* expression, whose transcription program modulates aerobic vs. anaerobic metabolism. Inhibition of aerobic mitochondrial metabolism by Hif1α programs is thought to result in a reduction in ROS generation. Loss of *Meis1*, hence *Hif1α* has been proposed to favor aerobic metabolism and ROS generation that results in a loss of HSC quiescence and self-renewal. NAC is theorized to eliminate these ROS and thus prevent loss of HSC quiescence and function as a result of *Meis1* deletion. As NAC also stimulates Erk1/2 activity, loss of which has similar phenotypes in the HSC, megakaryocyte and erythrocyte as loss of Meis1, it is also possible that phenotypic/functional rescue by NAC in *Meis1*$^{-/-}$ cells is a result of compensatory Erk1/2 activity, versus a loss of ROS.

Confidence in true HSC rescue by NAC, be it via *Hif*/ROS or other pathways, would be best served by experiments that monitor long-term lineage engraftment and

transplantation as well as confirm *Meis1* deletion in the repopulating cell compartment. One such experiment would be to perform a similar experiment to the one we performed to examine cell intrinsic/extrinsic roles for *Meis1*. $Cre^{+}/Meis1^{fl/fl}$ or $Cre^{+}/Meis1^{fl/+}$ cells could be transplanted into recipients and Cre-expression induced concurrently with NAC/PBS control administration. Maintenance of multi-lineage engraftment as well as *Meis1*-deletion could be monitored over 16 weeks and/or secondary transplants could be performed to measure HSC maintenance and self-renewal. This type of experiment would irrefutably support NAC rescue of HSC numbers in the absence of *Meis1*.

HIF1α has been shown to positively influence TERT expression (Nishi *et al.,* 2004; Coussens *et al*., 2010), a key protein component of the telomerase complex, that has activity in both that complex and independently (reviewed Li *et al.* 2011). In the context of the hematopoietic stem cell and embryonic stem cells, TERT as a component of the telomerase complex is proposed to maintain chromosomal stability and prevent premature senescence to allow for life-long division via maintenance of chromosomal telomere ends. It would be of interest to explore levels of *Tert* mRNA as well as telomerase activity in $Meis1^{-/-}$ hematopoietic stem cells.

HIF pathways additionally regulate EPO synthesis in the spleen and osteoblastic niche to increase RBC number in response to hypoxia (Rankin *et al.*, 2012; reviewed in Lee & Percy, 2011). In addition to a diminished RBC number in the peripheral blood of $ERTCre/Meis1^{-/-}$ mice, hematopoathologist review of H&E staining of the spleen in our moribund mice revealed abnormal iron deposition that was somewhat counterintuitive, given the drop in erythroid progenitors by Ter119-staining (Figure 4.2, panel a). Loss of erythroid progenitors could thus be due to a reduction in *Hif1α* –regulated *Epo* expression, as opposed

to a hematopoietic cell intrinsic effect. This may implicate *Meis1* in the regulation of gene expression in previously unappreciated cell types, that is the osteoblast and splenocyte. We did not examine BFU-E numbers in our cell-extrinsic long-term transplantation experiments. In order to tease the various influences of *Meis1* on erythropoiesis, both hematopoietic cell intrinsic and possible extrinsic components, one could measure serum, spleen and marrow EPO levels by Enzyme-Linked-Immunosobent Assays following deletion of *Meis1* in *MxCre/Meis1*$^{fl/fl}$ or *ERTCre/Meis1*$^{fl/fl}$ mice transplanted with wild-type bone marrow and examining BFU-E output in the transplanted wild-type cells.

In addition, congenital mutations in VHL, a negative regulator of HIF1α, leads to erythrocytosis, that is, an increase in red cell mass that may be due to increased numbers of red blood cells or iron-containing hemoglobin (Hb) molecules. Given the accumulation of studies providing support for a network of VHL/HIF/MEIS interaction and the clinical phenotypes associated with mutations in VHL in erythrocytosis, conditional *Meis1* deletion mice may provide novel models for the study of this disease.

Conclusion

Our studies have provided strong evidence that *Meis1* is a requirement for adult hematopoiesis in terms of maintenance of stem cell numbers and self-renewal as well as in erythropoiesis and megakaryopoiesis. Perhaps most intriguing, however, is how the compilation and comparison of our results with that of others may suggest that further study using the conditional *Meis1* knock-out mouse would be of value in elucidating alternative mechanisms of the hematopoietic hierarchy from the canonical model of stepwise differentiation. Use of this *Meis1* conditional model will allow interrogation of the possibility

of multiple modes of derivation of megakaryocytic potential and if these are obligatorily linked to erythroid potential. In addition, differential response of the HSC and committed progenitor population to the effects of NAC will allow further study into if ROS regulation is at the root of this effect or more so a concomitant change with activation of MEK/ERK1/2 pathways. That cell cycling is apparently increased with loss of expression of *Meis1* in normal hematopoietic populations as well as with overexpression in leukemic populations raises the possibility that *Meis1* pathways could be differentially targeted for therapeutic benefit in the future. Overall, the work presented in this thesis demonstrates a robust model with which the function of *Meis1* in an array of processes can be delineated including development, normal homeostasis, lineage commitment and leukemic processes. Future work using the model outlined in this thesis in conjunction with complementary methods will ultimately be fruitful in delineating these processes.

References

Abu-Shaar, M., Ryoo, H. D., & Mann, R. S. (1999). Control of the nuclear localization of Extradenticle by competing nuclear import and export signals. *Genes & Development*, *13*, 935–945.

Adolfsson, J., Månsson, R., Buza-Vidas, N., Hultquist, A., Liuba, K., Jensen, C. T., et al. (2005). Identification of Flt3+ Lympho-Myeloid Stem Cells Lacking Erythro-Megakaryocytic Potential. *Cell*, *121*(2), 295–306. doi:10.1016/j.cell.2005.02.013

Afonja, O., Smith, J. E. J., Cheng, D. M., Goldenberg, A. S., Amorosi, E., Shimamoto, T., et al. (2000). MEIS1 and HOXA7 genes in human acute myeloid leukemia. *Leukemia Research*, *24*, 849–855.

Akala, O. O., & Clarke, M. F. (2006). Hematopoietic stem cell self-renewal. *Current Opinion in Genetics & Development*, *16*(5), 496–501. doi:10.1016/j.gde.2006.08.011

Akashi, K., Traver, D., Miyamoto, T., & Weissman, I. L. (2000). A clonogenic common myeloid progenitor that gives rise to all myeloid lineages. *Nature*, *404*, 193–197.

Alcalay, M., Alcalay, M., Tiacci, E., Bergomas, R., Bigerna, B., Venturini, E., et al. (2005). Acute myeloid leukemia bearing cytoplasmic nucleophosmin (NPMc+ AML) shows a distinct gene expression profile characterized by up-regulation of genes involved in stem-cell maintenance. *Blood*, *106*(3), 899–902. doi:10.1182/blood-2005-02-0560

Antonchuck, J., Sauvageau, G., & Humphries, R. K. (2002). *HOXB4*-INDUCED EXPANSION OF ADULT HEMATOPOIETIC STEM CELLS EX VIVO. *Cell*, *109*, 39–45.

Argiropoulos, B., & Humphries, R. K. (2007). Hox genes in hematopoiesis and leukemogenesis. *Oncogene*, *26*(47), 6766–6776. doi:10.1038/sj.onc.1210760

Argiropoulos, B., Palmqvist, L., Imren, S., Miller, M., Rouhi, A., Mager, D. L., & Humphries, R. K. (2010a). Meis1 disrupts the genomic imprint of Dlk1 in a NUP98-HOXD13 leukemia model. *Leukemia*, *24*(10), 1788–1791. doi:10.1038/leu.2010.161

Argiropoulos, B., Palmqvist, L., Yung, E., Kuchenbauer, F., Heuser, M., Sly, L. M., et al. (2008). Linkage of Meis1 leukemogenic activity to multiple downstream effectors including Trib2 and Ccl3. *Experimental Hematology*, *36*(7), 845–859. doi:10.1016/j.exphem.2008.02.011

Argiropoulos, B., Yung, E., Xiang, P., Lo, C. Y., Kuchenbauer, F., Palmqvist, L., et al. (2010b). Linkage of the potent leukemogenic activity of Meis1 to cell cycle entry and

transcriptional regulation of cyclin D3. *Blood*. doi:10.1182/blood-2009-06-225573

Arinobu, Y., Mizuno, S.-I., Chong, Y., Shigematsu, H., Iino, T., Iwasaki, H., et al. (2007). Reciprocal Activation of GATA-1 and PU.1 Marks Initial Specification of Hematopoietic Stem Cells into Myeloerythroid and Myelolymphoid Lineages. *Cell Stem Cell*, *1*(4), 416–427. doi:10.1016/j.stem.2007.07.004

Ayton, P. M., & Cleary, M. L. (2003). Transformation of myeloid progenitors by MLL oncoproteins is dependent on Hoxa7 and Hoxa9. *Genes & Development*, *17*(18), 2298–2307. doi:10.1101/gad.1111603

Azcoitia, V., Aracil, M., Martínez-A, C., & Torres, M. (2005). The homeodomain protein Meis1 is essential for definitive hematopoiesis and vascular patterning in the mouse embryo. *Developmental Biology*, *280*(2), 307–320. doi:10.1016/j.ydbio.2005.01.004

Badea, T. C., Wang, Y., & Nathans, J. (2003). A noninvasive genetic/pharmacologic strategy for visualizing cell morphology and clonal relationships in the mouse. *The Journal of Neuroscience : the Official Journal of the Society for Neuroscience*, *23*(6), 2314–2322.

Becker, M. W., & Jordan, C. T. (2011). Leukemia stem cells in 2010: Current understanding and future directions. *Yblre*, *25*(2), 75–81. doi:10.1016/j.blre.2010.11.001

Benjamini, Y., & Hochberg, Y. J. (1995). *Controlling the false discovery rate: a practical and powerful approach to multiple testing* (Vol. 57, pp. 289–300). R. Stat. Soc.

Berthelsen, J., Kilstrup-Nielsen, C., Blasi, F., Mavilio, F., & Zappavigna, V. (1999). The subcellular localization of PBX1 and EXD proteins depends on nuclear import and export signals and is modulated by association with PREP1 and HTH. *Genes & Development*, *13*(8), 946–953.

Bessa, J., Tavares, M. J., Santos, J., Kikuta, H., Laplante, M., Becker, T. S., et al. (2008). meis1 regulates cyclin D1 and c-myc expression, and controls the proliferation of the multipotent cells in the early developing zebrafish eye. *Development*, *135*(5), 799–803. doi:10.1242/dev.011932

Bisaillon, R., Wilhelm, B. T., Krosl, J., & Sauvageau, G. (2011). C-terminal domain of MEIS1 converts PKNOX1 (PREP1) into a HOXA9-collaborating oncoprotein. *Blood*, *118*(17), 4682–4689. doi:10.1182/blood-2011-05-354076

Björnsson, J. M., Larsson, N., Brun, A. C. M., Magnusson, M., Andersson, E., Lundström, P., et al. (2003). Reduced proliferative capacity of hematopoietic stem cells deficient in Hoxb3 and Hoxb4. *Mol Cell Biol*, *23*(11), 3872–3883.

Bockamp, E. O., McLaughlin, F., Murrell, A. M., Gottgens, B., Robb, L., Begley, C. G., & Green, A. R. (1995). Lineage-restricted regulation of the murine SCL/TAL-1 promoter.

Blood, *86*(4), 1502–1514.

Bonnet, D., & Dick, J. E. (1997). Human acute myeloid leukemia is organized as a hierarchy that originates from a primitive hematopoietic cell. *Nature Medicine*, *3*(7), 730–737.

Bowie, M. B., Kent, D. G., Dykstra, B., McKnight, K. D., McCaffrey, L., Hoodless, P. A., & Eaves, C. J. (2007). Identification of a new intrinsically timed developmental checkpoint that reprograms key hematopoietic stem cell properties. *Proceedings of the National Academy of Sciences of the United States of America*, *104*(14), 5878–5882. doi:10.1073/pnas.0700460104

Boyer, S. W., Beaudin, A. E., & Forsberg, E. C. (2012). Mapping differentiation pathways from hematopoietic stem cells using Flk2/Flt3 lineage tracing. *Cell Cycle (Georgetown, Tex.)*, *11*(17), 3180–3188. doi:10.4161/cc.21279

Brun, A. C. M., Björnsson, J. M., Magnusson, M., Larsson, N., Leveén, P., Ehinger, M., et al. (2004). Hoxb4-deficient mice undergo normal hematopoietic development but exhibit a mild proliferation defect in hematopoietic stem cells. *Blood*, *103*(11), 4126–4133. doi:10.1182/blood-2003-10-3557

Buzzeo, M. P., Scott, E. W., & Cogle, C. R. (2007). The hunt for cancer-initiating cells: a history stemming from leukemia. *Leukemia*, *21*(8), 1619–1627. doi:10.1038/sj.leu.2404768

Byers, R. J., Currie, T., Tholouli, E., Rodig, S. J., & Kutok, J. L. (2011). MSI2 protein expression predicts unfavorable outcome in acute myeloid leukemia. *Blood*, *118*(10), 2857–2867. doi:10.1182/blood-2011-04-346767

Cai, M., Langer, E. M., Gill, J. G., Satpathy, A. T., Albring, J. C., Kc, W., et al. (2012). Dual actions of Meis1 inhibit erythroid progenitor development and sustain general hematopoietic cell proliferation. *Blood*. doi:10.1182/blood-2012-01-403139

Calero-Nieto, F. J., Joshi, A., Bonadies, N., Kinston, S., Chan, W.-I., Gudgin, E., et al. (2013). HOX-mediated LMO2 expression in embryonic mesoderm is recapitulated in acute leukaemias. *Oncogene*. doi:10.1038/onc.2013.175

Calvo, K. R., Sykes, D. B., Pasillas, M. P., & Kamps, M. P. (2000). Hoxa9 Immortalizes a Granulocyte-Macrophage Colony-Stimulating Factor-Dependent Promyelocyte Capable of Biphenotypic Differentiation to Neutrophils or Macrophages, Independent of Enforced Meis Expression. *Molecular and Cellular Biology*, *20*, 3274–3285.

Camós, M., Esteve, J., Jares, P., Colomer, D., Rozman, M., Villamor, N., et al. (2006). Gene expression profiling of acute myeloid leukemia with translocation t(8;16)(p11;p13) and MYST3-CREBBP rearrangement reveals a distinctive signature with a specific pattern of HOX gene expression. *Cancer Research*, *66*(14), 6947–6954. doi:10.1158/0008-

5472.CAN-05-4601

Capron, C., Lacout, C., Lécluse, Y., Wagner-Ballon, O., Kaushik, A.-L., Cramer-Bordé, E., et al. (2011). LYL-1 deficiency induces a stress erythropoiesis. *Experimental Hematology*, *39*(6), 629–642. doi:10.1016/j.exphem.2011.02.014

Chan, G., Gu, S., & Neel, B. G. (2013). Erk1 and Erk2 are required for maintenance of hematopoietic stem cells and adult hematopoiesis. *Blood*, *121*(18), 3594–3598. doi:10.1182/blood-2012-12-476200

Chang, C. P., Brocchieri, L., Shen, W. F., Largman, C., & Cleary, M. L. (1996). Pbx modulation of Hox homeodomain amino-terminal arms establishes different DNA-binding specificities across the Hox locus. *Mol Cell Biol*, *16*(4), 1734–1745.

Chang, C. P., Shen, W. F., Rozenfeld, S., Lawrence, H. J., Largman, C., & Cleary, M. L. (1995). Pbx proteins display hexapeptide-dependent cooperative DNA binding with a subset of Hox proteins. *Genes & Development*, *9*(6), 663–674.

Chang, H., Nayar, R., Li, D., & Sutherland, D. (2005). Clonality analysis of cell lineages in acute myeloid leukemia with inversion 16. *Cancer Genetics and Cytogenetics*, *156*(2), 175–178. doi:10.1016/j.cancergencyto.2004.03.017

Chang, M. J., Wu, H., Achille, N. J., Reisenauer, M. R., Chou, C. W., Zeleznik-Le, N. J., et al. (2010). Histone H3 Lysine 79 Methyltransferase Dot1 Is Required for Immortalization by MLL Oncogenes. *Cancer Research*, *70*(24), 10234–10242. doi:10.1158/0008-5472.CAN-10-3294

Chen, S., Su, Y., & Wang, J. (2013). ROS-mediated platelet generation: a microenvironment-dependent manner for megakaryocyte proliferation, differentiation, and maturation. *Cell Death & Disease*, *4*, e722. doi:10.1038/cddis.2013.253

Chen, W., Kumar, A. R., Hudson, W. A., Li, Q., Wu, B., Staggs, R. A., et al. (2008). Malignant transformation initiated by *Mll-AF9*: Gene dosage and critical target cells. *Cancer Cell*, *13*, 432–440.

Choe, S.-K., Lu, P., Nakamura, M., Lee, J., & SagerstrOm, C. G. (2009). Meis Cofactors Control HDAC and CBP Accessibility at Hox-Regulated Promoters during Zebrafish Embryogenesis. *Developmental Cell*, *17*(4), 561–567. doi:10.1016/j.devcel.2009.08.007

Chowdhury, A. H., Ramroop, J. R., Upadhyay, G., Sengupta, A., Andrzejczyk, A., & Saleque, S. (2013). Differential Transcriptional Regulation of meis1 by Gfi1b and Its Co-Factors LSD1 and CoREST. *PLoS ONE*, *8*(1), e53666. doi:10.1371/journal.pone.0053666

Christensen, J. L., & Weissman, I. L. (2001). Flk-2 is a marker in hematopoietic stem cell differentiation: a simple method to isolate long-term stem cells. *Proceedings of the*

National Academy of Sciences of the United States of America, *98*(25), 14541–14546. doi:10.1073/pnas.261562798

Collins, L. S., & Dorshkind, K. (1987). A stromal cell line from myeloid long-term bone marrow cultures can support myelopoiesis and B lymphopoiesis. *Journal of Immunology (Baltimore, Md. : 1950)*, *138*(4), 1082–1087.

Coussens, M., Davy, P., Brown, L., Foster, C., Andrews, W. H., Nagata, M., & Allsopp, R. (2010). RNAi screen for telomerase reverse transcriptase transcriptional regulators identifies HIF1alpha as critical for telomerase function in murine embryonic stem cells. *Proceedings of the National Academy of Sciences*, *107*(31), 13842–13847. doi:10.1073/pnas.0913834107

Craig, N. L. (1988). The mechanism of conservative site-specific recombination. *Annu. Rev. Genet.*, *22*, 77–105.

Crans-Vargas, H. N., Landaw, E. M., Bhatia, S., Sandusky, G., Moore, T. B., & Sakamoto, K. M. (2002). Expression of cyclic adenosine monophosphate response-element binding protein in acute leukemia. *Blood*, *99*(7), 2617–2619.

Crijns, A. P. G., de Graeff, P., Geerts, D., Hoor, Ten, K. A., Hollema, H., van der Sluis, T., et al. (2007). MEIS and PBX homeobox proteins in ovarian cancer. *European Journal of Cancer (Oxford, England : 1990)*, *43*(17), 2495–2505. doi:10.1016/j.ejca.2007.08.025

Cvejic, A., Serbanovic-Canic, J., Stemple, D. L., & Ouwehand, W. H. (2011). The role of meis1 in primitive and definitive hematopoiesis during zebrafish development. *Haematologica*, *96*(2), 190–198. doi:10.3324/haematol.2010.027698

Danielian, P. S., Muccino, D., Rowitch, D. H., Michael, S. K., & McMahon, A. P. (1998). Modification of gene activity in mouse embryos in utero by a tamoxifen-inducible form of Cre recombinase. *Current Biology*, *24*, 1323–1326.

de Andrés-Aguayo, L., Varas, F., & Graf, T. (2012). Musashi 2 in hematopoiesis. *Current Opinion in Hematology*, *19*(4), 268–272. doi:10.1097/MOH.0b013e328353c778

de Boer, J., Yeung, J., Ellu, J., Ramanujachar, R., Bornhauser, B., Solarska, O., et al. (2011). The E2A-HLF oncogenic fusion protein acts through Lmo2 and Bcl-2 to immortalize hematopoietic progenitors. *Leukemia*, *25*(2), 321–330. doi:10.1038/leu.2010.253

Dick, J. E. (2008). Stem cell concepts renew cancer research. *Blood*, *112*(13), 4793–4807. doi:10.1182/blood-2008-08-077941

DiMartino, J. F., Selleri, L., Traver, D., Firpo, M. T., Rhee, J., Warnke, R., et al. (2001). The Hox cofactor and proto-oncogene Pbx1 is required for maintenance of definitive hematopoiesis in the fetal liver. *Blood*, *98*, 618–626.

Drabkin, H. A., Parsy, C., Ferguson, K., Guilhot, F., La. (2002). Quantitative HOX expression in chromosomally defined subsets of acute myelogenous leukemia. *Leukemia*, *16*, 186–195. doi:10.1038/sj/leu/2402354

Elefanty, A. G., Begley, C. G., Hartley, L., Papaevangeliou, B., & Robb, L. (1999). SCL expression in the mouse embryo detected with a targeted lacZ reporter gene demonstrates its localization to hematopoietic, vascular, and neural tissues. *Blood*, *94*(11), 3754–3763.

Esparza, S. D., Chang, J., Shankar, D. B., Zhang, B., Nelson, S. F., & Sakamoto, K. M. (2008). CREB regulates Meis1 expression in normal and malignant hematopoietic cells. *Leukemia*, *22*(3), 665–667. doi:10.1038/sj.leu.2404933

Ferrando, A. A., Armstrong, S. A., Neuberg, D. S., Sallan, S. E., Silverman, L. B., Korsmeyer, S. J., & Look, A. T. (2003). Gene expression signatures in MLL-rearranged T-lineage and B-precursor acute leukemias: dominance of HOX dysregulation. *Blood*, *102*(1), 262–268. doi:10.1182/blood-2002-10-3221

Ferretti, E., Villaescusa, J. C., Di Rosa, P., Fernandez-Diaz, L. C., Longobardi, E., Mazzieri, R., et al. (2006). Hypomorphic mutation of the TALE gene Prep1 (pKnox1) causes a major reduction of Pbx and Meis proteins and a pleiotropic embryonic phenotype. *Mol Cell Biol*, *26*(15), 5650–5662. doi:10.1128/MCB.00313-06

Fischbach, N. A. (2005). HOXB6 overexpression in murine bone marrow immortalizes a myelomonocytic precursor in vitro and causes hematopoietic stem cell expansion and acute myeloid leukemia in vivo. *Blood*, *105*(4), 1456–1466. doi:10.1182/blood-2004-04-1583

Franco, R., Panayiotidis, M. I., & Cidlowski, J. A. (2007). Glutathione depletion is necessary for apoptosis in lymphoid cells independent of reactive oxygen species formation. *The Journal of Biological Chemistry*, *282*(42), 30452–30465. doi:10.1074/jbc.M703091200

Frisch, B. J., Porter, R. L., Gigliotti, B. J., Olm-Shipman, A. J., Weber, J. M., O'Keefe, R. J., et al. (2009). In vivo prostaglandin E2 treatment alters the bone marrow microenvironment and preferentially expands short-term hematopoietic stem cells. *Blood*, *114*(19), 4054–4063. doi:10.1182/blood-2009-03-205823

Fulwyler, M. J. (1980). Flow cytometry and cell sorting. *Blood Cells*, *6*(2), 173–184.
Gan, B., Sahina, E., Jiang, S., Sanchez-Aguilerac, A., Scott, K. L., Chin, L., et al. (2008). mTORC1-dependent and -independent regulation of stem cell renewal, differentiation, and mobilization. *Pnas*, *105*, 19384–19389.

Garcez, R. C., Teixeira, B. L., Schmitt, S. D. S., Alvarez-Silva, M., & Trentin, A. G. (2009). Epidermal growth factor (EGF) promotes the in vitro differentiation of neural crest cells to neurons and melanocytes. *Cellular and Molecular Neurobiology*, *29*(8), 1087–1091.

doi:10.1007/s10571-009-9406-2

Geest, C. R., & Coffer, P. J. (2009). MAPK signaling pathways in the regulation of hematopoiesis. *Journal of Leukocyte Biology*, *86*(2), 237–250. doi:10.1189/jlb.0209097

Gibbs, K. D., Jager, A., Crespo, O., Goltsev, Y., Trejo, A., Richard, C. E., & Nolan, G. P. (2012). Decoupling of tumor-initiating activity from stable immunophenotype in HoxA9-Meis1-driven AML. *Cell Stem Cell*, *10*(2), 210–217. doi:10.1016/j.stem.2012.01.004

Gilliland, D. G., Jordan, C. T., & Felix, C. A. (2004). The Molecular Basis of Leukemia. *American Society of Hematology*, 1–18.

Goyama, S., Yamamoto, G., Shimabe, M., Sato, T., Ichikawa, M., Ogawa, S., et al. (2008). Evi-1 Is a Critical Regulator for Hematopoietic Stem Cells and Transformed Leukemic Cells. *Cell Stem Cell*, *3*(2), 207–220. doi:10.1016/j.stem.2008.06.002

Grier, D., Thompson, A., Kwasniewska, A., McGonigle, G., Halliday, H., & Lappin, T. (2005). The pathophysiology of HOX genes and their role in cancer. *The Journal of Pathology*, *205*(2), 154–171. doi:10.1002/path.1710

Grubach, L., Juhl-Christensen, C., Rethmeier, A., Olesen, L. H., Aggerholm, A., Hokland, P., & Østergaard, M. (2008). Gene expression profiling of Polycomb, Hox and Meis genes in patients with acute myeloid leukaemia. *European Journal of Haematology*, *81*(2), 112–122. doi:10.1111/j.1600-0609.2008.01083.x

Gurumurthy, S., Xie, S. Z., Alagesan, B., Kim, J., Yusuf, R. Z., Saez, B., et al. (2010). The Lkb1 metabolic sensor maintains haematopoietic stem cell survival. *Nature*, *468*(7324), 659–663. doi:10.1038/nature09572

Halder, S. K., Cho, Y.-J., Datta, A., Anumanthan, G., Ham, A.-J. L., Carbone, D. P., & Datta, P. K. (2011). Elucidating the mechanism of regulation of transforming growth factor β Type II receptor expression in human lung cancer cell lines. *Neoplasia (New York, N.Y.)*, *13*(10), 912–922.

Hara, T., Schwieger, M., Kazama, R., Okamoto, S., Minehata, K., Ziegler, M., et al. (2008). Acceleration of chronic myeloproliferation by enforced expression of Meis1 or Meis3 in Icsbp-deficient bone marrow cells. *Oncogene*, *27*(27), 3865–3869. doi:10.1038/sj.onc.1211043

Hayashi, S., & McMahon, A. P. (2002). Efficient recombination in diverse tissues by a tamoxifen-inducible form of Cre: a tool for temporally regulated gene activation/inactivation in the mouse. *Developmental Biology*, *244*(2), 305–318. doi:10.1006/dbio.2002.0597

Haylock, D. N., & Nilsson, S. K. (2006). Osteopontin: a bridge between bone and blood. *British Journal of Haematology*, *134*(5), 467–474. doi:10.1111/j.1365-2141.2006.06218.x

Heazlewood, S. Y., Neaves, R. J., Williams, B., Haylock, D. N., Adams, T. E., & Nilsson, S. K. (2013). Megakaryocytes co-localise with hemopoietic stem cells and release cytokines that up-regulate stem cell proliferation. *Stem Cell Research*, *11*(2), 782–792. doi:10.1016/j.scr.2013.05.007

Heine, P., Dohle, E., Bumsted-O'Brien, K., Engelkamp, D., & Schulte, D. (2008). Evidence for an evolutionary conserved role of homothorax/Meis1/2 during vertebrate retina development. *Development*, *135*(5), 805–811. doi:10.1242/dev.012088

Herault, O., Hope, K. J., Deneault, E., Mayotte, N., Chagraoui, J., Wilhelm, B. T., et al. (2012). A role for GPx3 in activity of normal and leukemia stem cells. *Journal of Experimental Medicine*, *209*(5), 895–901. doi:10.1084/jem.20102386

Heuser, M., Argiropoulos, B., Kuchenbauer, F., Yung, E., Piper, J., Fung, S., et al. (2007). MN1 overexpression induces acute myeloid leukemia in mice and predicts ATRA resistance in patients with AML. *Blood*, *110*(5), 1639–1647. doi:10.1182/blood-2007-03-080523

Heuser, M., Yun, H., Berg, T., Yung, E., Argiropoulos, B., Kuchenbauer, F., et al. (2011). Cell of origin in AML: susceptibility to MN1-induced transformation is regulated by the MEIS1/AbdB-like HOX protein complex. *Cancer Cell*, *20*(1), 39–52. doi:10.1016/j.ccr.2011.06.020

Hirose, K., Abramovich, C., Argiropoulos, B., & Humphries, R. K. (2008). Leukemogenic properties of NUP98-PMX1 are linked to NUP98 and homeodomain sequence functions but not to binding properties of PMX1 to serum response factor. *Oncogene*, *27*(46), 6056–6067. doi:10.1038/onc.2008.210

Hisa, T., Spence, S. E., Rachel, R. A., Fujita, M., Nakamura, T., Ward, J. M., et al. (2004). Hematopoietic, angiogenic and eye defects in Meis1 mutant animals. *The EMBO Journal*, *23*(2), 450–459.

Hock, H., Meade, E., Medeiros, S., Schindler, J. W., Valk, P. J. M., Fujiwara, Y., & Orkin, S. H. (2004). Tel/Etv6 is an essential and selective regulator of adult hematopoietic stem cell survival. *Genes & Development*, *18*(19), 2336–2341. doi:10.1101/gad.1239604

Hope, K. J., & Sauvageau, G. (2011). Roles for MSI2 and PROX1 in hematopoietic stem cell activity. *Current Opinion in Hematology*, *18*(4), 203–207. doi:10.1097/MOH.0b013e328347888a

Hope, K. J., Cellot, S., Ting, S. B., MacRae, T., Mayotte, N., Iscove, N. N., & Sauvageau, G. (2010). An RNAi Screen Identifies Msi2 and Prox1 as Having Opposite Roles in the

Regulation of Hematopoietic Stem Cell Activity. *Stem Cell*, *7*(1), 101–113. doi:10.1016/j.stem.2010.06.007

Hope, K. J., Jin, L., & Dick, J. E. (2003). Human acute myeloid leukemia stem cells. *Archives of Medical Research*, *34*(6), 507–514. doi:10.1016/j.arcmed.2003.08.007
Horman, S. R., Velu, C. S., Chaubey, A., Bourdeau, T., Zhu, J., Paul, W. E., et al. (2009). Gfi1 integrates progenitor versus granulocytic transcriptional programming. *Blood*, *113*(22), 5466–5475. doi:10.1182/blood-2008-09-179747

Hu, Y. L., Fong, S., Ferrell, C., Largman, C., & Shen, W. F. (2009). HOXA9 Modulates Its Oncogenic Partner Meis1 To Influence Normal Hematopoiesis. *Molecular and Cellular Biology*, *29*(18), 5181–5192. doi:10.1128/MCB.00545-09

Huang, H., Rastegar, M., Bodner, C., Goh, S. L., Rambaldi, I., & Featherstone, M. (2005). MEIS C Termini Harbor Transcriptional Activation Domains That Respond to Cell Signaling. *Journal of Biological Chemistry*, *280*(11), 10119–10127. doi:10.1074/jbc.M413963200

Huang, Y., Sitwala, K., Bronstein, J., Sanders, D., Dandekar, M., Collins, C., et al. (2012). Identification and characterization of Hoxa9 binding sites in hematopoietic cells. *Blood*, *119*(2), 388–398. doi:10.1182/blood-2011-03-341081

Huntly, B. J. P., & Gilliland, D. G. (2005). Leukaemia stem cells and the evolution of cancer-stem-cell research. *Nature Reviews Cancer*, *5*, 311–321.

Huntly, B. J. P., Shigematsu, H., Deguchi, K., Lee, B. H., Mizuno, S., Duclos, N., et al. (2004). MOZ-TIF2, but not BCR-ABL, confers properties of leukemic stem cells to committed murine hematopoietic progenitors. *Cancer Cell*, *6*(6), 587–596. doi:10.1016/j.ccr.2004.10.015

Ichikawa, M., Asai, T., Saito, T., Seo, S., Yamazaki, I., Yamagata, T., et al. (2004). AML-1 is required for megakaryocytic maturation and lymphocytic differentiation, but not for maintenance of hematopoietic stem cells in adult hematopoiesis. *Nature Medicine*, *10*(3), 299–304. doi:10.1038/nm997

Imamura, T., Morimoto, A., Ikushima, S., Kakazu, N., Hada, S., Tabata, Y., et al. (2002a). A novel infant acute lymphoblastic leukemia cell line with MLL-AF5q31 fusion transcript. *Leukemia*, *16*(11), 2302–2308. doi:10.1038/sj.leu.2402665

Imamura, T., Morimoto, A., Takanashi, M., Hibi, S., Sugimoto, T., Ishii, E., & Imashuku, S. (2002b). Frequent co-expression of HoxA9 and Meis1 genes in infant acute lymphoblastic leukaemia with MLL rearrangement. *British Journal of Haematology*, *119*(1), 119–121.

Ito, K., Hirao, A., Arai, F., Takubo, K., Matsuoka, S., Miyamoto, K., et al. (2006). Reactive oxygen species act through p38 MAPK to limit the lifespan of hematopoietic stem cells.

Nature Medicine, *12*(4), 446–451. doi:10.1038/nm1388

Iwasaki, M. (2005). Identification of cooperative genes for NUP98-HOXA9 in myeloid leukemogenesis using a mouse model. *Blood*, *105*(2), 784–793. doi:10.1182/blood-2004-04-1508

Jaw, T. J., You, L. R., Knoepfler, P. S., Yao, L. C., Pai, C. Y., Tang, C. Y., et al. (2000). Direct interaction of two homeoproteins, homothorax and extradenticle, is essential for EXD nuclear localization and function. *Mechanisms of Development*, *91*(1-2), 279–291.

Ji, H., Ehrlich, L. I. R., Seita, J., Murakami, P., Doi, A., Lindau, P., et al. (2010). Comprehensive methylome map of lineage commitment from haematopoietic progenitors. *Nature*, *467*(7313), 338–342. doi:10.1038/nature09367

Jo, S. Y., Granowicz, E. M., Maillard, I., Thomas, D., & Hess, J. L. (2011). Requirement for Dot1l in murine postnatal hematopoiesis and leukemogenesis by MLL translocation. *Blood*, *117*(18), 4759–4768. doi:10.1182/blood-2010-12-327668

Jojic, V., Shay, T., Sylvia, K., Zuk, O., Sun, X., Kang, J., et al. (2013). Identification of transcriptional regulators in the mouse immune system. *Nature Immunology*, *14*(6), 633–643. doi:10.1038/ni.2587

Jones, T. A., Flomen, R. H., Senger, G., Nizetić, D., & Sheer, D. (2000). The homeobox gene MEIS1 is amplified in IMR-32 and highly expressed in other neuroblastoma cell lines. *European Journal of Cancer (Oxford, England : 1990)*, *36*(18), 2368–2374.

Jordan, C. T. (2004). Cancer stem cell biology: from leukemia to solid tumors. *Current Opinion in Cell Biology*, *16*(6), 708–712. doi:10.1016/j.ceb.2004.09.002

Jordan, C. T., & Guzman, M. L. (2004). Mechanisms controlling pathogenesis and survival of leukemic stem cells. *Oncogene*, *23*(43), 7178–7187. doi:10.1038/sj.onc.1207935

Kalberer, C. P., Antonchuck, J., & Humphries, R. K. (2002). Genetic Modification of Murine Hematopoietic Stem Cells by Retroviruses. In C. A. Klug & C. T. Jordan (Eds.), *Hematopoietic Stem Cell Protocols* (1st ed., pp. 231–242). Totowa, New Jersey: Humana Press.

Kamps, M. P., Murre, C., Sun, X. H., & Baltimore, D. (1990). A new homeobox gene contributes the DNA binding domain of the t(1;19) translocation protein in pre-B ALL. *Cell*, *60*(4), 547–555.

Kawagoe, H., Humphries, R. K., Blair, A., SUTHERLAND, H. J., & Hogge, D. (1999). Expression of HOX genes, HOX cofactors, and MLL in phenotypically and functionally defines subpopulations of leukemic and normal human hematopoietic cells. *Leukemia*, *13*, 687–698.

Kent, D. G., Copley, M. R., Benz, C., Wohrer, S., Dykstra, B. J., Ma, E., et al. (2009). Prospective isolation and molecular characterization of hematopoietic stem cells with durable self-renewal potential. *Blood*, *113*(25), 6342–6350. doi:10.1182/blood-2008-12-192054

Kiel, M. J., Yilmaz, O. H., Iwashita, T., Yilmaz, O. H., Terhorst, C., & Morrison, S. J. (2005). SLAM family receptors distinguish hematopoietic stem and progenitor cells and reveal endothelial niches for stem cells. *Cell*, *121*(7), 1109–1121. doi:10.1016/j.cell.2005.05.026

Kocabas, F., Zheng, J., Thet, S., Copeland, N. G., Jenkins, N. A., DeBerardinis, R. J., et al. (2012). Meis1 regulates the metabolic phenotype and oxidant defense of hematopoietic stem cells. *Blood*. doi:10.1182/blood-2012-05-432260

Kohlmann, A., Schoch, C., Dugas, M., Schnittger, S., Hiddemann, W., Kern, W., & Haferlach, T. (2005). New insights into MLL gene rearranged acute leukemias using gene expression profiling: shared pathways, lineage commitment, and partner genes. *Leukemia*, *19*(6), 953–964. doi:10.1038/sj.leu.2403746

Kondo, M., Weissman, I. L., & Akashi, K. (1997). Identification of clonogenic common lymphoid progenitors in mouse bone marrow. *Cell*, *91*(5), 661–672.

Kroon, E., Krosl, J., Thorsteinsdottir, U., Baban, S., Buchberg, A. M., & Sauvageau, G. (1998). Hoxa9 transforms primary bone marrow cells through specific collaboration with Meis1a but not Pbx1b. *The EMBO Journal*, *17*(13), 3714–3725.

Krosl, J., Austin, P., Beslu, N., Kroon, E., Humphries, R. K., & Sauvageau, G. (2003a). In vitro expansion of hematopoietic stem cells by recombinant TAT-HOXB4 protein. *Nature Medicine*, *9*(11), 1428–1432. doi:10.1038/nm951

Krosl, J., Beslu, N., Mayotte, N., Humphries, R. K., & Sauvageau, G. (2003b). The Competitive Nature of HOXB4-Transduced HSC Is Limited by PBX1: The Generation of Ultra-Competitive Stem Cells Retaining Full Differentiation Potential. *Immunity*, *18*, 561–571.

Krystal, G., Lam, V., Dragowska, W., Takahashi, C., Appel, J., Gontier, A., et al. (1994). Transforming growth factor beta 1 is an inducer of erythroid differentiation. *The Journal of Experimental Medicine*, *180*(3), 851–860.

Kuhn, R., Schwenk, F., Aguet, M., & Rajewsky, K. (1995). Inducible gene targeting in mice. *Science*, *269*(5229), 1427–1429.

Kumar, A. R., Li, Q., Hudson, W. A., Chen, W., Sam, T., Yao, Q., et al. (2009). A role for MEIS1 in MLL-fusion gene leukemia. *Blood*, *113*(8), 1756–1758. doi:10.1182/blood-2008-06-163287

Kumar, A. R., Sarver, A. L., Wu, B., & Kersey, J. H. (2010). Meis1 maintains stemness signature in MLL-AF9 leukemia. *Blood*, *114*, 3642–3643.

Lawrence, H. J., Christensen, J., Fong, S., Hu, Y.-L., Weissman, I., Sauvageau, G., et al. (2005). Loss of expression of the Hoxa-9 homeobox gene impairs the proliferation and repopulating ability of hematopoietic stem cells. *Blood*, *106*(12), 3988–3994. doi:10.1182/blood-2005-05-2003

Lawrence, H. J., Helgason, C. D., Sauvageau, G., Fong, S., Izon, D. J., Humphries, R. K., & Largman, C. (1997). Mice bearing a targeted interruption of the homeobox gene HOXA9 have defects in myeloid, erythroid, and lymphoid hematopoiesis. *Blood*, *89*(6), 1922–1930.

Lawrence, H. J., Rozenfeld, S., Cruz, C., Matsukuma, K., KWONG, A., KOMUVES, L. G., et al. (1999). Frequent co-expression of the HOXA9 and MEIS1 homeobox genes in human myeloid leukemias. *Leukemia*, *13*, 1993–1999.

Lee, F. S., & Percy, M. J. (2011). The HIF Pathway and Erythrocytosis. *Annual Review of Pathology: Mechanisms of Disease*, *6*(1), 165–192. doi:10.1146/annurev-pathol-011110-130321

Li, J., Tang, B., Qu, Y., & Mu, D. (2011). International Journal of Developmental Neuroscience. *International Journal of Developmental Neuroscience*, *29*(8), 867–872. doi:10.1016/j.ijdevneu.2011.07.010

Lieu, Y. K., & Reddy, E. P. (2009). Conditional c-myb knockout in adult hematopoietic stem cells leads to loss of self-renewal due to impaired proliferation and accelerated differentiation. *Pnas*, *106*, 21689–21694.

Lindsey, S., & Papoutsakis, E. T. (2012). The evolving role of the aryl hydrocarbon receptor (AHR) in the normophysiology of hematopoiesis. *Stem Cell Reviews and Reports*, *8*(4), 1223–1235. doi:10.1007/s12015-012-9384-5

Longobardi, E., Iotti, G., Di Rosa, P., Mejetta, S., Bianchi, F., Fernandez-Diaz, L. C., et al. (2010). Prep1 (pKnox1)-deficiency leads to spontaneous tumor development in mice and accelerates EmuMyc lymphomagenesis: a tumor suppressor role for Prep1. *Molecular Oncology*, *4*(2), 126–134. doi:10.1016/j.molonc.2010.01.001

Loonstra, A., Vooijs, M., Beverloo, H. B., Allak, Al, B., van Drunen, E., Kanaar, R., et al. (2001). Growth inhibition and DNA damage induced by Cre recombinase in mammalian cells
. *Pnas*, *98*, 9209–9214.

Lu, Q., Knoepfler, P. S., Scheele, J., Wright, D. D., & Kamps, M. P. (1995). Both Pbx1 and E2A-Pbx1 bind the DNA motif ATCAATCAA cooperatively with the products of multiple murine Hox genes, some of which are themselves oncogenes. *Molecular and*

Cellular Biology, *15*, 3786–3795.

Maeda, R., Ishimura, A., Mood, K., Park, E. K., Buchberg, A. M., & Daar, I. O. (2002). Xpbx1b and Xmeis1b play a collaborative role inhindbrain and neural crest gene expressionin Xenopus embryos. *Pnas*, *99*(8), 5448–5453.

Maguer-Satta, V., Petzer, A. L., Eaves, A. C., & Eaves, C. J. (1996). BCR-ABL expression in different subpopulations of functionally characterized Ph+ CD34+ cells from patients with chronic myeloid leukemia. *Blood*, *88*(5), 1796–1804.

Mamo, A., Krosl, J., Kroon, E., Bijl, J., Thompson, A., Mayotte, N., et al. (2006). Molecular dissection of Meis1 reveals 2 domains required for leukemia induction and a key role for Hoxa gene activation. *Blood*, *108*(2), 622–629. doi:10.1182/blood-2005-06-2244

Mann, R. S., & Abu-Shaar, M. (1996). Nuclear import of the homeodomain protein extradenticle in response to Wg and Dpp signalling. *Nature*, *383*(6601), 630–633. doi:10.1038/383630a0

Matsumoto, A., & Nakayama, K. I. (2012). Role of key regulators of the cell cycle in maintenance of hematopoietic stem cells. *Biochimica Et Biophysica Acta*. doi:10.1016/j.bbagen.2012.07.004

McMahon, K. A., Hiew, S. Y. L., Hadjur, S., Veiga-Fernandes, H., Menzel, U., Price, A. J., et al. (2007). Mll Has a Critical Role in Fetal and Adult Hematopoietic Stem Cell Self-Renewal. *Cell Stem Cell*, *1*(3), 338–345. doi:10.1016/j.stem.2007.07.002

Mikkola, H. K. A., Klintman, J., Yang, H., Hock, H., Schlaeger, T. M., Fujiwara, Y., & Orkin, S. H. (2003). Haematopoietic stem cells retain long-term repopulating activity and multipotency in the absence of stem-cell leukaemia SCL/tal-1 gene. *Nature*, *421*, 547–551.

Misaghian, N., Ligresti, G., Steelman, L. S., Bertrand, F. E., Bäsecke, J., Libra, M., et al. (2008). Targeting the leukemic stem cell: the Holy Grail of leukemia therapy. *Leukemia*, *23*(1), 25–42. doi:10.1038/leu.2008.246

Miyamoto, K., Araki, K. Y., Naka, K., Arai, F., Takubo, K., Yamazaki, S., et al. (2007). Foxo3a Is Essential for Maintenance of the Hematopoietic Stem Cell Pool. *Cell Stem Cell*, *1*(1), 101–112. doi:10.1016/j.stem.2007.02.001

Moens, C., & Selleri, L. (2006). Hox cofactors in vertebrate development. *Developmental Biology*, *291*(2), 193–206. doi:10.1016/j.ydbio.2005.10.032

Mojsin, M., & Stevanovic, M. (2009). PBX1 and MEIS1 up-regulate SOX3gene expression by direct interaction with a consensus binding site within the basal promoter region. *Biochemical Journal*, *425*(1), 107–116. doi:10.1042/BJ20090694

Morgado, E., Albouhair, S., & Lavau, C. (2007). Flt3 is dispensable to the Hoxa9/Meis1 leukemogenic cooperation. *Blood*, *109*(9), 4020–4022. doi:10.1182/blood-2006-01-039586

Moskow, J. J. (1995). *Meis1,* a *PBX1-Related* Homeobox Gene Involved in Myeloid Leukemia in BXH-2 Mice. *Mol Cell Biol*, 1–10.

Mulloy, J. C., Cammenga, J., MacKenzie, K. L., Berguido, F. J., Moore, M., & Nimer, S. D. (2002). The AML1-ETO fusion protein promotes the expansion of human hematopoietic stem cells. *Blood*, *99*(1), 15–23. doi:10.1182/blood.V99.1.15

Murone, M., Carpenter, D. A., & de Sauvage, F. J. (1998, January 1). Hematopoietic Deficiencies in c-mpl and TPO Knockout Mice. *Stem Cells*. Retrieved July 17, 2012, from http://onlinelibrary.wiley.com/doi/10.1002/stem.160001/abstract;jsessionid=234D6F3A83927E5F1D45CC2EEF52D498.d03t02

Müller, A. M., Medvinsky, A., Strouboulis, J., Grosveld, F., & Dzierzak, E. (1994). Development of hematopoietic stem cell activity in the mouse embryo. *Immunity*, *1*(4), 291–301.

Nakamura, T., Largaespada, D. A., Shaughnessy, J. D., Jenkins, N. A., & Copeland, N. G. (1996). Cooperative activation of Hoxa and Pbx1-related genes in murine myeloid leukaemias. *Nature Genetics*, *12*(2), 149–153. doi:10.1038/ng0296-149

Nishi, H., Nakada, T., Kyo, S., Inoue, M., Shay, J. W., & Isaka, K. (2004). Hypoxia-Inducible Factor 1 Mediates Upregulation of Telomerase (hTERT). *Mol Cell Biol*, *24*(13), 6076–6083. doi:10.1128/MCB.24.13.6076-6083.2004

Nürnberg, S. T., Rendon, A., Smethurst, P. A., Paul, D. S., Voss, K., Thon, J. N., et al. (2012). A GWAS sequence variant for platelet volume marks an alternative DNM3 promoter in megakaryocytes near a MEIS1 binding site. *Blood*, *120*(24), 4859–4868. doi:10.1182/blood-2012-01-401893

Ohta, H., Sekulovic, S., Bakovic, S., Eaves, C. J., Pineault, N., Gasparetto, M., et al. (2007). Near-maximal expansions of hematopoietic stem cells in culture using NUP98-HOX fusions. *Experimental Hematology*, *35*(5), 817–830. doi:10.1016/j.exphem.2007.02.012

Okada, Y., Nagai, R., Sato, T., Matsuura, E., Minami, T., Morita, I., & Doi, T. (2003). Homeodomain proteins MEIS1 and PBXs regulate the lineage-specific transcription of the platelet factor 4 gene. *Blood*, *101*(12), 4748–4756. doi:10.1182/blood-2002-02-0380

Okuda, T., van Deursen, J., Hiebert, S. W., Grosveld, G., & Downing, J. R. (1996). AML1, the target of multiple chromosomal translocations in human leukemia, is essential for normal fetal liver hematopoiesis. *Cell*, *84*(2), 321–330.

Orford, K. W., & Scadden, D. T. (2008). Deconstructing stem cell self-renewal: genetic insights into cell-cycle regulation. *Nature Reviews Genetics*, *9*(2), 115–128. doi:10.1038/nrg2269

Orkin, S. H., & Zon, L. I. (2008). Hematopoiesis: An Evolving Paradigm for Stem Cell Biology. *Cell*, *132*(4), 631–644. doi:10.1016/j.cell.2008.01.025

Orlovsky, K., Kalinkovich, A., Rozovskaia, T., Shezen, E., Itkin, T., Alder, H., et al. (2011). Down-regulation of homeobox genes MEIS1 and HOXA in MLL-rearranged acute leukemia impairs engraftment and reduces proliferation. *Proceedings of the National Academy of Sciences*, *108*(19), 7956–7961. doi:10.1073/pnas.1103154108

Pai, C.-Y., Kuo, T.-S., Jaw, T. J., Kurant, E., Chen, C.-T., Bessarab, D. A., et al. (1998). The Homothorax homeoprotein activates the nuclear localization of another homeoprotein, Extradenticle, and suppresses eye development in Drosophila. *Genes & Development*, 435–446.

Palmqvist, L., Argiropoulos, B., Pineault, N., Abramovich, C., Sly, L. M., Krystal, G., et al. (2006). The Flt3 receptor tyrosine kinase collaborates with NUP98-HOX fusions in acute myeloid leukemia. *Blood*, *108*(3), 1030–1036. doi:10.1182/blood-2005-12-007005

Passegue, E., Jamieson, C. H. M., Ailles, L. E., & Weissman, I. L. (2003). Normal and leukemic hematopoiesis: Are leukemiasa stem cell disorder or a reacquisition of stemcell characteristics? *Pnas*, *100*, 11842–11849.

Pawliuk, R., Kay, R., Lansdorp, P., & Humphries, R. K. (1994). Selection of retrovirally transduced hematopoietic cells using CD24 as a marker of gene transfer. *Blood*, *84*(9), 2868–2877.

Peifer, M., & Wieschaus, E. (1990). Mutations in the Drosophila gene extradenticle affect the way specific homeo domain proteins regulate segmental identity. *Genes & Development*, *4*(7), 1209–1223.

Perry, J. M., Harandi, O. F., & Paulson, R. F. (2007). BMP4, SCF, and hypoxia cooperatively regulate the expansion of murine stress erythroid progenitors. *Blood*, *109*(10), 4494–4502. doi:10.1182/blood-2006-04-016154

Phelan, M. L., Rambaldi, I., & Featherstone, M. S. (1995). Cooperative interactions between HOX andPBX proteins mediated by a conserved peptide motif. *Molecular and Cellular Biology*, *15*(8), 3989–3997.

Pineault, N., Abramovich, C., & Humphries, R. K. (2005). Transplantable cell lines generated with NUP98–Hox fusion genes undergo leukemic progression by Meis1 independent of its binding to DNA. *Leukemia*. doi:10.1038/sj.leu.2403696

Pineault, N., Abramovich, C., Ohta, H., & Humphries, R. K. (2004). Differential and Common Leukemogenic Potentials of Multiple NUP98-Hox Fusion Proteins Alone or with Meis1. *Molecular and Cellular Biology*, *24*, 1907–1917. doi:10.1128/MCB.24.5.1907–1917.2004

Pineault, N., Buske, C., Feuring-Buske, M., Abramovich, C., Rosten, P., Hogge, D. E., et al. (2003). Induction of acute myeloid leukemia in mice by the human leukemia-specific fusion gene NUP98-HOXD13 in concert with Meis1. *Blood*, *101*(11), 4529–4538. doi:10.1182/blood-2002-08-2484

Pineault, N., Helgason, C. D., Lawrence, H. J., & Humphries, R. K. (2002). Differential expression of *Hox, Meis1* and *Pbx1* genes in primitive cells throughout murine hematopoietic ontogeny. *Experimental Hematology*, *30*, 49–57.

Piper, D. E., Batchelor, A. H., Chang, C.-P., Cleary, M. L., & Wolberger, C. (1999). Structure of a HoxB1–Pbx1 Heterodimer Bound to DNA: Role of the Hexapeptide and a Fourth Homeodomain Helix in Complex Formation. *Cell*, *96*, 587–597.

Pronk, C. J. H., Rossi, D. J., Månsson, R., Attema, J. L., Norddahl, G. L., Chan, C. K. F., et al. (2007). Elucidation of the phenotypic, functional, and molecular topography of a myeloerythroid progenitor cell hierarchy. *Cell Stem Cell*, *1*(4), 428–442. doi:10.1016/j.stem.2007.07.005

Purton, L. E., & Scadden, D. T. (2007). Limiting factors in murine hematopoietic stem cell assays. *Cell Stem Cell*, *1*(3), 263–270. doi:10.1016/j.stem.2007.08.016

Rankin, E. B., Wu, C., Khatri, R., Wilson, T. L. S., Andersen, R., Araldi, E., et al. (2012). The HIF Signaling Pathway in Osteoblasts Directly Modulates Erythropoiesis through the Production of EPO. *Cell*, *149*(1), 63–74. doi:10.1016/j.cell.2012.01.051

Rauskolb, C., & Wieschaus, E. (1994). Coordinate regulation of downstream genes by extradenticle and the homeotic selector proteins. *The EMBO Journal*, *13*(15), 3561–3569.

Rauskolb, C., Peifer, M., & Wieschaus, E. (1993). extradenticle, a regulator of homeotic gene activity, is a homolog of the homeobox-containing human proto-oncogene pbx1. *Cell*, *74*(6), 1101–1112.

Rave-Harel, N., Givens, M. L., Nelson, S. B., Duong, H. A., Coss, D., Clark, M. E., et al. (2004). TALE homeodomain proteins regulate gonadotropin-releasing hormone gene expression independently and via interactions with Oct-1. *The Journal of Biological Chemistry*, *279*(29), 30287–30297. doi:10.1074/jbc.M402960200

Rebel, V. I., Miller, C. L., Eaves, C. J., & Lansdorp, P. M. (1996). The repopulation potential of fetal liver hematopoietic stem cells in mice exceeds that of their liver adult bone

marrow counterparts. *Blood*, *87*, 3500–3507.

Reya, T. (2003). Regulation of Hematopoietic Stem Cell Self-Renewal. *Recent Prog Horm Res*, *58*, 283–295.

Rieckhof, G. E., Casares, F., Ryoo, H. D., Abu-Shaar, M., & Mann, R. S. (1997). Nuclear translocation of extradenticle requires homothorax, which encodes an extradenticle-related homeodomain protein. *Cell*, *91*(2), 171–183.

Rizo, A. (2006). Signaling pathways in self-renewing hematopoietic and leukemic stem cells: do all stem cells need a niche? *Human Molecular Genetics*, *15*(Review Issue 2), R210–R219. doi:10.1093/hmg/ddl175

Roche, J., Zeng, C., Barón, A., Gadgil, S., Gemmill, R. M., Tigaud, I., et al. (2004). Hox expression in AML identifies a distinct subset of patients with intermediate cytogenetics. *Leukemia*, *18*(6), 1059–1063. doi:10.1038/sj.leu.2403366

Rosales-Aviña, J. A., Torres-Flores, J., Aguilar-Lemarroy, A., Gurrola-Díaz, C., Hernández-Flores, G., Ortiz-Lazareno, P. C., et al. (2011). MEIS1, PREP1, and PBX4 are differentially expressed in acute lymphoblastic leukemia: association of MEIS1 expression with higher proliferation and chemotherapy resistance. *Journal of Experimental & Clinical Cancer Research : CR*, *30*, 112. doi:10.1186/1756-9966-30-112

Roy, S., Tripathy, M., Mathur, N., Jain, A., & Mukhopadhyay, A. (2012). Hypoxia improves expansion potential of human cord blood-derived hematopoietic stem cells and marrow repopulation efficiency. *European Journal of Haematology*, *88*(5), 396–405. doi:10.1111/j.1600-0609.2012.01759.x

Royo, J. L., Bessa, J., Hidalgo, C., Fernández-Miñán, A., Tena, J. J., Roncero, Y., et al. (2012). Identification and analysis of conserved cis-regulatory regions of the MEIS1 gene. *PLoS ONE*, *7*(3), e33617. doi:10.1371/journal.pone.0033617

Rozovskaia, T., Feinstein, F., Mor, O., Foà, R., Blechman, J., Nakamura, T., et al. (2001). Upregulation of Meis1 and Hoxa9 in Acute Lymphocytic Leukemias with the T(4:11) Abnormality. *Oncogene*, *20*, 874–878.

Ryoo, H. D., Marty, T., Casares, F., Affolter, M., & Mann, R. S. (1999). Regulation of Hox target genes by a DNA bound Homothorax/Hox/Extradenticle complex. *Development*, *126*(22), 5137–5148.

Saleh, M., Huang, H., Green, N. C., & Featherstone, M. S. (2000). A conformational change in PBX1A is necessary for its nuclear localization. *Experimental Cell Research*, *260*(1), 105–115. doi:10.1006/excr.2000.5010

Sardina, J. L., López-Ruano, G., Sánchez-Sánchez, B., Llanillo, M., & Hernández-Hernández, A. (2012). Reactive oxygen species: are they important for haematopoiesis?

Critical Reviews in Oncology/Hematology, *81*(3), 257–274. doi:10.1016/j.critrevonc.2011.03.005

Sashida, G., & Iwama, A. (2012). Epigenetic regulation of hematopoiesis. *International Journal of Hematology*, *96*(4), 405–412. doi:10.1007/s12185-012-1183-x

Sauvageau, G., Lansdorp, P. M., Eaves, C. J., Hogge, D. E., Dragowska, W., Reid, D. S., et al. (1994). Differential expression of homeobox genes in functionally distinct CD34+ subpopulations of human bone marrow cells. *Proceedings of the National Academy of Sciences of the United States of America*, *91*(25), 12223–12227.

Sauvageau, G., Thorsteinsdottir, U., Eaves, C. J., Lawrence, H. J., Largman, C., Lansdorp, P. M., & Humphries, R. K. (1995). Overexpression of HOXB4 in hematopoietic cells causes the selective expansion of more primitive populations in vitro and in vivo. *Genes & Development*, *9*(14), 1753–1765. doi:10.1101/gad.9.14.1753

Shanmugam, K., Green, N. C., Rambaldi, I., Saragovi, H. U., & Featherstone, M. (1999). PBX and MEIS as Non-DNA-Binding Partners in Trimeric Complexes with HOX Proteins. *Molecular and Cellular Biology*, *19*, 7577–7588.

Shen, W., Montgomery, J., Rozenfeld, S., Moskow, J., Lawrence, H. J., Buchberg, A., & Largman, C. (1997). AbdB-Like Hox Proteins Stabilize DNA Binding by the Meis1 Homeodomain Proteins. *Molecular and Cellular Biology*, *17*(11), 6448–6458.

Shen, W.F., Rozenfelf, S., Kwong, A., Komulves, L. G., Lawrence, H. J., & Largman, C. (1999). HOXA9 Forms Triple Complexes with PBX2 and MEIS1 in Myeloid Cells. *Molecular and Cellular Biology*, *19*(4), 3051–3061.

Shinnick, K. M., Eklund, E. A., & McGarry, T. J. (2010). Geminin deletion from hematopoietic cells causes anemia and thrombocytosis in mice. *Journal of Clinical Investigation*, *120*(12), 4303–4315. doi:10.1172/JCI43556DS1

Shivdasani, R. A., & Schulze, H. (2005). Culture, expansion, and differentiation of murine megakaryocytes. *Current Protocols in Immunology / Edited by John E. Coligan ... [Et Al.]*, *Chapter 22*, Unit 22F.6. doi:10.1002/0471142735.im22f06s67

Simsek, T., Kocabas, F., Zheng, J., DeBerardinis, R. J., Mahmoud, A. I., Olson, E. N., et al. (2010). The Distinct Metabolic Profile of Hematopoietic Stem Cells Reflects Their Location in a Hypoxic Niche. *Stem Cell*, *7*(3), 380–390. doi:10.1016/j.stem.2010.07.011

Socolovsky, M., Nam, H., Fleming, M. D., Haase, V. H., Brugnara, C., & Lodish, H. F. (2001). Ineffective erythropoiesis in Stat5a(-/-)5b(-/-) mice due to decreased survival of early erythroblasts. *Blood*, *98*(12), 3261–3273.

Somervaille, T. C. P., & Cleary, M. L. (2010). Grist for the MLL: how do MLL oncogenic fusion proteins generate leukemia stem cells? *International Journal of Hematology*,

91(5), 735–741. doi:10.1007/s12185-010-0579-8

Song, X., Krelin, Y., Dvorkin, T., Bjorkdahl, O., Segal, S., Dinarello, C. A., et al. (2005). CD11b+/Gr-1+ immature myeloid cells mediate suppression of T cells in mice bearing tumors of IL-1beta-secreting cells. *Journal of Immunology (Baltimore, Md. : 1950)*, *175*(12), 8200–8208.

Spangrude, G. J., Smith, L., Uchida, N., Ikuta, K., Heimfeld, S., Friedman, J., & Weissman, I. L. (1991). Mouse hematopoietic stem cells. *Blood*, *78*(6), 1395–1402.

Spieker, N., van Sluis, P., Beitsma, M., Boon, K., van Schaik, B. D., van Kampen, A. H., et al. (2001). The MEIS1 oncogene is highly expressed in neuroblastoma and amplified in cell line IMR32. *Genomics*, *71*(2), 214–221. doi:10.1006/geno.2000.6408

Sprüssel, A., Schulte, J. H., Weber, S., Necke, M., Händschke, K., Thor, T., et al. (2012). Lysine-specific demethylase 1 restricts hematopoietic progenitor proliferation and is essential for terminal differentiation. *Leukemia*. doi:10.1038/leu.2012.157

Stankunas, K., Shang, C., Twu, K. Y., Kao, S. C., Jenkins, N. A., Copeland, N. G., et al. (2008). Pbx/Meis Deficiencies Demonstrate Multigenetic Origins of Congenital Heart Disease. *Circulation Research*, *103*(7), 702–709. doi:10.1161/CIRCRESAHA.108.175489

Szilvassy, S. J., Humphries, R. K., Lansdorp, P. M., Eaves, A. C., & Eaves, C. J. (1990). Quantitative Assay for Totipotent Reconstituting Hematopoietic Stem Cells by a Competitive Repopulation Strategy. *Pnas*, *87*(22), 8736–8740.

Takeda, A., Goolsby, C., & Yaseen, N. R. (2006). NUP98-HOXA9 induces long-term proliferation and blocks differentiation of primary human CD34+ hematopoietic cells. *Cancer Research*, *66*(13), 6628–6637. doi:10.1158/0008-5472.CAN-06-0458

Takubo, K., Goda, N., Yamada, W., Iriuchishima, H., Ikeda, E., Kubota, Y., et al. (2010). Regulation of the HIF-1α Level Is Essential for Hematopoietic Stem Cells. *Stem Cell*, *7*(3), 391–402. doi:10.1016/j.stem.2010.06.020

Tamai, H., & Inokuchi, K. (2010). 11q23/MLL acute leukemia : update of clinical aspects. *Journal of Clinical and Experimental Hematopathology : JCEH*, *50*(2), 91–98.

Thorsteinsdottir, U., Mamo, A., Kroon, E., Jerome, L., Bijl, J., Lawrence, H. J., et al. (2002). Overexpression of the myeloid leukemia-associated Hoxa9 gene in bone marrow cells induces stem cell expansion. *Blood*, *99*(1), 121–129. doi:10.1182/blood.V99.1.121

Tothova, Z., Kollipara, R., Huntly, B. J., Lee, B. H., Castrillon, D. H., Cullen, D. E., et al. (2007). FoxOs Are Critical Mediators of Hematopoietic Stem Cell Resistance to Physiologic Oxidative Stress. *Cell*, *128*(2), 325–339. doi:10.1016/j.cell.2007.01.003

Trentin, L., Giordan, M., Dingermann, T., Basso, G., Kronnie, te, G., & Marschalek, R. (2009). Two independent gene signatures in pediatric t(4;11) acute lymphoblastic leukemia patients. *European Journal of Haematology*, *83*(5), 406–419. doi:10.1111/j.1600-0609.2009.01305.x

Unnisa, Z., Clark, J. P., Roychoudhury, J., Thomas, E., Tessarollo, L., Copeland, N. G., et al. (2012). Meis1 preserves hematopoietic stem cells in mice by limiting oxidative stress. *Blood*. doi:10.1182/blood-2012-06-435800

Van Zant, G. (1984). Studies of hematopoietic stem cells spared by 5-fluorouracil. *The Journal of Experimental Medicine*, *159*(3), 679–690.

Vu, H. A., Xinh, P. T., Masuda, M., Motoji, T., Toyoda, A., Sakaki, Y., et al. (2006). FLT3 is fused to ETV6 in a myeloproliferative disorder with hypereosinophilia and a t(12;13)(p13;q12) translocation. *Leukemia*, *20*(8), 1414–1421. doi:10.1038/sj.leu.2404266

Wang, G. G., Cai, L., Pasillas, M. P., & Kamps, M. P. (2007). NUP98–NSD1 links H3K36 methylation to Hox-A gene activation and leukaemogenesis. *Nature Cell Biology*, *9*(7), 804–812. doi:10.1038/ncb1608

Wang, G. G., Pasillas, M. P., & Kamps, M. P. (2005). Meis1 programs transcription of FLT3 and cancer stem cell character, using a mechanism that requires interaction with Pbx and a novel function of the Meis1 C-terminus. *Blood*, *106*(1), 254–264. doi:10.1182/blood-2004-12-4664

Wang, G. G., Pasillas, M. P., & Kamps, M. P. (2006). Persistent Transactivation by Meis1 Replaces Hox Function in Myeloid Leukemogenesis Models: Evidence for Co-Occupancy of Meis1-Pbx and Hox-Pbx Complexes on Promoters of Leukemia-Associated Genes. *Molecular and Cellular Biology*, *26*, 3902–3916. doi:10.1128/MCB.26.10.3902–3916.2006

Warner, J. K., Wang, J. C. Y., Hope, K. J., Jin, L., & Dick, J. E. (2004). Concepts of human leukemic development. *Oncogene*, *23*(43), 7164–7177. doi:10.1038/sj.onc.1207933

Waskiewicz, A. J., rikhof, H. A., Hernandez, R. E., & Moens, C. B. (2001). Zebrafish Meis functions to stabilize PBX proteins and regulate hindbrain patterning. *Development*, *128*, 4139–4151.

Williams, T. M., Williams, M. E., & Innis, J. W. (2005). Range of HOX/TALE superclass associations and protein domain requirements for HOXA13:MEIS interaction. *Developmental Biology*, *277*(2), 457–471. doi:10.1016/j.ydbio.2004.10.004

Wilson, N. K., Foster, S. D., Wang, X., Knezevic, K., Schütte, J., Kaimakis, P., et al. (2010). Combinatorial Transcriptional Control In Blood Stem/Progenitor Cells: Genome-wide Analysis of Ten Major Transcriptional Regulators. *Stem Cell*, *7*(4), 532–544.

doi:10.1016/j.stem.2010.07.016

Wong, P., Iwasaki, M., Somervaille, T. C. P., So, C. W. E., & Cleary, M. L. (2007). Meis1 is an essential and rate-limiting regulator of MLL leukemia stem cell potential. *Genes & Development*, *21*(21), 2762–2774. doi:10.1101/gad.1602107

Woolthuis, C. M., Han, L., Verkaik-Schakel, R. N., van Gosliga, D., Kluin, P. M., Vellenga, E., et al. (2012). Downregulation of MEIS1 impairs long-term expansion of CD34+ NPM1-mutated acute myeloid leukemia cells. *Leukemia*, *26*(4), 848–853. doi:10.1038/leu.2011.277

Xiang, P., Lo, C., Argiropoulos, B., Lai, C. B., Rouhi, A., Imren, S., et al. (2010). Identification of E74-like factor 1 (ELF1) as a transcriptional regulator of the Hox cofactor MEIS1. *Experimental Hematology*, *38*(9), 798–808.e2. doi:10.1016/j.exphem.2010.06.006

Xu, B., Geerts, D., Qian, K., Zhang, H., & Zhu, G. (2008a). Myeloid ecotropic viral integration site 1 (MEIS) 1 involvement in embryonic implantation. *Human Reproduction (Oxford, England)*, *23*(6), 1394–1406. doi:10.1093/humrep/den082

Xu, J., Suzuki, M., Niwa, Y., Hiraga, J., Nagasaka, T., Ito, M., et al. (2008b). Clinical significance of nuclear non-phosphorylated beta-catenin in acute myeloid leukaemia and myelodysplastic syndrome. *British Journal of Haematology*, *140*(4), 394–401. doi:10.1111/j.1365-2141.2007.06914.x

Yang, J., Su, Y., & Richmond, A. (2007). Antioxidants tiron and N-acetyl-L-cysteine differentially mediate apoptosis in melanoma cells via a reactive oxygen species-independent NF-kappaB pathway. *Free Radical Biology & Medicine*, *42*(9), 1369–1380. doi:10.1016/j.freeradbiomed.2007.01.036

Yilmaz, O. H., Valdez, R., Theisen, B. K., Guo, W., Ferguson, D. O., Wu, H., & Morrison, S. J. (2006). Pten dependence distinguishes haematopoietic stem cells from leukaemia-initiating cells. *Nature Publishing Group*, *441*(7092), 475–482. doi:10.1038/nature04703

Zangenberg, M., Grubach, L., Aggerholm, A., Silkjaer, T., Juhl-Christensen, C., Nyvold, C. G., et al. (2009). The combined expression of HOXA4 and MEIS1 is an independent prognostic factor in patients with AML. *European Journal of Haematology*, *83*(5), 439–448. doi:10.1111/j.1600-0609.2009.01309.x

Zeisig, B. B., Milne, T., Garcia-Cuellar, M.-P., Schreiner, S., Martin, M.-E., Fuchs, U., et al. (2004). *Hoxa9* and *Meis1* Are Key Targets for MLL-ENL-Mediated Cellular Immortalization. *Mol Cell Biol*, *24*, 617–628. doi:10.1128/MCB.24.2.617–628.2004

Zhang, F., Lau, S. S., & Monks, T. J. (2011). The cytoprotective effect of N-acetyl-L-cysteine against ROS-induced cytotoxicity is independent of its ability to enhance glutathione synthesis. *Toxicological Sciences : an Official Journal of the Society of*

Toxicology, *120*(1), 87–97. doi:10.1093/toxsci/kfq364

Zhang, X., Friedman, A., Heaney, S., Purcell, P., & Maas, R. L. (2002). Meis homeoproteins directly regulate Pax6 during vertebrate lens morphogenesis. *Genes & Development*, *16*(16), 2097–2107. doi:10.1101/gad.1007602

Zhou, J., Wu, J., Li, B., Liu, D., Yu, J., Yan, X., et al. (2013). PU.1 is essential for MLL leukemia partially via crosstalk with the MEIS/HOX pathway. *Leukemia*. doi:10.1038/leu.2013.384

Zon, L. I. (2008). Intrinsic and extrinsic control of haematopoietic stem-cell self-renewal. *Nature*, *453*(7193), 306–313. doi:10.1038/nature07038